SPATIO-TEMPORAL VARIABILITY OF COMPOUND DROUGHT AND HEATWAVE EVENTS (CDHEs) IN AUSTRALIAN AGRICULTURAL REGIONS AND THEIR IMPACTS ON CEREAL CROPS

Michela Skipp

Supervisor:

A/Prof Danielle Verdon-Kidd

A thesis submitted for the degree of Honours (Earth Science) The University of Newcastle

Declaration

This thesis contains no material which has been accepted for the award of any other degree or diploma in any university. To the best of the author's knowledge, it contains no material previously published or written by another person, except where due reference is made in the text.

Michela Skipp

October 2024

Availability of data and material

On request.

Code availability

On request.

Compliance with ethical standards

Conflict of interest

The author declare that they have no conflict of interest.

Acknowledgements

I would like to extend my sincere gratitude to my supervisor, Dr. Danielle Verdon-Kidd, whose invaluable guidance, expertise, and encouragement made this thesis possible and supported me throughout this challenging and rewarding journey. I also thank the University of Newcastle for providing the opportunity, space, and resources necessary to complete this honours year.

Abstract

The impact of climate-related hazards is an increasing concern for cereal crop production globally, with food security being a major issue. Among these hazards, compound drought and heatwave events (CDHEs) are particularly important. CDHEs are linked to significant crop yield losses globally; however, their impacts on cereal crop yield at a regional scale remain understudied in Australia. This study, for the first time, quantified the historical 1910-2022 spatio-temporal variability in CDHE characteristics across Australian Bureau of Agricultural and Resource Economics and Sciences (ABARES) crop growing regions using yield impact-based definitions of heatwaves and droughts. Heatwaves of all durations were detected using 5 km by 5 km gridded temperature data from the Australia Gridded Climate Data (AGCD) and the Excess Heat Factor (EHF) with a seasonal 15-day window 90th percentile threshold from 1961-1990. Drought was detected using 55 km by 55 km gridded data of the self-calibrating Palmer Drought Severity Index (scPDSI) to capture agricultural drought over the same time periods as heatwaves. CDHE days were then defined by intersecting values from both indices.

Frequency, intensity, duration and area impacted were analysed for individual events and across monthly, growing season and annual timescales. Sen Slope and Mann–Kendall tests were applied to detect trends in gridded frequency and severity of heatwaves and CDHEs over the 113-year period. Average statistics for the periods 1910–1999 and 2000–2022 were also spatially analysed to identify recent changes in heatwaves and CDHEs. The results show that the frequency, severity, and area of heatwaves and CDHEs have abruptly increased since the 2000s, particularly over western and eastern Australia. Extreme variability in both heatwaves and CDHEs is also aligned with growing regions and during the growing season.

The relationship between CDHEs and cereal crop yields of wheat, oats, barley and sorghum was assessed for ABARES regions using the Pearson's Correlation Coefficient. Statistically significant negative correlations between CDHE frequency, intensity, and detrended crop yield were found in Southern and Eastern Victoria wheat and barley (-0.49, -0.45), Tasmania wheat (-0.37), NSW Tablelands barley (-0.39), and Central North Victoria barley (-0.41). This study examines statistical yield loss anomalies, finding increased frequency and magnitude in all cereal crop yield anomalies over the 32-year ABARES record, indicating a response to a range of extreme weather and natural hazards. Several yield anomalies aligned with high CDHE frequency and intensity during the growing period, underlining the potential of Australian CDHEs to drive climate- related yield loss. However, not all years with yield anomalies were associated with CDHEs, highlighting the complexity of the effects of climate hazards on yield. Future research could identify the potential drivers of non-CDHE crop declines (such as combined flood and heat events).

This work is important for not only understanding the past climate variability and extremes of both heatwaves and CDHEs, but also works towards understanding how this is linked to crop yield. This is in efforts towards ongoing research in Australia to address challenges of the future climate in agriculture and better prepare for, adapt to, and mitigate CDHEs in the future.

Table of Contents

List of Tables

List of Figures

List of Supplementary Tables

List of Supplementary Figures

List of Abbreviations

Australian State / Territory

1. Australian Capital Territory: ACT

2. New South Wales: NSW

3. Northern Territory: NT

4. Queensland: QLD

5. South Australia: SA

6. Tasmania: TAS

7. Victoria: VIC

8. Western Australia: WA

Departments:

9. Intergovernmental Panel on Climate Change: IPCC

10. Australian Bureau of Agricultural and Resource Economics and Science Regions: ABARES

Other Regions

11. Murray Darling Basin: MDB

12. Australian agricultural growing regions: ABARES regions, growing regions

Scientific Terms:

13. Compound Events: CEs

14. Compound Drought and Heatwave Events: CDHEs

15. Excess Heat Factor: EHF

16. Self-calibrating Palmer Drought Severity Index: sc-PDSI

17. Standardised Precipitation Evapotranspiration Index: SPEI

18. Standardised Precipitation Index: SPI

Chapter 1 Introduction and Literature Review

1.1 Introduction

Assessing natural hazards, including climate and weather extremes, has been a central topic in earth sciences due to the associated severe social, economic, and environmental impacts (Schneiderbauer & Ehrlich, 2004). Natural hazards are defined as potentially damaging physical events or phenomena that can trigger the loss of life or injury, property damage, social and economic disruption, or environmental degradation, posing substantial risks to people and communities (Cui et al., 2021). Natural hazards become 'disasters' when they result in significant casualties, property loss, and hindered social and economic development (Aubrecht et al., 2013). Natural hazards also directly and indirectly affect natural resources and exacerbate constraints on agriculture and food production (Schneiderbauer & Ehrlich, 2004).

Changes in the Earth's climate system have altered the intensity and frequency of climate-related natural hazards such as cyclones, floods, droughts, heatwaves, and bushfires, significantly increasing the risk due to greater exposure and vulnerability of affected sectors (Aubrecht et al., 2013; Leonard et al., 2014). In recent decades, the extreme impact of natural hazards, including large-scale, cascading, and compound disasters, has intensified, further straining resources and increasing communities vulnerability to long-term socioeconomic consequences (Cui et al., 2021). Furthermore, the complex landscape of climate hazards and drivers has made it increasingly challenging to predict extreme events (Leonard et al., 2014). Therefore, understanding the spatio-temporal variability of natural hazards, which refers to changes over space and time, is critical for adaptation and mitigation.

While there has been significant research into the nature and impacts of individual climate hazards, driven by a growing interest in understanding how climate change has altered their frequency and severity, there remains limited understanding of how multiple climate hazards interact when occurring concurrently or consecutively. These interactions, known as Compound Events (CEs), happen when two or more climate hazards converge within a specific area during the same time period or in quick succession, often resulting in amplified impacts (Ridder et al., 2020). Examples of CEs include combinations of heat, drought, wind, bushfires, and heavy rainfall driven by meteorological/weather events such as heatwaves, droughts and cyclones (Ridder, Pitman, & Ukkola, 2022). Research into CEs has gained traction recently as they appear to have become more frequent and led to more severe socioeconomic impacts than single events (Afroz et al., 2023). CEs have been acknowledged as a distinct class since multiple hazards do not occur independently, necessitating studying together. This interdependence in CEs arises because certain climate drivers or hazards are interrelated, leading to extreme events occurring concurrently, such as heatwaves and drought, or heavy rain and strong winds (Zhang et al., 2022).

The nature of CEs, including their spatio-temporal variability and impacts, is complex, requiring multidisciplinary and interdisciplinary work in defining, mapping, analysing statistics, attributing impacts

and communicating risk (Leonard et al., 2014). Zscheischler et al. (2020) categorise the impacts of CEs into four typologies: (1) preconditioned impacts, where each hazard worsens due to existing conditions; (2) multivariate amplified impacts, which exceed those of individual occurrences, even if the individual occurrences are not extreme; (3) temporal impacts from a rapid succession of hazards; (4) spatially compounding impacts from the simultaneous occurrence of extremes.

Compound Drought and Heatwave events (CDHEs) are a category of CEs that can align with all four typologies listed above and can lead to severe consequences, such as intensified water shortages, crop failures, and increased bushfire risk, posing complex challenges for communities and ecosystems (Afroz et al., 2023; Tabari & Willems, 2023; Tripathy et al., 2023). To date, research into CDHEs has focused on understanding the drivers and impacts of CDHEs using multivariate approaches. However, understanding the nature of CDHEs (i.e. spatio-temporal variability of intensity, duration, frequency, onset, timing, extent, hazard combinations and dynamic drivers) remains an underexplored area in climate research, with very few global studies and detailed regional assessments (Ridder, Ukkola, et al., 2022). Australia, Southeast Asia, South Asia, South Africa, South America and the United States of America are the most frequently reported global hotspots for CDHEs, resulting in severe repercussions for agriculture (Afroz et al., 2023). Therefore, developing a better understanding of the nature of CDHEs is crucial for these regions.

This study addresses knowledge gaps in Australian CDHEs by quantifying spatio-temporal trends across agricultural growing regions and assessing the impact on cereal crops, which are critical to the nation's economy and food security. This study also seeks to quantify the impact of CDHE components on cereal crop yield, which is not well understood. This will build a foundation for understanding and mitigating climate-related risks from CDHEs in Australian agriculture, which is a crucial step in building resilience and safeguarding future generations.

1.2 Literature Review

As CDHEs are a combination of both drought and heatwaves, the literature review first delves into the impacts and characteristics of drought, followed by a review of heatwaves and then the combination of the two to form CDHEs. A brief discussion of potential CDHE impacts is also provided.

1.21 Characteristics and Impacts of Droughts

Droughts are generally defined by a deficiency of precipitation over an extended period (Redmond, 2002). Severe droughts are characterised by water shortages, which directly affect food, water and energy security (Ndayiragije & Li, 2022). There are several categories of droughts, including meteorological droughts (rainfall deficiency), agricultural droughts (soil moisture deficiency and plant stress), and hydrological droughts (surface and groundwater shortages) (Ndayiragije & Li, 2022). The sixth assessment report by the Intergovernmental Panel on Climate Change (IPCC) reported the intensification of droughts across Africa,

North and South America, Europe, Asia, and Australia, attributing to both anthropogenic climate change and natural variability (IPCC, 2021).

As global temperatures rise due to increased greenhouse gas emissions, the hydrological cycle undergoes significant changes (Mukherjee et al., 2018). Warmer temperatures accelerate evaporation from land and water surfaces, leading to drier soils and reduced water availability (Perkins-Kirkpatrick et al., 2015). Dry soils further elevate land surface temperatures by increasing sensible heat fluxes, creating a positive feedback loop that intensifies both droughts and heatwaves (Kiem et al., 2016). Limited moisture availability diminishes the cooling effect of evaporation, further exacerbating heating effects. Conversely, higher temperatures can increase atmospheric moisture, triggering more rainfall in some areas and resulting in complex patterns of intensifying wetting and drying (IPCC, 2021). Climate shocks, including drops in precipitation, more intense but less frequent rainfall and more frequent extreme droughts and heatwaves, can disrupt the water balance system, leading to prolonged dry spells and slower recovery from droughts (Gallic & Vermandel, 2020).

Australia is the driest inhabited continent on Earth, with a long history of droughts (BOM, 2020; Verdon-Kidd & Kiem, 2009). The drivers and impacts of droughts are well-studied in Australia (Gibson et al., 2022; Palmer et al., 2024; Verdon-Kidd & Kiem, 2009). Most notably, the prolonged dry conditions associated with the 1997-2010 Millennium Drought triggered stringent domestic and irrigation water restrictions in the Murray Darling Basin (MDB), which is the largest agricultural region in Australia (Fig. 1, Panel A) (Kiem et al., 2016). The Millennium Drought had major socioeconomic and environmental impacts, including disrupted agricultural production, natural habitats, and water availability, as well as increased bushfire risk (Verdon-Kidd & Kiem, 2009). It has been estimated that this drought reduced the gross domestic product of the MDB by 5.7% below forecasts between 2006-2009, with the Australian federal government having paid a total of 4.4 billion in drought assistance by mid-2010 (Climate Council, 2015). More recently, the 2017-2019 drought, known as the Tinderbox Drought, also had severe consequences (Fig. 1, Panel B). During this period, rainfall, particularly from April to September, was substantially below average across the MDB (BOM, 2020). The drought led to cascading and compounding impacts across socioeconomic and natural sectors, including bringing rural townships to the brink of running out of water, causing severe agricultural losses, and even threatening the water supply of Australia's largest city, Sydney (Devanand et al., 2024).

Prolonged multiyear droughts such as the Millenium Drought and Tinder Box Drought have severe impacts on people, society and natural systems (Gibson et al., 2022). Unlike most other climate hazards, droughts develop slowly (often described as a creeping hazard) and can go unnoticed until soil and or surface water shortages become apparent. Water stress occurs when water demand exceeds availability, resulting in water supply shortages for domestic, agricultural and industrial water use, causing crop yield declines, livestock

mortality, and disruption of services (Ding et al., 2011; Lamaoui et al., 2018). Signs of drought-affected agriculture include dried crops, withering and yellowing (Ding et al., 2011). Crop yield is compromised, particularly if drought stress coincides with key crop development phases in winter and spring (Muleke et al., 2022). Persistent agricultural drought stress is also known to disrupt plant development, including seed sowing, germination, reproduction, and maturation, thus reducing productivity (Sehgal et al., 2018).
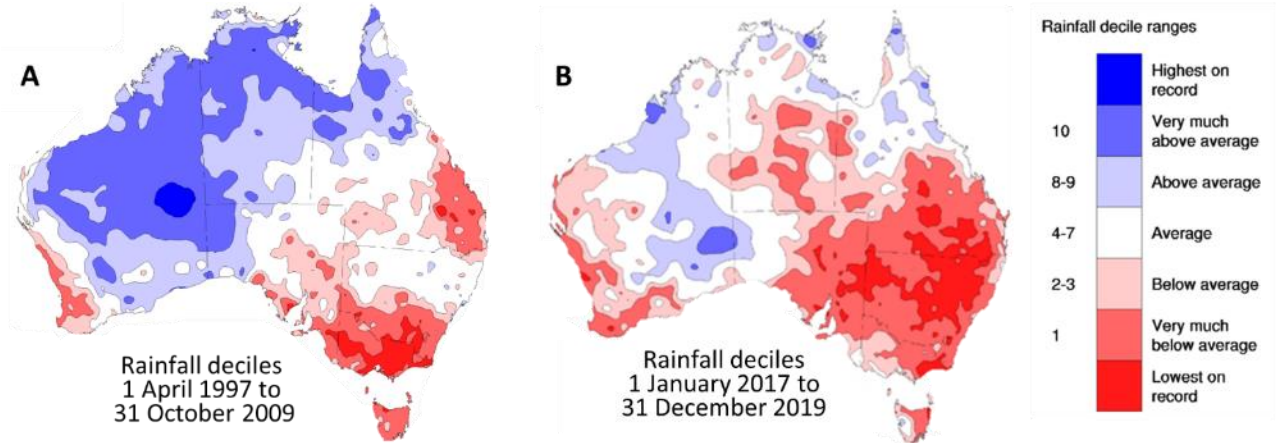
Fig. 1 Australian Rainfall Deciles for A: Millennial Drought and B: Tinderbox Drought (BOM, 2020)

Indirect impacts from drought include the effects on human health, socioeconomics, and the environment (Kiem et al., 2016). The health impacts of droughts arise from reduced nutrition, poor health, mental health issues, and exacerbated respiratory and cardiovascular conditions (Stanke et al., 2013). Socioeconomic impacts result from unemployment and reduced incomes, decreased productivity, and increased cost of living (Ding et al., 2011). Droughts are also linked to environmental consequences, such as heightened disease transmission, elevated dust levels, and reduced flow to water reservoirs (Ding et al., 2011; Stanke et al., 2013). Environmental impacts of droughts also include erosion, soil degradation, and loss of biodiversity (Qiu et al., 2021).

1.22 Characteristics and Impacts of Heatwaves

Heatwaves are defined as prolonged periods of unusually high temperatures, which can exceed normal ranges for humans and natural systems and cause heat stress (Sherwood & Huber, 2010). Heatwaves are a substantial hazard, killing more people globally than any other natural disaster, yet are often overlooked due to a focus on other natural disasters (Argüeso et al., 2015). The recent near-global intensification of heatwaves has been well documented in the literature, with the IPCC's sixth assessment report confirming that anthropogenic climate change has been the primary driver of increased heatwave frequency and intensity across most land regions since the 1950s (IPCC, 2021). The last decade has seen an unprecedented number of heatwaves. Anthropogenic climate change is projected to exacerbate the heatwave crisis in the future.

Consistent with global studies, Australia is expected to experience an increase in heatwave exposure in the future. Argüeso et al. (2015) predict a 2% increase in heatwave frequency and a 2-day extension in duration in NSW in the near future (2020-2039), escalating to a 6% rise and six additional days by the far future

(2060-2079). Trancoso et al. (2020) found that under 3°C warming, heatwave duration could exceed a month, with events up to 85% more frequent by the end of the 21st century. As climate change continues to exacerbate the heatwave crisis, it is crucial for governments to implement mitigation and adaptation strategies, along with emergency response plans, to minimise heatwave impacts and unnecessary fatalities.

Australia is no stranger to heatwaves, with much of the nation having experienced prolonged and significant heatwaves over the last 70 years (Trancoso et al., 2020). Notable events in Australia's history include the 'Black Saturday' heatwave disaster in late January to early February 2009, which was one of the most severe heatwaves since 1939, particularly for TAS, border areas of NSW and southern VIC (Fig 2, Panel A) (Nairn & Fawcett, 2015). This heatwave event had multiple spells of temperatures above 40 degrees Celsius and was associated with widespread power outages, transport disruptions, and a dramatic increase in hospital admissions for heat-related illnesses, with an estimated 432 heat-related deaths in VIC and SA (Nairn & Fawcett, 2015; Perkins-Kirkpatrick et al., 2016). More recently, the 2018-2019 'Black Summer' heatwave was another record-breaking event, impacting WA, the NT, SA, NSW/ACT, and VIC (Fig. 2, Panel B) (BOM, 2019). High temperatures, combined with record rainfall deficits, created tinder-dry fuels and an environment susceptible to heatwaves (Nairn et al., 2021). The heatwaves brought severe respiratory health impacts across NSW and the ACT, including 473 deaths, disproportionately affecting the most vulnerable (Nairn et al., 2021; Zhang et al., 2020). Both of these record heatwave events occurred at the end of significant multi-year droughts (the Millennium and Tinderbox drought) and were accompanied by some of the most devastating bushfire outbreaks in Australia (Perkins-Kirkpatrick et al., 2016).
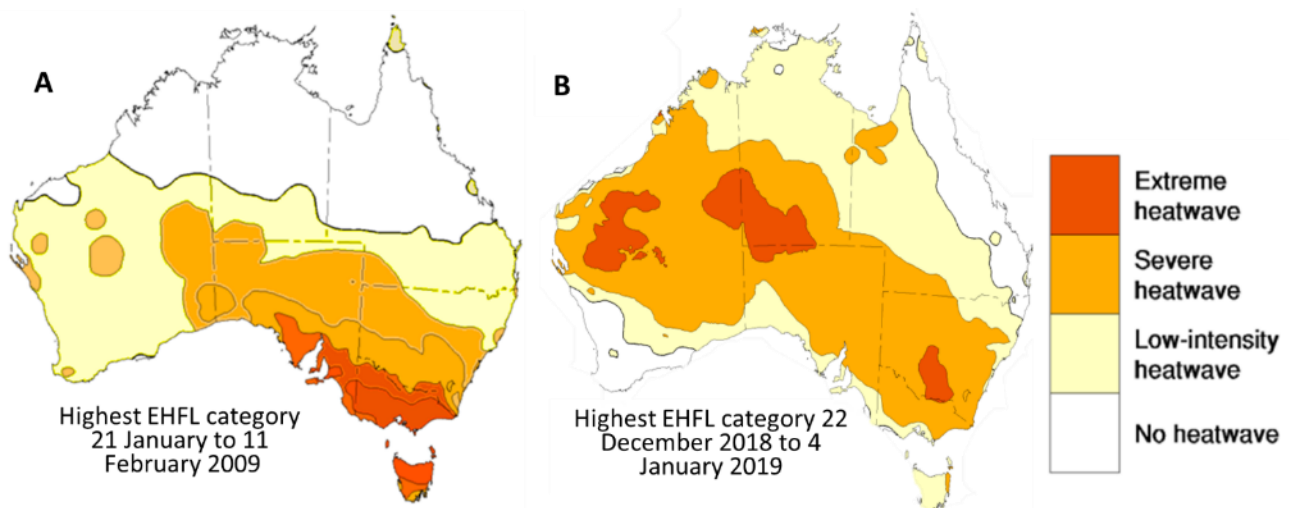
Fig. 2 Australian Heatwaves for A: 2009 Black Saturday and B: 2018-19 'Black Summer' (BOM, 2019)

Heatwaves have a range of significant impacts on society, the environment, and the economy. For example, heat stress in people can result in hyperthermia, where the body absorbs more heat than it dissipates, which can progress to heat exhaustion, heat stroke or death (Maughan, 2012). Heat-related deaths account for 85% of natural disaster fatalities in Australia (Argüeso et al., 2015). High intensity heatwaves are correlated with increased mortality and morbidity, leading to a surge in heat-related deaths, illnesses and demand for ambulances and hospital admissions (Cheng et al., 2021).

Heat stress can also severely damage plants and animals, leading to lowered agricultural productivity and adverse ecological effects (Breshears et al., 2021). In plants, heat stress occurs when a rise in soil and air temperature reaches a threshold, causing permanent harm to the plant's development (Lamaoui et al., 2018). Heat stress directly affects crop yield by shortening the growing season and damaging plant cells (Feng et al., 2019). Unusually high temperatures are not just constrained to the summer and can occur during any season (Perkins & Alexander, 2013). For example, winter heatwaves affect crop growth efficiency, which can significantly impact flowering times and fruit sets, thus affecting the quantity and quality of the harvest (Webb, 2013). The impact of heatwaves on native animals is also devastating, with one study attributing the 2019 Australian heatwave event to 72,000 flying fox deaths, significantly reducing critical ecological functions of pollination and seed dispersal (Welbergen et al., 2008). Aquatic ecosystems are particularly vulnerable, as higher temperatures can lead to lower oxygen levels in water bodies, harming fish and other aquatic life (McArley et al., 2022). Further impacts of heatwaves include increased energy demands and damage to infrastructure, including roads, railways, and bridges (IPCC, 2022).

1.23 Characteristics and Impacts of CDHEs

As discussed in the previous sections, the impacts of droughts and heatwaves are far-reaching across society and the environment; however, CDHEs have additional risks not accounted for when studying hazards individually. During the last two decades, CDHEs have been associated with significant economic losses globally, as illustrated in Fig. 3. For instance, extreme impacts of heatwaves and droughts in summer 2003 Europe cost approximately $7.90 billion in damages and China 2006 cost $3.91 billion (Zengchao Hao et al., 2022). Similarly, in the USA, extreme heatwaves and droughts between 2011 and 2013 incurred a total cost of $60 billion, with half of this attributed directly to crop losses (Feng et al., 2019). Thus, CDHEs pose heightened risks from multivariate and cumulative impacts, necessitating more comprehensive impact and risk assessments. Notably, CDHEs can exhibit impacts across four CE typology classes, leading to catastrophic effects and complicating efforts to disentangle drivers, characteristics, and impacts. The additional impacts from CDHEs for each typology are provided in Table 1.
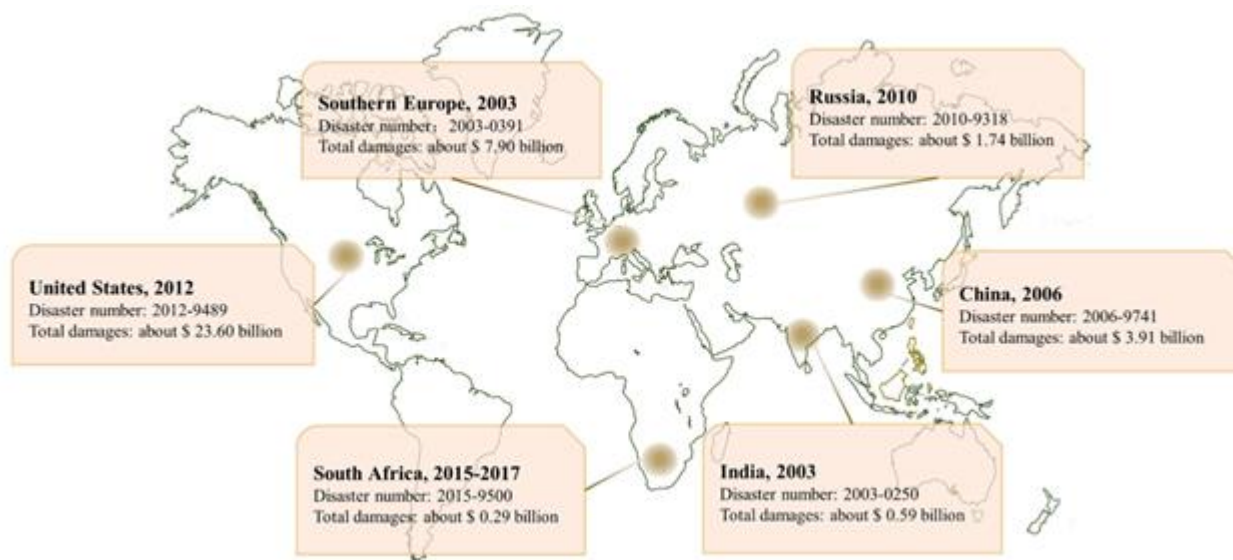
Fig. 3 Cost of Global Droughts and Hot Extreme Disasters (Zengchao Hao et al., 2022)

Table 1. Additional Impacts of CDHEs (Bevacqua et al., 2021; Zscheischler et al., 2020)

Typology	Examples	Impacts
Preconditioned	1. False Spring: Early bud breaks due to temperature anomalies in winter 2. High temperatures and/or droughts lead to growth stress 3. Feedback loops between droughts and heatwaves 4. Droughts due to earlier precipitation and/or soil moisture deficits	Crop yield, reductions in carbon uptake, biodiversity, wildfires
Multivariate	1. Extreme CDHEs (impacted area and/or severity) 2. Long-lasting CDHEs	<u>Extreme cascading impacts</u>: Crop yields, crop failure, larger reductions in carbon uptake, livestock mortality, human health, productivity, supply chain disruptions, economic losses, infrastructure damages, food, water and energy security, recovery efforts, vegetation, biodiversity, wildfires
Spatial and/or Temporal	1. More frequent and/or larger CDHEs 2. Shorter return period of CDHEs 3. Increased exposure and vulnerability from CDHEs occurring in cities and agricultural zones. 4. Impact from CDHEs in the same locations with or without a time lag 5. Increased impact of CDHEs from co-occurring with key crop phenological phases 6. More than one CDHE occurring in various locations leading to synchronous crop impacts	Crop yields, reductions in carbon uptake, livestock mortality, human health, productivity, infrastructure damages, food, water and energy security, recovery efforts, vegetation, biodiversity

The risks posed by CDHEs are particularly severe across the agricultural sector, adversely affecting crop quality and quantity and altering planting, growing, and harvesting times (Zengchao. Hao et al., 2022). CDHEs are widely acknowledged as the most damaging climatic stressors for food crops, resulting in significant global yield reductions (Afroz et al., 2023). This is attributed to the increased physiological damage inflicted by drought and heat stress on crops, compounded by the synergistic interactions between droughts and heatwaves (Zengchao. Hao et al., 2022). Combined drought and heat stress inhibit

photosynthesis and stunt growth during the vegetative stage, slow grain development during the reproductive stage, and shorten the grain-filling period, reducing grain kernel weights and crop yields (Zengchao. Hao et al., 2022). The timing of CDHEs in winter can also trigger early bud breaks in crops, inducing a 'false spring'. This premature growth exposes crops to frost damage when cold conditions return and disrupts the timing of later development, leading to reduced yields (Zscheischler et al., 2020).

The impacts of CDHEs extend beyond crop yields to encompass broader ecosystem effects, including decreased vegetation coverage, impacts on biodiversity, and disruptions to the carbon cycle by reducing plants ability to uptake carbon dioxide (Zengchao. Hao et al., 2022). These complex interactions underscore the multivariate nature of CDHEs, which affect agricultural and natural systems.

On a global scale, there is considerable evidence that the frequency of CDHEs has increased, largely driven by rising high-temperature extremes, as shown in Fig. 4. These events can create cascading socioeconomic impacts, often surpassing those of individual hazards by overwhelming both human and natural systems (Tabari & Willems, 2023). Most communities are ill-equipped to handle multiple hazards simultaneously, increasing recovery times (Ridder, Pitman, & Ukkola, 2022). For example, heatwaves occurring during long droughts exacerbate water scarcity by depleting already diminished water supplies and increasing demand. Growing regions with limited irrigation also suffer disproportionate yield losses due to increased exposure to drought and heat stress (Zengchao. Hao et al., 2022). Global studies indicate that cropland exposure to CDHEs will increase 1.7-1.8 times by the end of the 21st century, posing a major threat to global food security (Afroz et al., 2023). Greater overlap between CDHEs and exposed populations has also been identified, amplifying the health impacts of dehydration and heat stress (Ridder et al., 2020). CDHEs will likely exhibit increased return frequencies in the same regions in the future, placing a further strain on recovery and resources (Afroz et al., 2023).
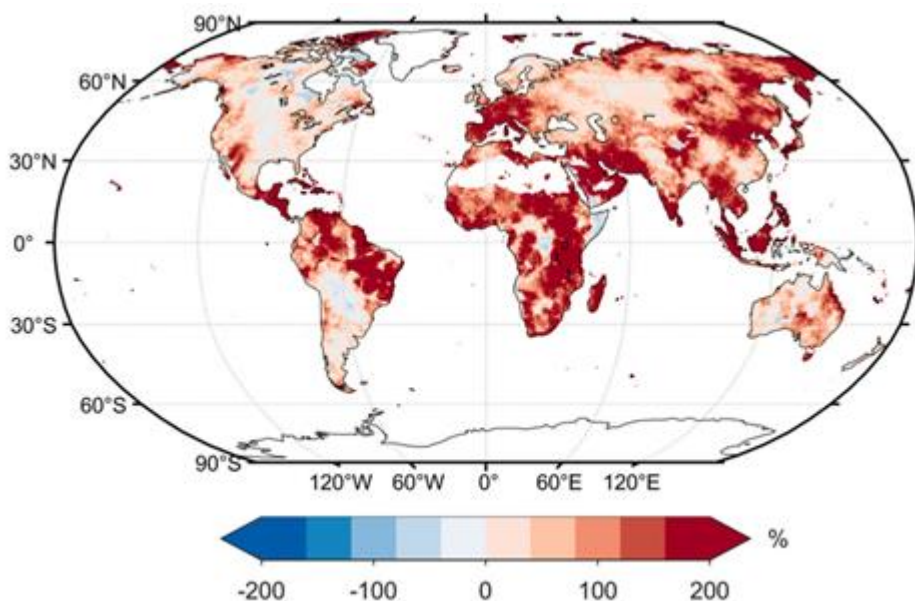
Fig. 4 Change in CDHE Frequency between 1951-1984 and 1985-2018 (Zengchao Hao et al., 2022)

8

Several Australian studies have quantified the spatio-temporal characteristics of CDHEs, and the results agree significant increases in CDHE characteristics have occurred in the last two decades compared to relatively stable historical patterns (Ridder, Pitman, & Ukkola, 2022). Laz et al. (2023) mapped CDHE trends in Southeastern Australia from 1971 to 2021, identifying hotspots in eastern NSW and QLD. The results found over the past two decades, these hotspots have expanded west towards Southeastern Australia. Laz et al. (2023) also identify the recent period 2001-2021 has experienced an increase in CDHEs with heatwaves and moderate drought by 63% in annual frequency and 65% in the 90th percentile extreme. Another study by Reddy et al. (2022) identified spatio-temporal trends of CDHEs Australia-wide from 1958 to 2020. The results indicated positive trends for southeast and west Australia, including increased frequency (3-5 days/season), duration (1.5-2.5 days/season) and amplitude (10-12°C^2/season). Larger and more widespread trends were identified for CDHEs with mild drought.

The vulnerability and risk of CDHEs are closely related to the return frequency in the same location. An assessment in Australia by Ridder, Pitman and Ukkola (2022) modelled the return period of CDHE events using both observational and climate-simulated data and noted that CDHEs returned less than one year for most of Australia and 0.5 years for eastern Australia between 1990 and 2014. Under moderate and high emissions scenarios, the return period of CDHEs increased the most in Northern Australia (0.1 to 0.5 years sooner) and Southern Australia (0.75 and 1 year).

While previous Australian studies have laid a foundational understanding of CDHE risk and its broad effects on society, there is a gap in detailed impact and vulnerability assessments on specific sectors, such as agriculture. Understanding these impacts is essential for implementing effective disaster adaptation and mitigation strategies. As climate change and natural variability amplify the risk of CDHEs, society is confronted with significant challenges in adapting to these changes amidst ongoing population growth.

1.24 Potential CDHE Impacts on Australian Agriculture

Understanding the relationship between climate extremes and crop yields is critical for ensuring food security and mitigating the impacts of CDHEs under a changing climate (Feng et al., 2019). Crop yields in Australia are highly dynamic across regions, with both harvested area and volume produced changing annually (Wang et al., 2015). Cereal crops are important staple crops in Australia, worth 19.31 billion in 2021-2022 (ABS, 2022). Wheat is Australia's highest-revenue cereal crop, making up 13.1 billion of the total revenue (ABS, 2022).

While many studies have referred to crop production and yield interchangeably, this study distinguishes between crop production as the total tons produced and crop yield as the total produced per unit of area (Brás et al., 2021). To provide additional context, Table 2 shows crop production data by State/Territory, offering insights into which regions have the highest levels of agricultural output and may be more affected by yield impacts. Trends in crop production are largely driven by trends in yield (Brás et al., 2021). Most

9

cereal crops are produced in WA (35%) which is the largest producer of wheat (36%), oats (54%) and barley (40%). NSW is the second largest cereal crop producer, dominating the production of rice (99%) and producing moderate amounts of wheat (33%), oats (20%), barley (24%) and sorghum (35%). QLD produces the most sorghum (65%) and lesser amounts of wheat, oats, and barley. SA and VIC are also small wheat, oats, and barley producers. TAS and the NT grow little cereal crops.

Table 2. Percentage of Cereal Crops Grown by State/Territory (ABS, 2022)

State/Territory	Wheat	Oats	Barley	Sorghum	Rice	Total
New South Wales (NSW)	33.20%	19.85%	24.77%	34.96%	99.13%	31.51%
Victoria (VIC)	11.72%	13.48%	15.79%	0.09%	0.24%	12.13%
Queensland (QLD)	6.13%	3.86%	4.29%	64.85%	0.48%	8.31%
South Australia (SA)	13.11%	8.40%	14.92%	0%	0%	12.64%
Western Australia (WA)	35.65%	54.04%	40.05%	0%	0%	35.23%
Tasmania (TAS)	0.19%	0.38%	0.17%	0%	0%	0.18%
Northern Territory (NT)	0%	0%	0%	0%	0.14%	0.002%

The annual variability of State cereal crop production, shown in Fig. 5 clearly demonstrates that WA and NSW experience the greatest magnitude of crop production losses and the most significant year-to-year variability (Kingwell, 2019). Understanding the impacts of yield variability on a regional scale is crucial for maintaining profitable production and productivity as well as developing feasible strategies for climate adaptation (Wang et al., 2015).
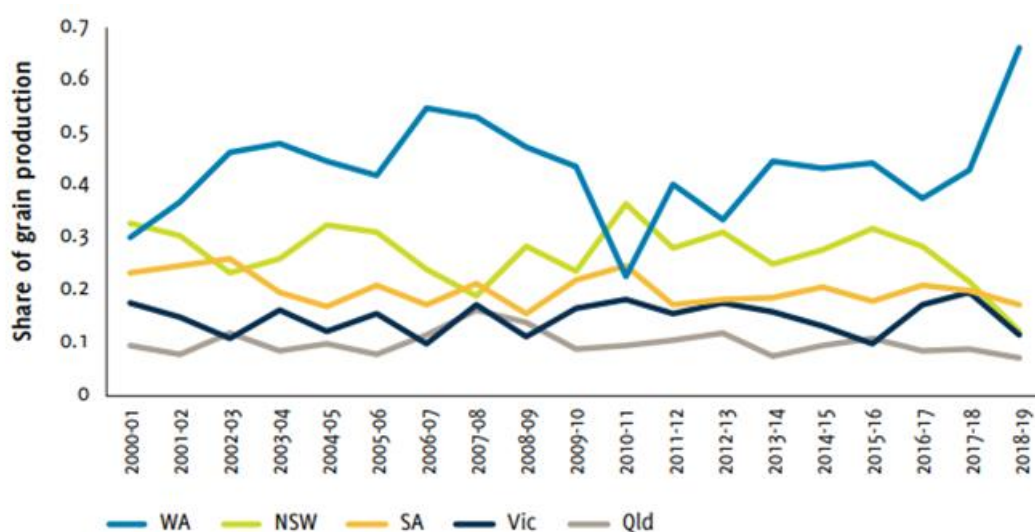
Fig. 5 Australian Grain Production shares by State since 2001-2018 (Kingwell, 2019)

Past research on crop yield and climate interactions in Australia has focused on specific climate hazards. For instance, using multiple linear regression, Hague et al. (2016) investigated the effects of heatwave days, total rainfall, and various climate drivers on wheat yield at the State/Territory level. Their findings revealed that the total rainfall over the preceding 12 months accounted for up to 36% of the variability in wheat yield. However, after removing the effects of rainfall, heatwaves further exacerbated yield loss during August, September, and October. Notably, the detrimental impact of heatwaves on yield intensified during severe drought conditions, suggesting CDHEs have dual effects (though not specifically studied as a CDHE). Wang et al. (2015) conducted a similar regression analysis focusing on maximum and minimum

temperature, rainfall, solar radiation, and the occurrence of heat and frost stress days across four wheat regions in NSW. The results revealed that rainfall did not consistently emerge as the primary factor influencing yield variation across all regions, with the wheat belt's eastern slopes and northern areas exhibiting greater sensitivity to temperature fluctuations. Consequently, identifying dominant variables affecting crop yield varies across different variables, seasons, and locations. While existing research has extensively examined the impact of individual climate hazards on yield, there remains a notable gap in understanding the influence of CDHEs on yield in Australia and characterising the complex spatial, temporal, and climate interaction.

As highlighted in Section 1.23, understanding the risk of compound events is crucial, as it necessitates studying not just the individual hazards but also their combined effects. Developing a new model specifically for the combined effects of heatwaves and droughts on crop yield allows the additional risk to be accounted for. However, this has not yet been done in Australia. Addressing this knowledge gap is essential, given that droughts and heatwaves will become more extreme in the future, drastically increasing risk to the agricultural sector.

1.3 Summary of Knowledge Gaps, Aims and Objectives

The proposed research endeavours to generate significant new knowledge about CDHEs, particularly focusing on their impacts on cereal crop yield in Australian growing regions. A notable knowledge gap has been identified in regional studies within Australia, particularly regarding the assessment of CDHE impacts on agriculture and crop yield. While existing research in Australia has concentrated on conventional single-hazard risk assessments in crop climate impacts, it has overlooked the amplified risks posed by CDHEs. Additionally, there are knowledge gaps in defining CDHEs that specifically impact agriculture and in applying impact assessment methods tailored to these events.

This study aims to quantify the spatio-temporal trends of CDHEs across growing regions in Australia and evaluate the impacts of CDHEs on cereal crop yields. This will be achieved through the following objectives:

1) Explore historical (1910-2022) trends in heatwaves and droughts including frequency, severity, duration, extent, and seasonality Australia-wide and for each growing region
2) Develop a historical (1910-2022) gridded CDHE data set for Australia
3) Quantify gridded spatio-temporal heatwave and CDHE characteristics (frequency, severity)
4) Analyse trends and statistics in CDHEs for each regional growing area
5) Quantify impacts of CDHEs on cereal crop yields using Pearson's Correlation and rank by exposure risk

By addressing these objectives, this study will provide valuable insights into the impacts of CDHEs on agriculture in Australia, facilitating broader climate governance and improved hazard mitigation.

Chapter 2 Data and Methods

2.1 Historical Cereal Crop Yields for Agricultural Growing Regions in Australia

Data for cereal crop production and harvested areas for growing regions in Australia from 1990 to 2022 were obtained from the Australian Bureau of Agricultural and Resource Economics and Sciences records (ABARES, 2023). The crops used for this study include wheat, barley, oats, and sorghum, which were selected due to being grown in multiple regions in different climates in Australia. Yield was calculated by dividing the total crop production (tons) by the sowing area (hectares). The ABARES dataset had no missing production data. However, there were minimal cases of missing sown area values (fewer than 5), which were filled using the most frequently occurring values to ensure valid yield calculations. The yield data was also filtered to remove regions with less than 30 years of data, including non-growing areas in the NT, WA Pilbara, and sorghum regions in Tasmania, South Australia, and Victoria, as regions that did not cultivate the crops for enough years. Regions with at least 30 years of data were used to ensure a sufficiently large sample size for meaningful statistical analysis and to avoid underfitting. Lastly, any years without crop production were flagged as missing for yield, resulting in the final dataset (refer to Table 4). Most selected growing regions contained the full 33 years of yield data. A map of regions is also depicted in Fig. 6.

Table 3. ABARES Growing Regions Data Availability (Orange: Available, Black: Not Available)

1990-2022 Selected ABARES Regions	Abbreviated Name	Wheat	Barley	Oats	Sorghum
1. NSW Central West					
2. NSW Far West				2001, 2020, 2022	
3. NSW North West Slopes and Plains	NSW North West				
4. NSW Riverina					
5. NSW Tablelands (Northern Central and Southern)	NSW Tablelands		2015		
6. QLD Eastern Darling Downs					
7. QLD Southern Coastal - Curtis to Moreton	QLD Southern Coastal		2019	2002, 2007	
8. QLD Western Downs and Central Highlands	QLD Western Downs				
9. SA Eyre Peninsula					
10. SA Murray Lands and Yorke Peninsula	SA Murray Lands-Yorke Pen				
11. SA Northern Pastoral				2015	
12. SA South East					
13. TAS Tasmania					
14. VIC Central North					
15. VIC Mallee					
16. VIC Southern and Eastern Victoria	VIC Southern and Eastern				
17. VIC Wimmera					
18. WA Central and Southern Wheat Belt	WA Central-Southern WB.				
19. WA Northern and Eastern Wheat Belt	WA Northern-Eastern WB.				
20. WA South West Coastal					
	Total Missing	None	2 yrs	6 yrs	none
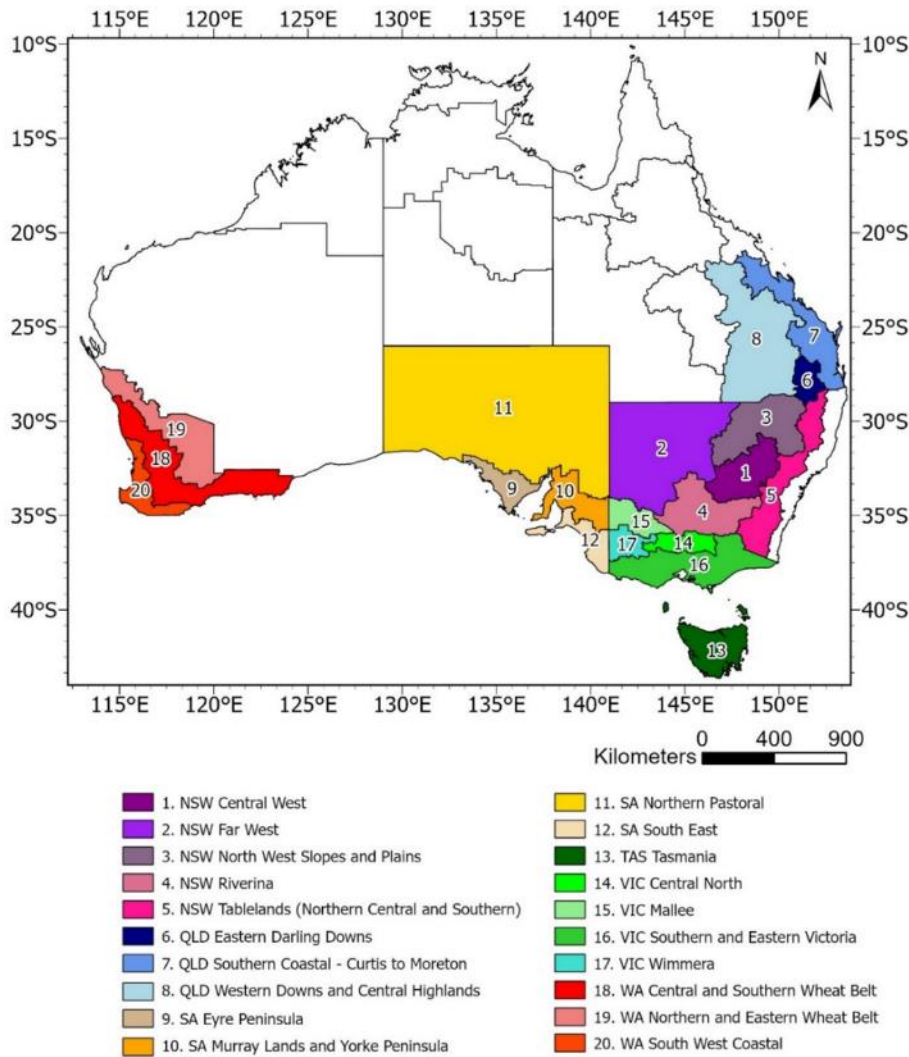
Fig. 6 Spatial Distribution of Selected Australian ABARES Growing Regions

The yield data was detrended consistent with previous studies (Hague et al., 2016; Wang et al., 2015). Detrending removes the influence of confounding effects, such as increasing trends due to technology, leaving only the inter-annual variability. A common approach is to subtract linear regression fitted slopes of each growing region from the yield data. This method was applied to the Australian cereal crop yield data in this study. An example of the effects of the detrending approach on yield is shown in Fig. 7. The raw yield data (brown series) displays an increasing trend which is very common as production increases with demand and improved technologies. However, after subtracting the linear trend, the detrended series has a centre of zero and correctly shows yield anomalies. That is, the detrended series shows yield variation year to year with the influence of other trends removed.
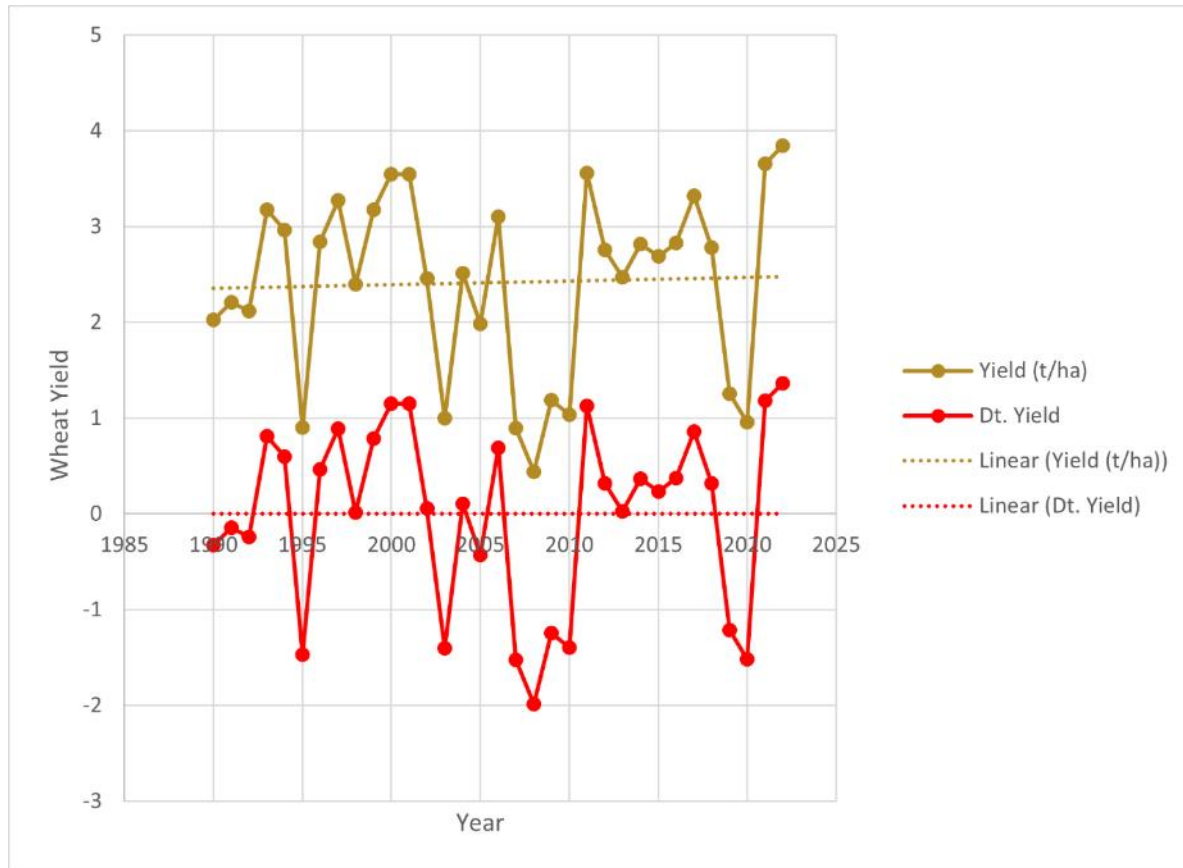
Fig. 7 Example of Detrended Wheat Yield Data for NSW Riverina ABARES Growing Region

2.2 Derivation of Historical CDHE Dataset for Australia

2.21 Measuring and Defining Droughts and Heatwaves

Defining both heatwaves and droughts involves considerable complexity due to varying characteristics and lack of universally observed conditions, leading to several methods (Argüeso et al., 2015; Ndayiragije & Li, 2022). For heatwaves, approaches relying on fixed thresholds, such as the 95th percentile or days exceeding 40 °C, primarily reflect trends in the hottest regions during summer (Perkins & Alexander, 2013). However, this limits the applicability to assessing heatwaves year-round and considering regional climate variations. Dynamic thresholds allow a more detailed understanding of what constitutes an 'extreme event' over time (Perkins & Alexander, 2013). The Excess Heat Factor (EHF) proposed by Perkins and Alexander (2013) has been adopted as the preferred metric and standard Australian heatwave definition, accounting for both the minimum and maximum temperatures and separating short- and long-term temperature anomalies. The EHF involves the accumulation of excess heat over three and 30 days, coupled with the difference between the three-day average and a threshold percentage based on a climatological baseline.

For droughts, there are multiple definitions and indices depending on where water shortages and the resulting impacts discussed in section 1.21. Given that this study concentrates on the impacts of drought on crops, which are primarily associated with agricultural drought, this study will specifically focus on agricultural drought. While the standardised Precipitation Index (SPI) has been used extensively to quantify

drought in CDHE studies, a major limitation is that only precipitation is included in the derivation of the index (Laz et al., 2023; Reddy et al., 2022). To improve agricultural drought attribution, the Standardised Precipitation Evapotranspiration Index (SPEI) and the self-calibrating Palmer Drought Severity Index (sc-PDSI) have been employed in CDHE studies, offering a more comprehensive measure of agricultural drought (Laz et al., 2023; Tripathy et al., 2023). The SPEI incorporates evaporation alongside rainfall (via a temperature relationship) and is useful for delineating short-term drought dynamics (Zhao et al., 2017). However, the SPEI may not fully capture the duration of severe droughts due to its exclusion of hydroclimate factors such as recharge rates, streamflow, runoff, and groundwater dynamics, which significantly influence water availability for crops over longer periods (Ndayiragije & Li, 2022). The sc-PDSI incorporates additional hydroclimate factors, replicating water balance, making it a powerful tool for measuring agricultural droughts over longer periods (Wells. et al.; Zhao et al., 2017).

The derivation of both the heatwave, drought, and combined events (CDHEs) datasets are further detailed in the following sections.

2.22 Drought Dataset

For the drought component of CDHEs, this study utilises pre-processed monthly 0.5° gridded sc-PDSI data from the Climatic Research Unit (2021). The sc-PDSI is based on a water balance model that considers precipitation, temperature, and local soil moisture conditions. It estimates the departure of moisture from normal conditions, which is crucial in determining whether an area is experiencing drought or excessively wet conditions (Wells. et al.). A summary of the composition of the sc-PDSI is shown in Fig. 8 for completeness. Droughts were classified into mild, moderate, severe, and extreme based on the thresholds outlined in Table 5.

Table 4. PDSI/sc-PDSI Drought Classification (Wells. et al.)

PDSI Value	Severity Category
0.49 to -0.49	Normal
-0.50 to -0.99	Incipient Drought
-1.00 to -1.99	Mild Drought
-2.00 to -2.99	Moderate Drought
-3.00 to -3.99	Severe Drought
Bellow -4.00	Extreme Drought
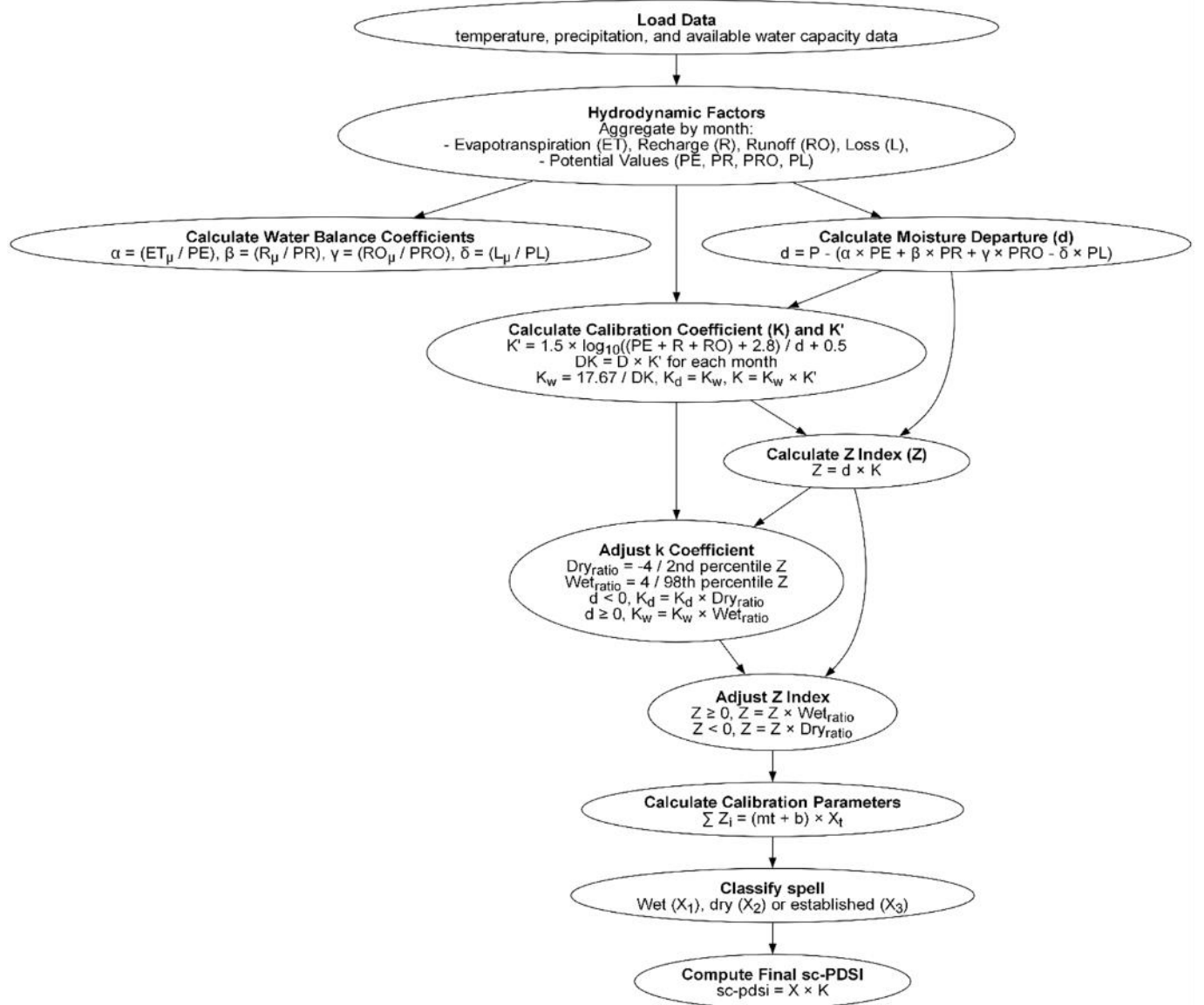
Fig. 8 Flow Chart Methodology for the Self-Calibrating Palmer Drought Severity Index

2.23 Heatwaves Dataset

Previous CDHE studies modified the EHF to consider one- and two-day heatwaves as crop yield is sensitive to short extreme heat (Hague et al., 2016). Therefore, the adapted EHF method was implemented (Hague et al., 2016; Perkins & Alexander, 2013) (refer to Eqn. 1) using 0.05° AGCD gridded temperature data (BOM, 2023) and Python source code from Argüeso (2024).

$$T = \frac{T_{max} + T_{min}}{2}$$

$$EHI_{accl} = (T_i + T_{i-1} + T_{i-2}) - (T_{i-3} + \cdots + T_{i-32})/30$$

$$\mathbf{EHI_{sig}} = \frac{\mathbf{T_i + T_{i-1} + T_{i-2}}}{\mathbf{3}} - \mathbf{pct}$$ Eqn. 1

$$EHF\ (C°)^2 = \max(1, EHI_{accl}) \times EHI_{sig}$$

Heatwave for $EHF \geq 0$

In the above equations, T_{max}, T_{min} and T are the daily maximum, minimum and mean air temperatures, respectively. The variable i represents the day of the year, and pct is the chosen threshold. The 90th percentile of 15-day moving windows for a base period from 1961 to 1990 was chosen as the pct threshold

for heatwaves (as shown in Appendix 1, Fig. i). Using a moving PCT threshold allows unusually high temperatures in cooler months to be classified without being constrained by a higher threshold that may only be crossed during warmer months.

After obtaining the EHF series, the data was re-gridded to match the 0.5° resolution of the sc-PDSI dataset and projected to Australian Albers CRS to ensure spatial consistency in the subsequent metric computations while retaining the original latitude and longitude coordinates as variables for tracking purposes. Using the heatwaves classification system by Nairn and Fawcett (2015), heatwaves were categorised into low-intense', 'severe' and 'extreme' for each day i to assess intensity (refer to Eqn. 2). This is a slight adaptation of the original classification, as computation occurs over each day of the heatwave rather than assigning a single category per event. In this way, a heatwave can be 'upgraded' or 'downgraded' during the event, similar to other natural hazards. Finally, the ABARES region shapefile was used in Python to extract heatwave events for the corresponding growing regions. The procedure for calculating the PCT and EHF with severity classification is depicted in Fig. 9-10.

$$\text{Heatwave Severity} = \begin{cases} \text{Low-Intense,} & \dfrac{\text{EHF}_i}{\text{EHF}_{85}} < 1 \\[2ex] \text{Severe,} & 1 \leq \dfrac{\text{EHF}_i}{\text{EHF}_{85}} < 3 \\[2ex] \text{Extreme,} & \dfrac{\text{EHF}_i}{\text{EHF}_{85}} \geq 3 \end{cases} \qquad \text{Eqn. 2}$$
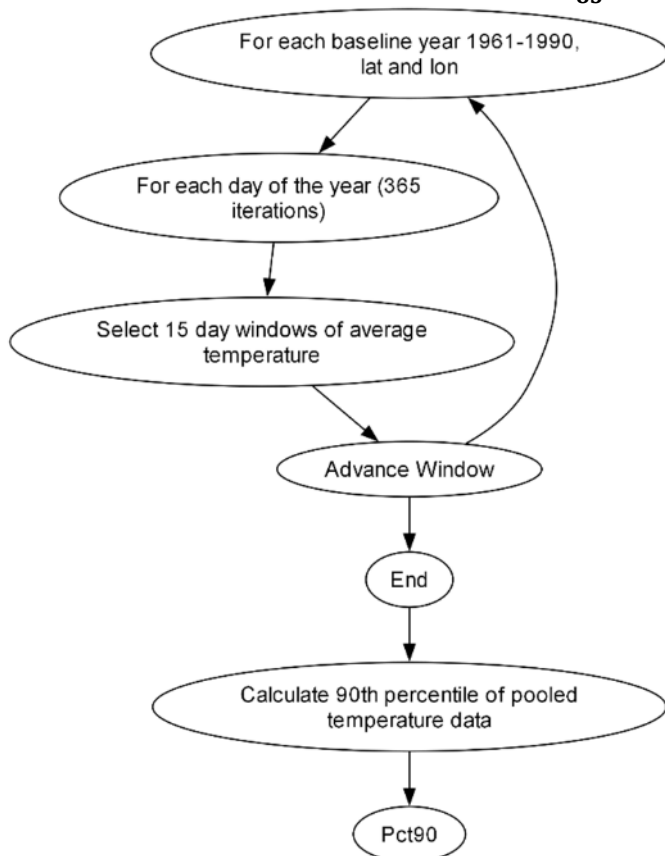
Fig. 9 Flow Chart Methodology for Heatwave PCT Threshold
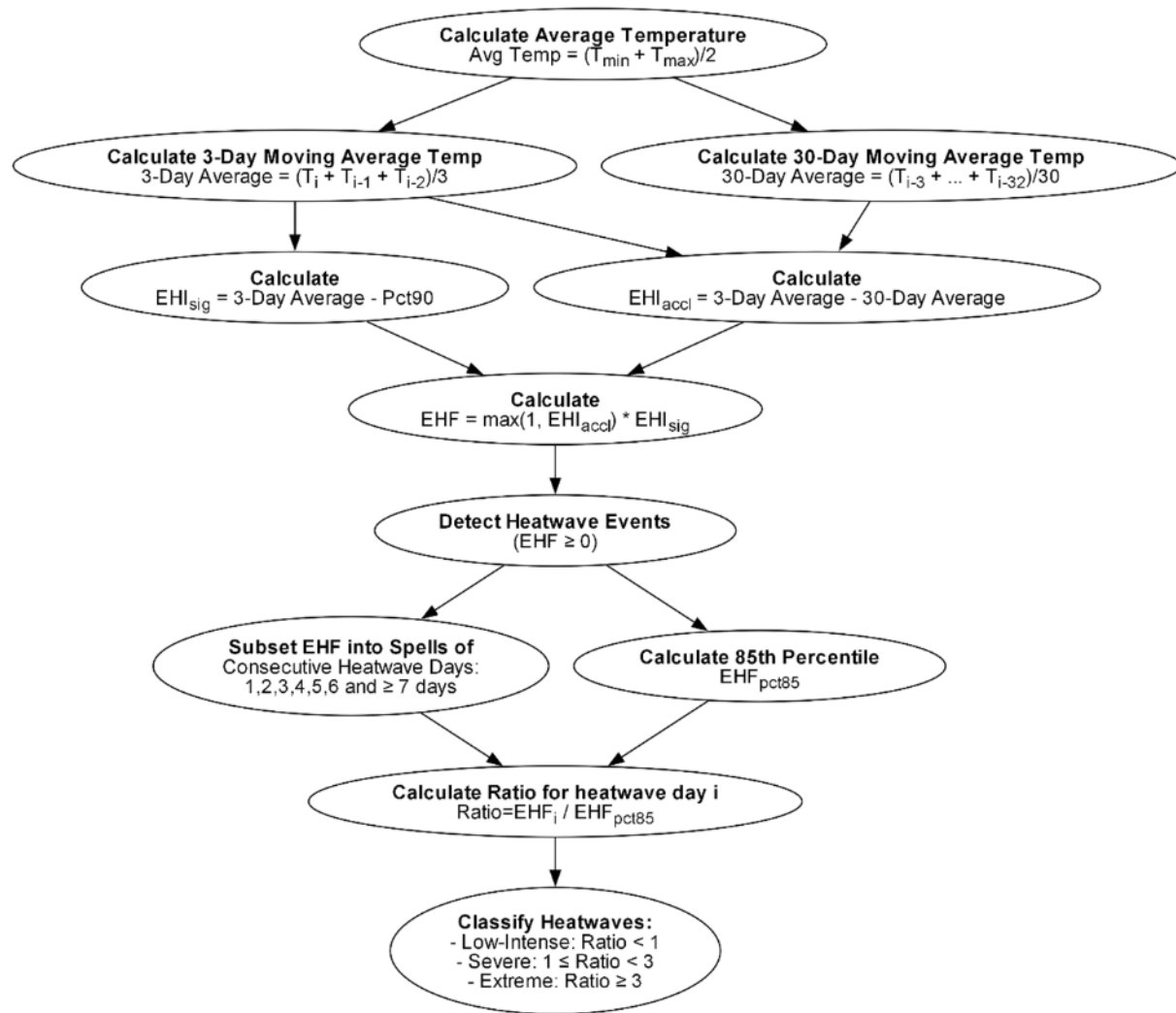
Fig. 10 Flow Chart Methodology for EHF and Severity Classification

2.24 CHDE Dataset

CDHEs in this study are defined as instances where heatwaves and drought conditions occur at the same time and location. To achieve this, the monthly sc-PDSI drought time series data was filtered to values ≤ -1 (corresponding to mild drought and below) to remove non-drought events. The data was then reprojected to Australian Albers CRS and resampled to daily (by simply assigning the same monthly value of sc-PDSI to each day of the month) to align with the heatwave's timescale. To find the joint occurrence of droughts and heatwaves, the classified EHF data was flattened into a csv, where each row contained the event attributes, including the time (date), location (latitude, longitude), ABARES region, severity, and EHF (see Fig. 11, Panel A). Next, heat events for each severity group were summarised by the start date, end date, and duration using R code (see Fig. 11, Panel B). A similar process was applied to droughts, reshaping the sc-PDSI into a flattened csv by coordinates and severity classification. The drought data was matched to the daily heatwave data, ensuring that only the overlapping events were included, while events with just drought or just heatwave were excluded. To calculate the daily CDHE magnitude, the sc-PDSI values were first multiplied by a negative one (to reverse the scale so drought intensity is positive) and then multiplied by the EHF values. This ensures that the resulting magnitude is always positive, reflecting the intensity of the combined events.

Next, CDHEs were categorised into 12 different heat and drought combinations, from extreme drought and extreme heatwave to mild drought and low-intense spells. For both heatwaves and CDHEs, each day was assigned two tags containing the coordinates, a unique event ID tracking each event group, and a multi-day ID tracking the specific event day. The event ID was also used to classify heatwave and CDHE days into seven duration categories including 1 day, 2 days, 3 days, 4 days, 5 days, 6 days, and ≥7 days (see Fig. 11, Panel C). The CDHE duration was also calculated for all CDHE events together, so the total length could be assessed separately.

A

Lat	Lon	Time	ABARES Region	Severity	EHF
-43.25	146.25	25/03/1910	TAS Tasmania	low intense	1.74
-43.25	146.25	25/05/1910	TAS Tasmania	low intense	0.02

B

Lat	Lon	Start date	End date	Duration	ABARES Region	Severity
-27.75	150.75	11/10/1922	14/10/1922	4	QLD Eastern Darling Downs	severe
-28.25	151.75	12/10/1922	12/10/1922	1	QLD Eastern Darling Downs	severe

C

Multi day ID	Event id	Event D	Duration	ABARES R.	CDHE cat	EHF	scpdsi	CDHE mag
2017-11-22-1-2017-11-23_-43.25_146.25	2017-11-22-2-2017-11-23_-43.25_146.25	1	2 days	TAS Tasmania	Extreme HW - Extreme Drought	37.83	-4.07	153.99
2017-11-22-2-2017-11-23_-43.25_146.25	2017-11-22-2-2017-11-23_-43.25_146.25	2	2 days	TAS Tasmania	Extreme HW - Extreme Drought	41.14	-4.07	167.46

Fig. 11 Sample of processed datasets for A: Heatwave Daily Events Summary, B: Heatwave Event Summary and C: CDHE Daily Events

2.25 Heatwave and CDHE Metrics

From the daily heatwave and CDHE data, metrics were calculated to characterise the temporal variability of heatwaves and CDHEs, including frequency, intensity, and impact measures (refer to Table 6). These were analysed over a range of spatial scales, from the smallest level of a grid cell through to Australia-wide.

The following definitions and methods were used to generate these metrics:

Spatial scales

- *Gridded*: Includes heatwaves and CDHEs for each coordinate (0.5° resolution)
- *Australia-wide*: This includes all heatwaves and CDHEs in Australia
- *ABARES Regions*: Includes all heatwaves and CDHEs with the centre of the cell inside the region boundary
- *Area (number of cells)*: Per number of cells in a region calculated as $Area\ Region\ (sqkm)/Cell\ Area\ (sqkm)$

Temporal Scales

- *Calander year:* Standard January to December dates.
- *Heatwave Year*: Years and days adjusted between July and June to keep summer events together
- *Growing Years and Days*: The months of the year when crops are typically grown are recorded in the year of the first harvest (marketing year).

Techniques

Regional Aggregation: Region aggregations (Australia-wide and by ABARES Regions) for heatwaves and CDHEs by calendar year, month, and growing period were performed using Python, where each grid cell centre was matched with the boundaries of the shapefile for each region.

Heatwave and CDHE Seasonality Year Adjustment: To calculate the first heatwave and CDHE event of the year, the day of the year was re-centred to align with heatwave years (July to June). Each day was represented as an integer, starting from July 1 as day one and continuing to June 30 of the following year. This ensured that summer events were not split across different years. As a result, the adjusted years 1909 (part of 1910) and 2022 (part of 2023) were excluded due to incomplete data.

Growing year adjustment for Heatwaves and CDHEs: The impact of CDHEs is likely to be the greatest during the growing season of the crop (Hague et al., 2016). Crop production from ABARES is recorded by the marketing year for consistency (when harvesting begins) and includes the full growing cycle from sowing (typically Autumn for winter crops and spring for summer crops) to the end of the harvest (ABARES, 2023b). Since exact growing periods were unavailable, typical planting months up to the end of the marketing period were used to approximate the growing cycle for each crop for aggregation, including:

- **Wheat**: April - October
- **Barley**: May - November
- **Oats**: March - November
- **Sorghum**: September - March

Consequently, in the CDHE growing season aggregated metrics for sorghum, the year is shifted to be aligned with the harvest year (e.g., the 2022 harvest year includes data from September 2021 through March 2022).

Table 5. Definition of Heatwave and CDHE Metrics *(Afroz et al., 2023; Reddy et al., 2022)*

	Metric	Description	Units
Gridded	**Daily**		
	CDHE Days	$D = \begin{cases} 0 \; if \; no \; CDHE \\ 1 \; if \; CDHE \end{cases}$	Boolean
	Daily CDHE Magnitude	$(-scPDSI_j)EHF_i$ $i = day; j = corr \; month$	°C² per day
	Heatwave Duration CDHE Duration	$diff_i = event_{day_{i+1}} - event_{day_i}$ $D = \begin{cases} 1 \; if \; diff_i \neq 1 \\ T_{end} - T_{start} + 1 \; if \; diff_i = 1 \end{cases}$	Event Length (days)
	Yearly		
	Heatwave Frequency CDHE Frequency	The sum of heatwave days The sum of CDHE days	Days/year
	CDHE Severity	The year sum of CDHE magnitude	°C²/year
Australia-wide	**Daily**		
	% Area Event (Heatwaves, CDHEs)	$\dfrac{Event \; Days}{Cells \; [Area]} \times 100$	% Area per day
	Yearly		
	Total % Area Event (Heatwaves, CDHEs)	$\sum_N \dfrac{\% \; Area \; Event}{365}$	% Area/yr
	Total CDHE Severity	$\left(\dfrac{\sum_N CDHE \; Severity}{Cells \; [Area]} \right)$	°C²/Area Cells per year
	Total CDHE Frequency	$\dfrac{\sum_N CDHE \; Frequency}{Cells \; [Area]}$	Days / Area Cells per year
ABARES Regions	**Yearly**		
	Heatwave Timming (HWT)	Day of the year (1-365) of the first heatwave	Heatwave year day
	Yearly, growing period and Monthly		
	Regional Heatwave Severity (EHF)[1]	$\left(\dfrac{\sum_N Total \; EHF \; (°c^2)}{Cells \; [Area]} \right)$	$°c^2/Area \; Cells$ per year, month, and growing period
	Regional CDHE Severity	$\left(\dfrac{\sum_N Total \; CDHE \; Severity \; (°c^2)}{Cells \; [Area]} \right)$	°C² / Area Cells per year, month, and growing period
	Regional Heatwave Frequency Regional CDHE Frequency	$\dfrac{\sum_N Event \; Days}{Cells \; [Area]}$	CDHE Days/Area Cells per year and growing period
	Regional Total Heatwave % Area Regional Total CDHE % Area	$\sum_N \dfrac{\% \; Area \; Event}{time \; (days)}$	% Area per year and growing period

[1] Some results for Regional Heatwave Severity have been expressed in the previous unit of °C²/Ha

2.3 Methods for Part 1: Spatio-temporal Trends in Heatwaves

Heatwave and CDHE metrics from 1910 to 2022 covering all of Australia and specific ABARES regions were visualised using R's ggplot library and ArcPro Software. The goal of this exploratory data analysis was to understand the statistical and spatial distribution of both heatwaves and CDHEs, including their variability, spread, centre, and location of extremes. The results for spatio-temporal trends and statistics in heatwaves are presented in Chapter 3 (Part 1) and CDHEs in Chapter 4 (Part 2). Supplementary figures and data may also be referred to in the results.

2.31 Methods Heatwave Trends and Statistics Australia-Wide

To analyse the composition of the heatwave dataset, frequency and stacked bar charts were used to summarise the proportion of events across severity and duration categories. Violin plots compared the variation among these categories, while a density histogram was employed to assess the frequency of heatwaves as probability density.

To assess spatial trends on the gridded heatwave frequency by heatwave severity and for all heatwave events, the Sen Slope and Mann Kendall p values were calculated using ArcPro's generate trend function. The Sen's slope, also known as the Theil-Sen estimator, is a non-parametric method used for estimating the slope of a trend in a time series and is particularly useful for climate time series where data often exhibit non-linear patterns and contain outliers (Sen, 1968). The Mann-Kendall (MK), also non-parametric, evaluates the significance of the trend, accommodating skewed data (Mann, 1945). Spatial averages between 1910-1999 and 2000-2022 were also calculated to compare the long-term trends in heatwave frequency with the recent period. The average and Sen Slope frequency trends were arranged into a 4X3 panel map using consistent colour scales. This included creating the same colour symbology for both average periods and applying standard deviation classification to the Sen Slope trends. Standard deviation is often used in spatial analysis to highlight how areas with unusually high or low values, as values beyond ±1 standard deviation from the mean (Reveiu & Dardala, 2011).

To investigate temporal variation in heatwaves, time series plots of the spatial extent (% area) were generated, highlighting both the yearly contribution of each severity level and the total, mean and maximum area covered (the yearly mean and maximum area statistics are available in Supplementary Data Table i).

2.32 Methods Heatwave Trends and Statistics by Growing Region

To characterise regional variation and spread, boxplots of both the daily heatwave magnitude (EHF), yearly regional frequency and severity, and duration for each heatwave category and growing region were visualised. A heatmap chart was created to show the extreme regional heatwave severity for each year and ABARES regions, with colours representing quantiles. This approach highlights which regions and years experienced the most extreme events and provides a detailed view of how the frequency of extremes has changed over time. Time series plots of annual area percent coverage were also produced in Supplementary Fig. ii.

2.33 Methods Heatwave Trends and Statistics by Seasonality and Growing Region

To gain a deeper understanding of heatwave seasonality, the distribution of monthly regional heatwave severity from 1990–2022 was examined for each heatwave category using polar plots. These plots effectively display both annual and interannual variations in heatwave patterns. Summary statistics for the average monthly heatwave severity are provided in Supplementary Data Table ii. Trends in the timing of the first heatwave of the year by region and severity were analysed using regression models. The response variable, year (indexed 1–113), was regressed against the day of the year (1–365) for the first heatwave occurrence (HWT), using R's 'lm' function (see Fig. 12). A map showing regional trends where the difference between intercept and slope exceeded 14 days was produced, and the full regression results are available in Supplementary Data Table iii.
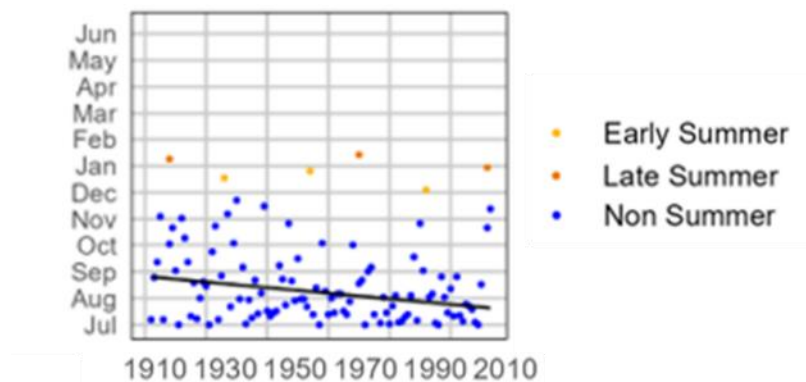
Fig. 12 Example Linear Regression of First Heatwave from July to June in QLD Western Downs

2.4 Methods for Part 2: Spatio-temporal Trends in CDHEs

2.41 Methods CDHE Trends and Statistics Australia-Wide

The composition of the CDHE dataset, across the twelve types, severity, and duration, was analysed using the same methods as for heatwaves, including frequency tables and violin plots. Due to the low frequency of severe and extreme droughts and extreme heatwaves, it was decided to present most of the CDHE results by heatwave category and all events together, which was common in other Australian CDHE studies (Laz et al., 2023). Supplementary figures iii-v include statistics of CDHEs by the respective heatwave and drought categories to complement the results presented.

The time series of yearly CDHE spatial extent (% area) were displayed by heatwave category, along with the mean and maximum daily extent and coverage for all CDHEs (data for the CDHE area statistics is presented in Supplementary Data Table iv). The CDHE severity across the twelve categories and years was also visualised using a heatmap to highlight the range of values of the metric. Finally, Spatial trend analysis of gridded CDHE frequency and severity for all events, including averages between 1910–1999 and 2022, as well as Sen Slope trends and MK significance, was conducted in the same manner as the heatwave analysis.

2.42 Methods CDHE Trends and Statistics by Growing Region

This section included a violin plot of CDHE magnitude as well as a split stacked bar chart comparing CDHE regional frequency between 1910-1999 and 200-2022 using each category. The remaining regional analysis used the total CDHE metrics, including regional boxplots for CDHE daily magnitude, yearly regional frequency and severity, and duration. In addition, supplementary results (fig v-vii) present some complementary boxplots.

2.43 Methods CDHE Trends and Statistics by Seasonality and Growing Region

CDHE seasonality on a monthly scale was examined using the same polar chart structure as heatwaves. Summary statistics for average monthly heatwave severity are provided in Supplementary Data Table v.

2.5 Methods for Part 3: CDHE impact on cereal crops and Yield

Preliminary exploration of the detrended yield data for each crop (wheat, oats, barley and sorghum) was conducted to contextualise variation and the years associated with reduced yields. The regional variability of detrended crop yield was first analysed using boxplots. Time series plots were generated for the wheat growing season, showing CDHE area percentage and severity with markers for years when yield anomalies (below one standard deviation) coincided with CDHE area or severity above the 75th percentile. These visualisations illustrate the relationship between CDHE events and yield fluctuations. Supplementary Data Table V presents a detailed list of years and regions with all crop yield anomalies, along with corresponding CDHE area and severity values. Time series plots of each detrended crop yield and yield anomalies defined in the same way were produced using a positive and negative split bar chart. Additionally, a bubble chart was used to show the frequency and magnitude of all yield anomalies by region, year, and type. Finally, to assess the strength of the relationship between CDHEs and yield, pair-wise Pearson's correlations between the regional CDHE severity and area across the growing season and detrended yield was conducted for each crop. Supplementary Fig. vii displayed the total yield anomalies by year and region.

Chapter 3 Results Part 1: Spatio-temporal Trends in Heatwaves

This chapter presents the findings from the analysis of heatwave trends and statistics (Part 1). The trends and statistics in compound drought-heatwave events (CDHEs) will be explored in Chapter 4 (Part 2), and the relationship between these events and cereal crop yields will be discussed in Chapter 5 (Part 3).

3.1 Heatwave Trends and Statistics Australia-Wide

The frequency of heatwaves varies considerably across duration and severity level. Duration was calculated for each heatwave category separately to assess each individually. In Fig 13, Panel A shows that the most frequent events are short-duration (1–3 days) and mid-to-long duration (≥4 days) low-intense spells, comprising 50.68% and 34.32% of events, respectively. This aligns with findings of Nairn et al. (2018) which reported 85% of heatwaves in Australia, defined using the EHF, are low-intense spells. Severe heatwaves account for 12.95%, with 1–3-day events making up 9.97% and ≥4-day events contributing 2.98%. Extreme heatwaves are the least common, representing 2.07% of events. Panel B, focusing on duration alone, reinforces that 1- and 2-day heatwave events are the most common, followed by mid and long-duration events. Panel C also shows a similar pattern in the severity proportion of each duration, with low-intense making up 80-90%, severe around 5-15% and extreme <5%. Overall, shorter heatwave events are most prevalent, however, longer events still make up a notable portion. There is also a high presence of extreme short events, supporting their inclusion in this analysis.
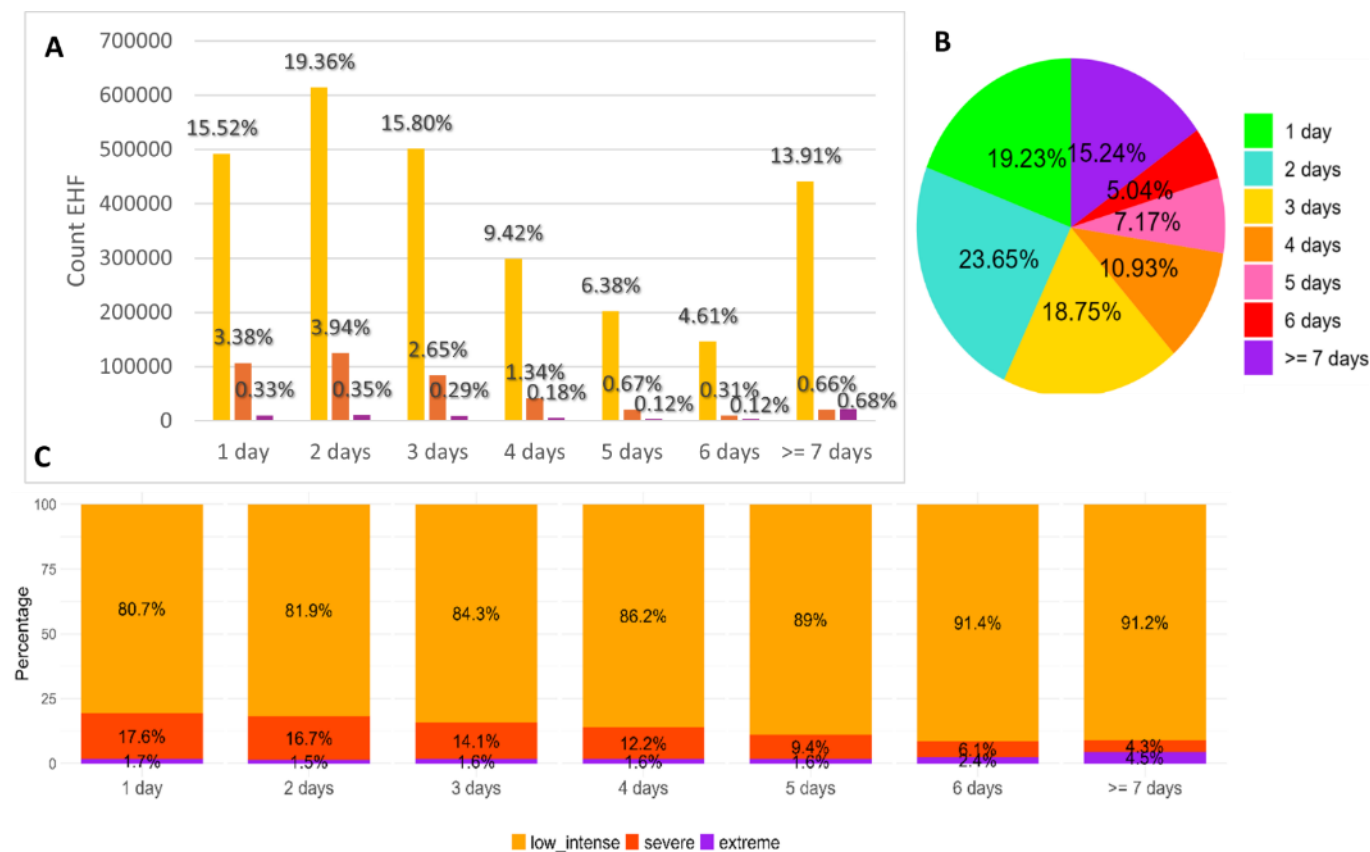
Fig. 13 Percentages of Heatwave Events by Severity and Duration: A: Bar Chart of Group Percentages, B: Pie Chart by Duration, C: 100% Stacked Chart of Heatwave Severity Proportions

Daily heatwave intensity (represented by the EHF) varies significantly across heatwave severity and duration. The violin plot in Fig. 14 shows that low-intense spells have the lowest variability, with minimal variation across duration, concentrated between 0.6-7 and up to 20. In contrast, severe heatwaves exhibit greater variability, particularly after four days, with a higher spread of EHF values concentrated between 10-30, and exceeding 100 in the 3–5-day range. Severe heatwaves also exhibit a stabilisation pattern where after 6 days, the values decrease. Extreme heatwaves have the highest and most variable daily intensity, with most values between 40-130 and peaking at 297 for heatwaves lasting seven or more days.
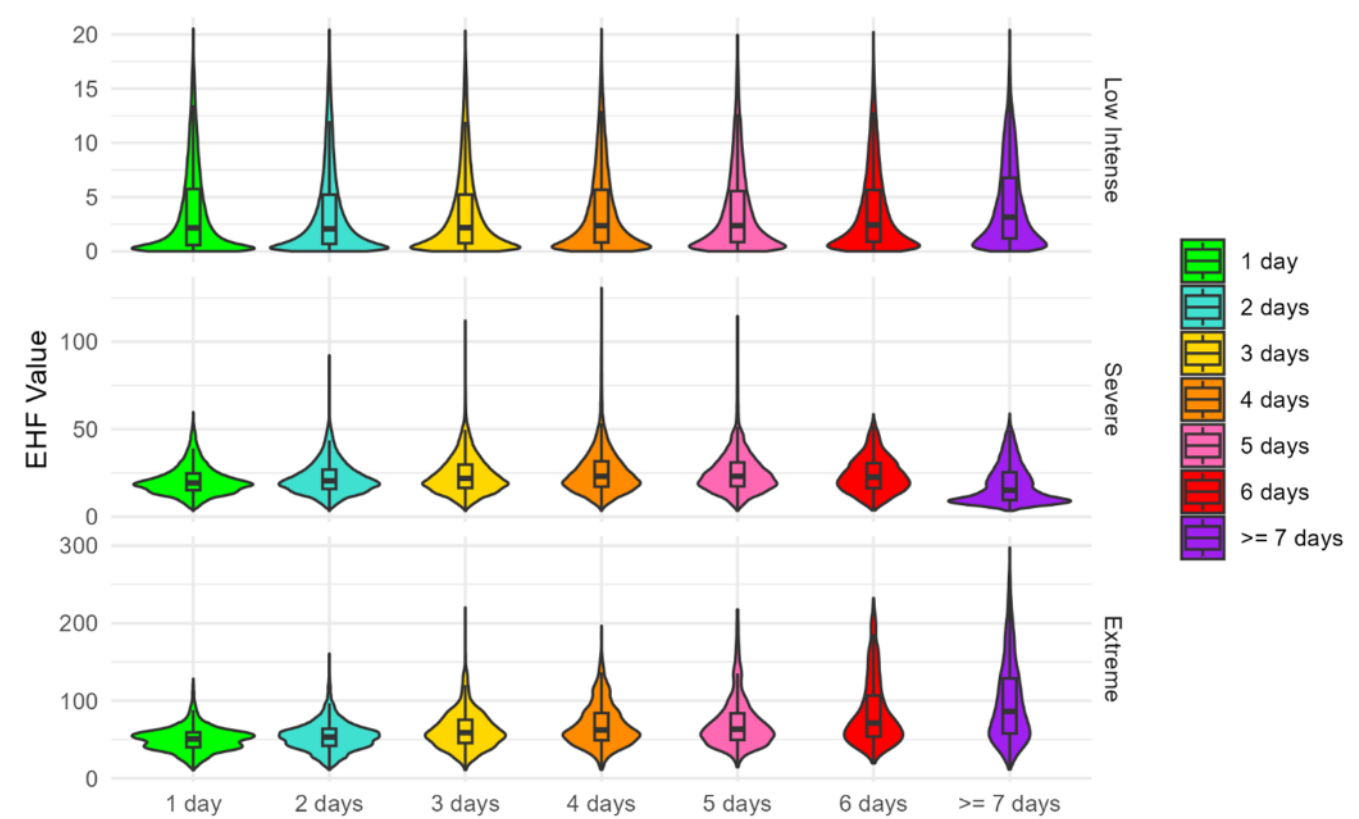
Fig. 14 Violin plot of EHF by Duration and Severity

Fig. 15 illustrates the density histogram of EHF values across different heatwave durations and severities. All panels display right-skewed, Pareto-like distributions, with a wide spread of values above the 90th percentile. The density for low-intense spells remains concentrated in lower EHF values, even as duration increases, suggesting these events don't accumulate extreme values. In contrast, severe and extreme heatwaves exhibit a broader distribution of EHF values, particularly in longer durations. In extreme heatwaves lasting 6 or more days, the 90th percentile threshold rises significantly, indicating a greater likelihood of exceptionally high heatwave intensity in prolonged extremes. The heatwave severity categories effectively partition events, capturing the rising intensity across each level.
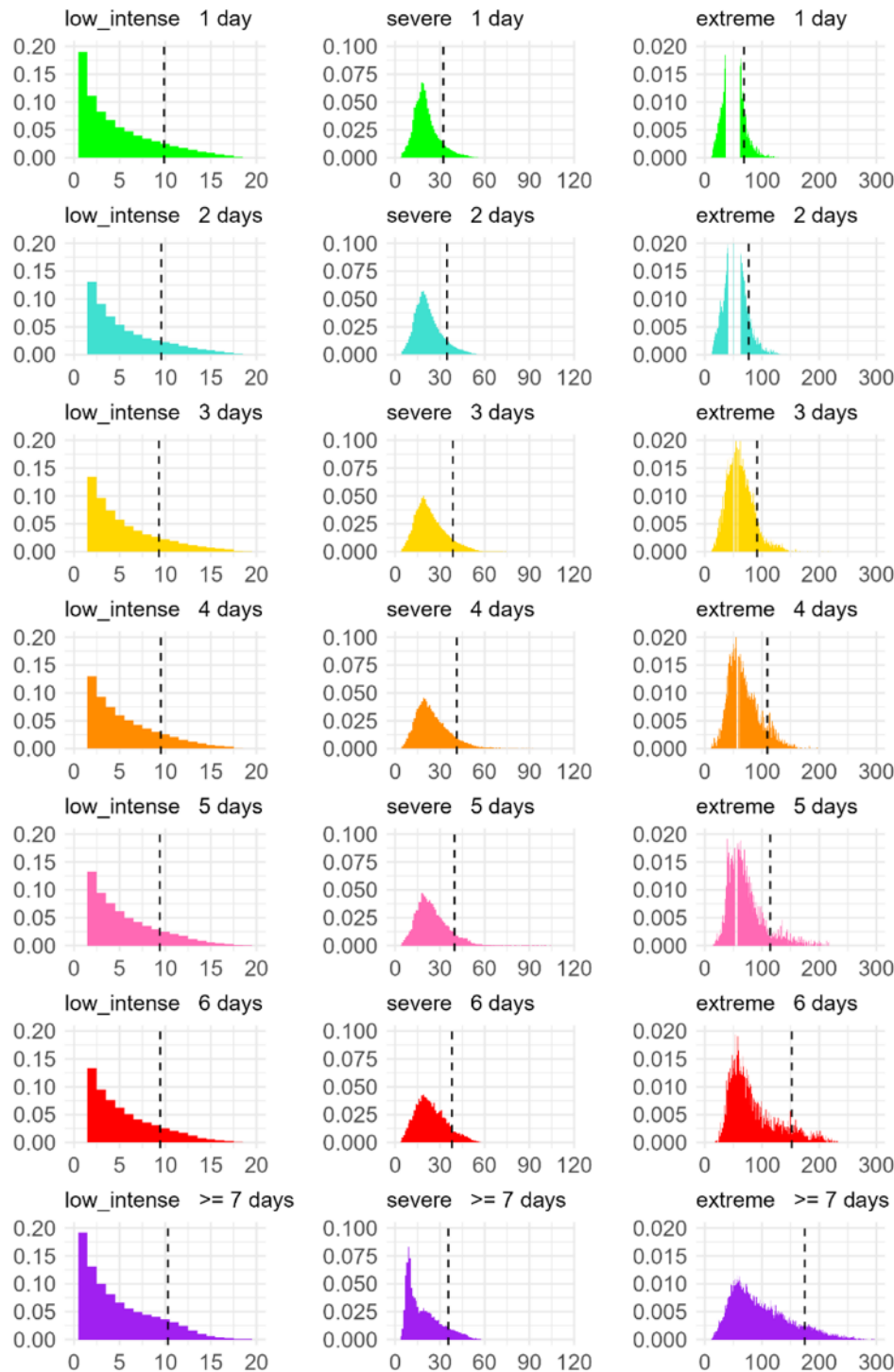
Fig. 15 Density Histogram of EHF by Severity and Duration (dotted line depicts the 90th percentile)

Fig. 16 shows the spatial distribution and trends in heatwave frequency across Australia by severity. The first two columns indicate an increase in mean annual frequency between 1910–1999 and 2000–2022 across all categories. Across all of Australia, the mean frequency of low-intense spells rose from 20 to 42 days (+22 days), severe from 3 to 11 days (+8 days), and extreme from 2 to 14 days (+12 days). Higher heatwave frequencies occur in the upper Northern Territory (NT), Queensland (QLD), and Western Australia (WA), with extreme heatwaves also prominent in NW South Australia (SA). The third column of Fig. 16 shows Sen Slopes indicating statistically significant positive trends for low-intense spells (0.07–1.09 days/year) and severe heatwaves (0.01–0.53 days/year) across most regions, except in parts of the NT and WA where decreases are observed. For severe heatwaves, significant positive trends are less widespread, while extreme heatwaves have too few events for statistical significance. Regions with trends exceeding 2 standard deviations for low-intense spells (0.41–1.09 days/year) and severe heatwaves (0.1–0.53 days/year) are found in central WA, northern NT, and northern QLD. Extreme heatwave frequency trends above 2 standard deviations are higher in magnitude (3.33–12.9 days/year) and are observed in East WA, NW SA, and SW NT.
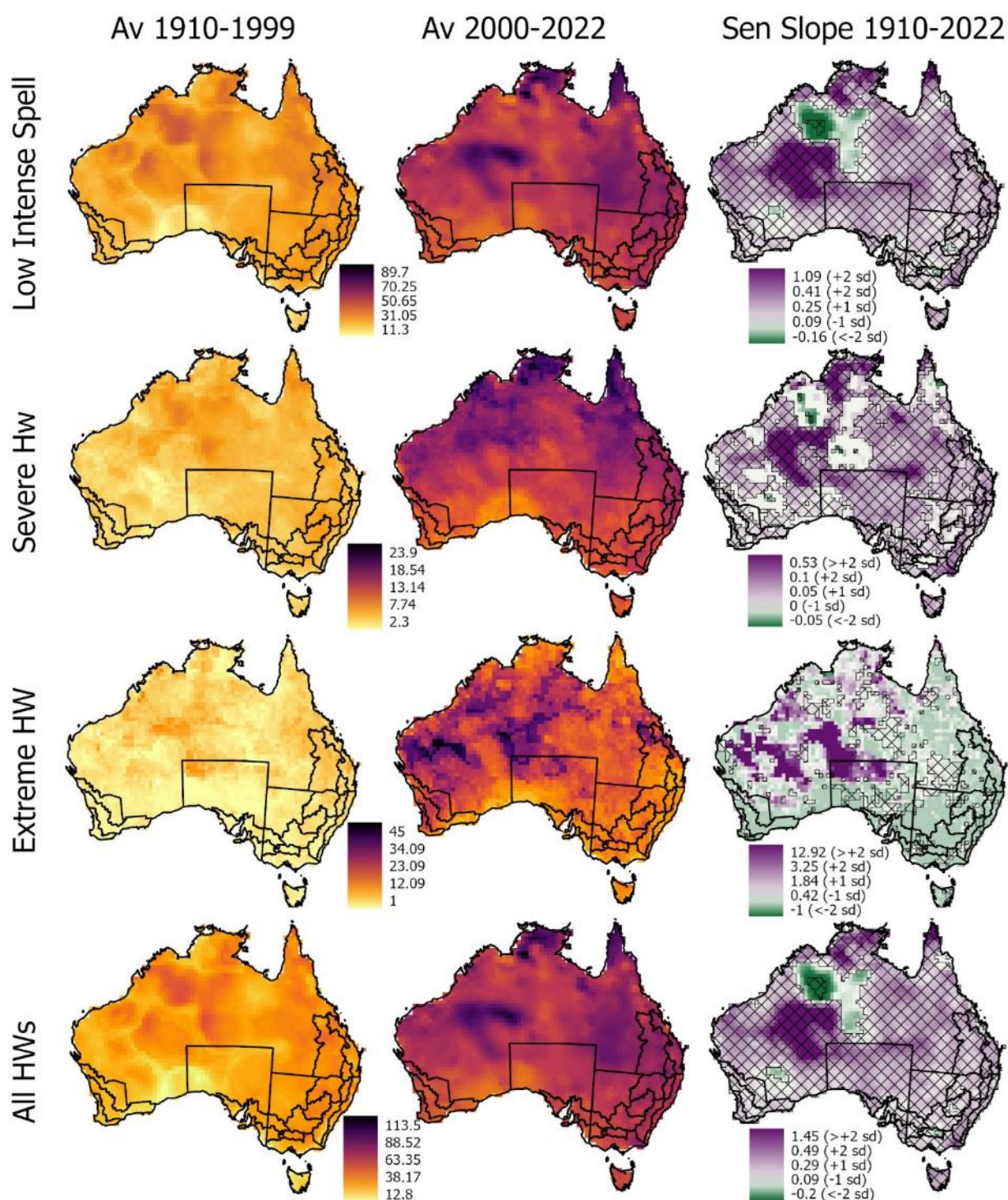
Fig. 16 Heatwave Frequency Trends by Severity

The first two columns show the average gridded heatwave frequency (days/year) from 1910–1999 and 2000–2022 using the same inferno colour scale. The third column displays the Sen Slope trend magnitude, with the Mann-Kendall significance (p < 0.05) overlaid as a mesh. The trend is represented using a purple-green diverging colour scale, where white indicates changes within ±1 standard deviation, purples indicate increases of more than +1 standard deviation, and greens represent decreases of more than -1 standard deviation.

Fig. 17 shows annual trends in heatwave coverage across Australia by severity. Panel A reveals that low-intense spells cover the largest land area, followed by severe and extreme heatwaves. The affected area has notably increased since the 1980s, with peak severe and extreme years in 1940, 1970, 1990, 1995, 1998, 2003, 2009, 2013, 2015, 2017-2019, and 2021-2022. Panel B shows the yearly mean (blue) and maximum single-day coverage (black). In recent years, the mean coverage spiked, peaking in 2019 (23.3%) and again in 2021-2022 (60%). Since the 2000s, more years have exceeded a mean coverage of 20%, indicating more frequent widespread heatwave events. Maximum single-day coverage has also increased, with April 2021 and 2022 reaching near 100%, which was mostly comprised from low-intense spells (97%). Additionally, mid-January 2021 saw an extreme heatwave day cover 97.6% of the land area, marking the highest recorded extent for an extreme heatwave day. Panel C consolidates these trends, showing that recent years frequently experience a yearly coverage between 10-40%.
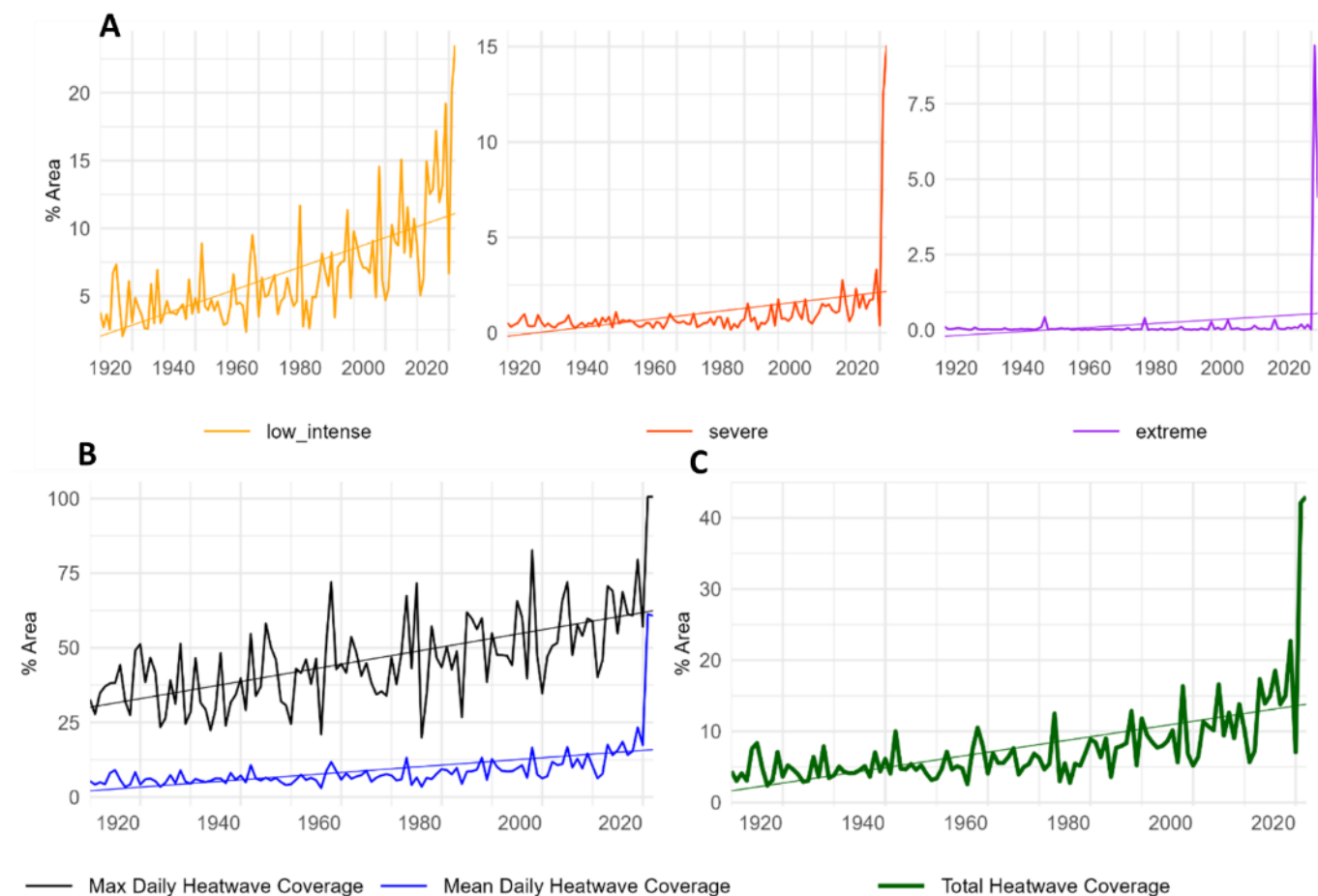
Fig. 17 Yearly Heatwave Coverage (A: Coverage % by Heatwave Severity, B: Max and Mean Daily Coverage %, C: Total coverage %)

Panel A shows the annual area percentage covered by heatwaves separated by heatwave severity on the y-axis, calculated as total heatwave days divided by the total number of grid cells Australia-wide. Panel B illustrates the daily area percentage affected by all heatwaves on the y-axis, with the black line representing the maximum percentage area of a single day and the blue line showing the mean percentage area across all days. Panel C contains the total annual area covered by all heatwaves. Linear trend lines are also displayed on each time series.

3.2 Heatwave Trends and Statistics by Growing Region

This section focuses on the variability of heatwaves across growing regions. Fig. 18 displays the ABARES regional boxplots of daily heatwave intensity (EHF) in Panel A and yearly regional heatwave frequency in Panel B for each heatwave category. For daily heatwave magnitude, growing regions in NSW (1,2 and 4), SA (9-12), and VIC (14,15, and 17) have greater magnitudes of low-intense, severe and extreme heatwaves (indicated by taller boxes and extreme outliers). For severe and extreme heatwaves, WA (18-20) has consistent extremes, however, the boxes are shorter and sit lower in comparison to the regions above. Queensland (6-8) consistently has lower EHF values. This is an expected result since the EHF and heatwave severity is not uniform across Australia, varying with latitude and regional temperature differences. Nairn and Fawcett (2015) note that in southern regions, higher temperatures are required for a heatwave to reach a severe level, whereas in the tropical north, lower temperature excursions can classify as severe heatwaves.

Fig. 18, Panel B reveals variability in heatwave occurrences across regions, with peaks in frequency in certain years appearing as outliers. Low-intense spells are the most frequent, occurring every year across all regions, with frequencies ranging from 1 to 138.25 days per cell, showing significant variability and fluctuations in occurrence. Severe heatwaves are observed in nearly every year (averaging 108 out of the 113-year record), and generally range between 0-6 days per cell but can reach up to 30-40 days per cell in periods of elevated severe heatwave activity. Extreme heatwaves are the rarest, occurring in an average of 47 years in the record, with frequencies primarily consistent across 0-3 days per cell, though occasional outliers reach 15-30 days per cell, highlighting rare periods of extreme heatwave frequency. The variability in both the daily heatwave magnitude and yearly frequency captures diverse heatwave dynamics, with each region experiencing fluctuations in heatwave behaviour.
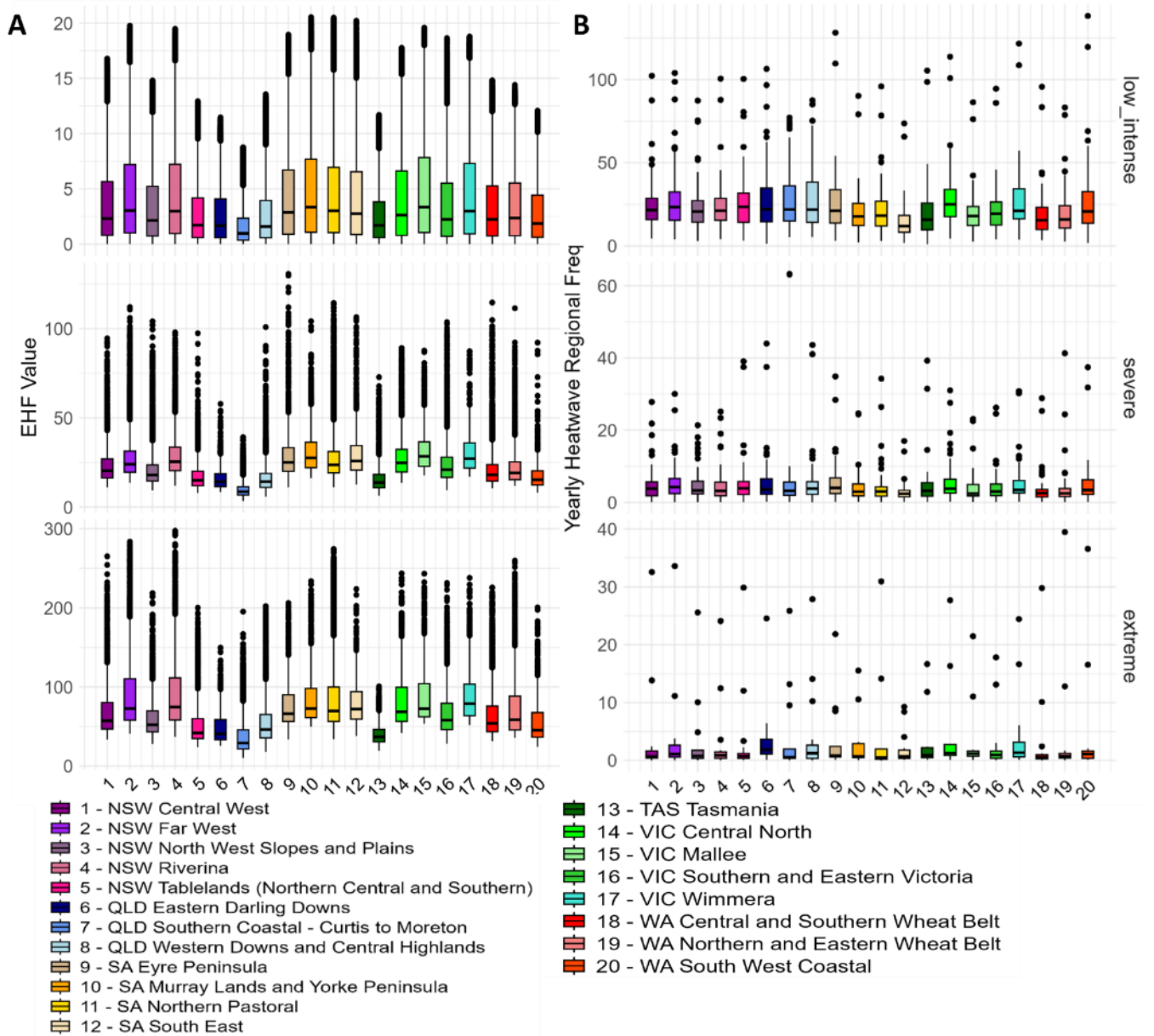
Fig. 18 ABARES Boxplots for A: EHF and B: Yearly Heatwave Regional Frequency

The x-axis lists the regions (numbered 1 to 20), while the y-axis indicates the heatwave daily magnitude (EHF) (A) and yearly heatwave regional frequency (days / area (no. cells))

Fig. 19 shows the ABARES regional boxplots of heatwave duration in panel A and yearly regional heatwave severity in Panel B for each heatwave category. Most low-intense spells have a duration less than 3 days, while longer occurrences between 5-60 days have occurred frequently across growing regions. Severe heatwaves typically range between 1-3 days across regions, while some instances have occurred for 7+ days. Regions 7-8: QLD Southern Coastal and Western Downs, and 5: NSW Tablelands have recorded the longest severe heatwaves, extending from 40-52 days. Extreme heatwaves show the greatest variability in duration, as indicated by the taller boxes and regional variation in outliers. Most extreme heatwaves are between 1-5 days, however, there are a number of extreme heatwaves (outliers) extending past 7 days. The longest extreme heatwaves occurred in region 2: NSW Far West, 3: North West Slopes, and 7-8: QLD Southern Coastal and Western Downs which reached 28-31 days.

Fig. 19, Panel B shows there is variability in the yearly heatwave severity (total EHF) across growing regions. The yearly severity of low-intense spells is typically between 0.32-150 °C² per cell and has peaked at 300-890 °C² per cell in periods of frequent low-intense spells. Regions in NSW (1-5), SA (9-12) and VIC (14-17) have greater variability of low-intense spell severity, as shown by the taller boxes. Values for yearly severe heatwaves mostly fall between 0.2-164 °C² per cell, extending up to 450-1038°C² per cell in years with elevated severe heatwaves. Regions in SA (9,10,11), and VIC (14, 17) reach the highest yearly severity values for severe heatwaves. For extreme heatwaves, yearly severity is mostly within 0.16-100 °C² per cell, however, has peaked at much higher severity between 1000-3000 °C² per cell. The high severity values in each region (outliers) indicate years with the most intense and frequent heatwave events, which varies between regions and fluctuations in heatwave behaviour.
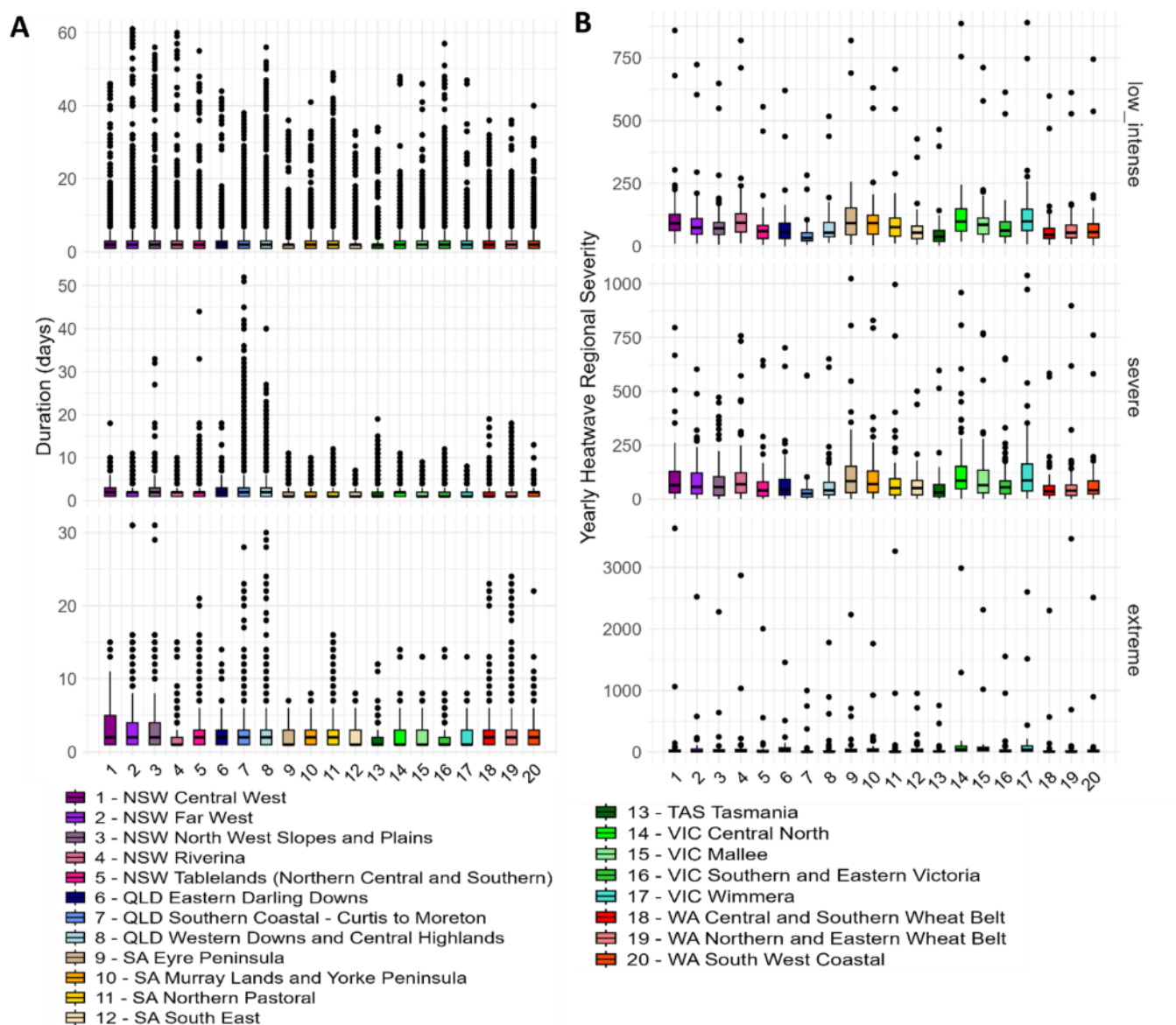
Fig. 19 ABARES Boxplots for A: Heatwave Duration and B: Yearly Heatwave Regional Severity

The x-axis lists the regions (numbered 1 to 20), while the y-axis indicates the heatwave duration in days (A) and yearly heatwave regional severity ($°C^2/area\ (no.cells)$)

Fig. 20 presents a heat map displaying the distribution of extreme heatwave severity by ABARES region and year, represented by thirty-two quantiles. The chart highlights a significant increase in the frequency and spread of extreme heatwave events in recent years, particularly from 2000 onwards, also observed Australia-wide. This is shown by the denser clustering of darker tiles and fewer lighter tiles, most apparent in regions 1-5: NSW, 7-8: QLD Southern Coastal and 11: SA Northern Pastoral. Regions with the highest frequency of extremes include 11: SA Northern Pastoral, 18: WA Central-Southern WB., 7-8: Queensland Southern Coastal and Western Downs, 16: VIC Southern and Eastern, and 5: NSW Tablelands (>60 years). Notably, four record-breaking consecutive extremes from 2021 to 2022 occurred in regions 2: NSW Far West (179.3), 14: VIC Central North (163.3), 11: SA Northern Pastoral (161.3) and 19: WA Northern-Eastern WB. (158.5). The top 5 severity tiles summarised in Table 7 further details the year and region records. The regional data also supports the increasing heatwave area coverage, with all growing regions experiencing an increase in the area affected by heatwaves (see Supplementary Fig. ii).
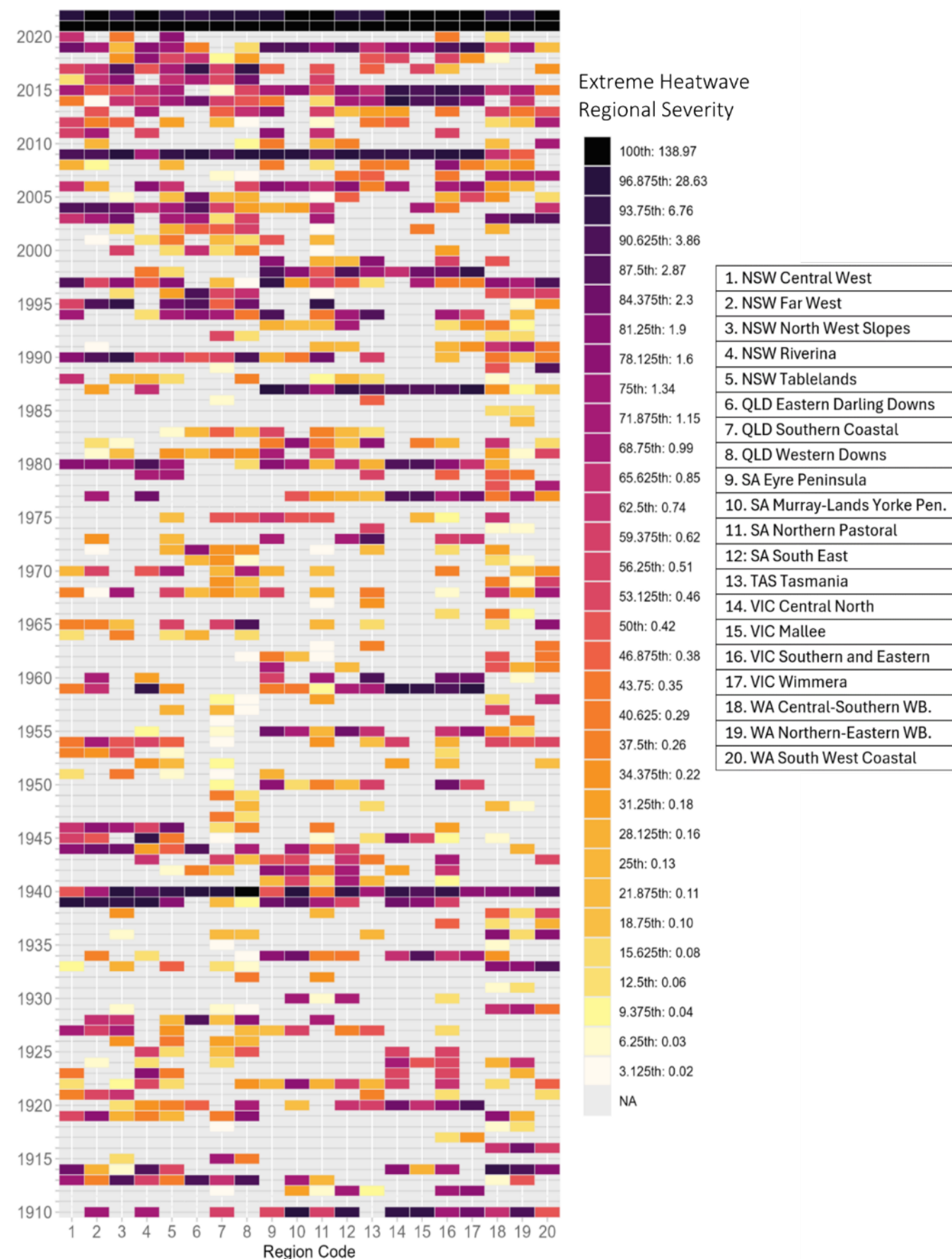
Fig. 20 Heat map of Extreme Heatwave Severity by ABARES Region and Year

The x-axis represents ABARES regions (numbered 1 to 20), while the y-axis shows the calendar years. Tile colours correspond to the yearly regional heatwave severity for extreme events, measured in °C²/ha, divided into 32 quantiles. Blank grey tiles indicate regions and years with no extreme heatwave events.

Table 6. Extreme Heatwave Records by Year and ABARES Region (consecutive records coloured)

Year			
1940	8: QLD Western Downs (34)	7: QLD Southern Coastal (28.3)	6: QLD Eastern Darling Downs (19.6)
	3: NSW North West (8.7)	10: SA Murray Lands-Yorke Pen (6.8)	16: VIC Southern and Eastern (6.7)
	12: SA South East (4.9)	14: VIC Central North (4.5)	5: NSW Tablelands (4.4)
	15: VIC Mallee (2.7)	4: NSW Riverina (2.7)	20: WA South West Coastal (2.6)
2009	9: SA Eyre Peninsula (22.1)	17: VIC Wimmera (16.6)	12: SA South East (10.8)
	6: QLD Eastern Darling Downs (9.4)	10:SA Murray Lands-Yorke Pen (7.9)	3: NSW North West (7.6)
	8: QLD Western Downs (7.1)	16: VIC Southern and Eastern (6.9)	14: VIC Central North (6)
	5: NSW Tablelands (5.7)	13: TAS Tasmania (4)	15: VIC Mallee (4)
	1: NSW Central West (3.8)	2: NSW Far West (3.6)	11: SA Northern Pastoral (2.8)
	7: QLD Southern Coastal (2.6)		
1987	9: SA Eyre Peninsula (7.8)	17: VIC Wimmera (7.7)	12: SA South East (5.5)
	10:SA Murray Lands-Yorke Pen (3.6)	13: TAS Tasmania (3.6)	16: VIC Southern and Eastern (3.5)
	15: VIC Mallee (2.9)	14: VIC Central North (2.6)	
1939	1: NSW Central West (9.3)	4: NSW Riverina (8.4)	2: NSW Far West (5.5)
	3: NSW North West (3.9)	10: SA Murray Lands-Yorke Pen (3.6)	
1959	17: VIC Wimmera (8.2)	14: VIC Central North (7)	15: VIC Mallee (4.8)
	4: NSW Riverina (4.6)	16: VIC Southern and Eastern (3.4)	
1910	10:SA Murray Lands-Yorke Pen (9.8)	12: SA South East (6.3)	14: VIC Central North (4.2)
	15: VIC Mallee (4)	19: WA Northern-Eastern WB. (3)	
2019	17: VIC Wimmera (5.1)	10:SA Murray Lands-Yorke Pen (3.8)	12: SA South East (3)
	16: VIC Southern and Eastern (2.4)	9: SA Eyre Peninsula (2.4)	
2015	14: VIC Central North (4)	16: VIC Southern and Eastern (3.9)	17: VIC Wimmera (3.8)
	15: VIC Mallee (3)		
1995	11: SA Northern Pastoral (4.4)	3: NSW North West (4.3)	2: NSW Far West (2.8)
	6: QLD Eastern Darling Downs (2.6)		
2014	14: VIC Central North (6.8)	16: VIC Southern and Eastern (3.8)	15: VIC Mallee (3)
2017	6: QLD Eastern Darling Downs (6.2)	8: QLD Western Downs (4.7)	3: NSW North West (2.5)
1914	18: WA Central-Southern WB. (5.3)	19: WA Northern-Eastern WB. (3.8)	4: NSW Riverina (2.5)
1990	3: NSW North West (4.4)	8: QLD Western Downs (3.5)	2: NSW Far West (2.9)
1998	17: VIC Wimmera (4.3)	12: SA South East (3.2)	9: SA Eyre Peninsula (3.2)
1913	6: QLD Eastern Darling Downs (3.8)	8: QLD Western Downs (3.7)	3: NSW North West (2.3)
1997	9: SA Eyre Peninsula (4.3)	20: WA South West Coastal (3.1)	1: NSW Central West (2.4)
1980	4: NSW Riverina (3.3)	15: VIC Mallee (2.9)	14: VIC Central North (2.4)
2004	6: QLD Eastern Darling Downs (2.7)	2: NSW Far West (2.4)	1: NSW Central West (2.3)

3.3 Heatwave Trends and Statistics by Seasonality and Growing Region

This section explores heatwave seasonality by monthly regional heatwave severity and for the timing of the first heatwave of the year (HWT). Polar plots in Fig. 21-23 illustrates in the most recent period (1990-2022), low-intense and severe heatwaves predominantly occur during the Austral summer months (September to March) and are most concentrated in summer, while extreme heatwaves are almost exclusively in summer. Compared to previous years, the recent period has seen a detectable increase in low-intense spell occurrences in February and March, particularly in NSW, SA, and VIC. Similarly, severe heatwaves have increased in February in NSW and December across NSW, SA, and VIC while extreme heatwaves have increased in April and August (refer to Supplementary Data Table ii). Furthermore, the charts reflect that extreme heatwaves are becoming more frequent earlier and later in the heatwave season, indicating a broader shift in extreme climate patterns. This shift suggests that the heatwave season is expanding beyond the traditional summer months, posing new challenges for agriculture as heatwaves start to occur more frequently in spring and autumn.
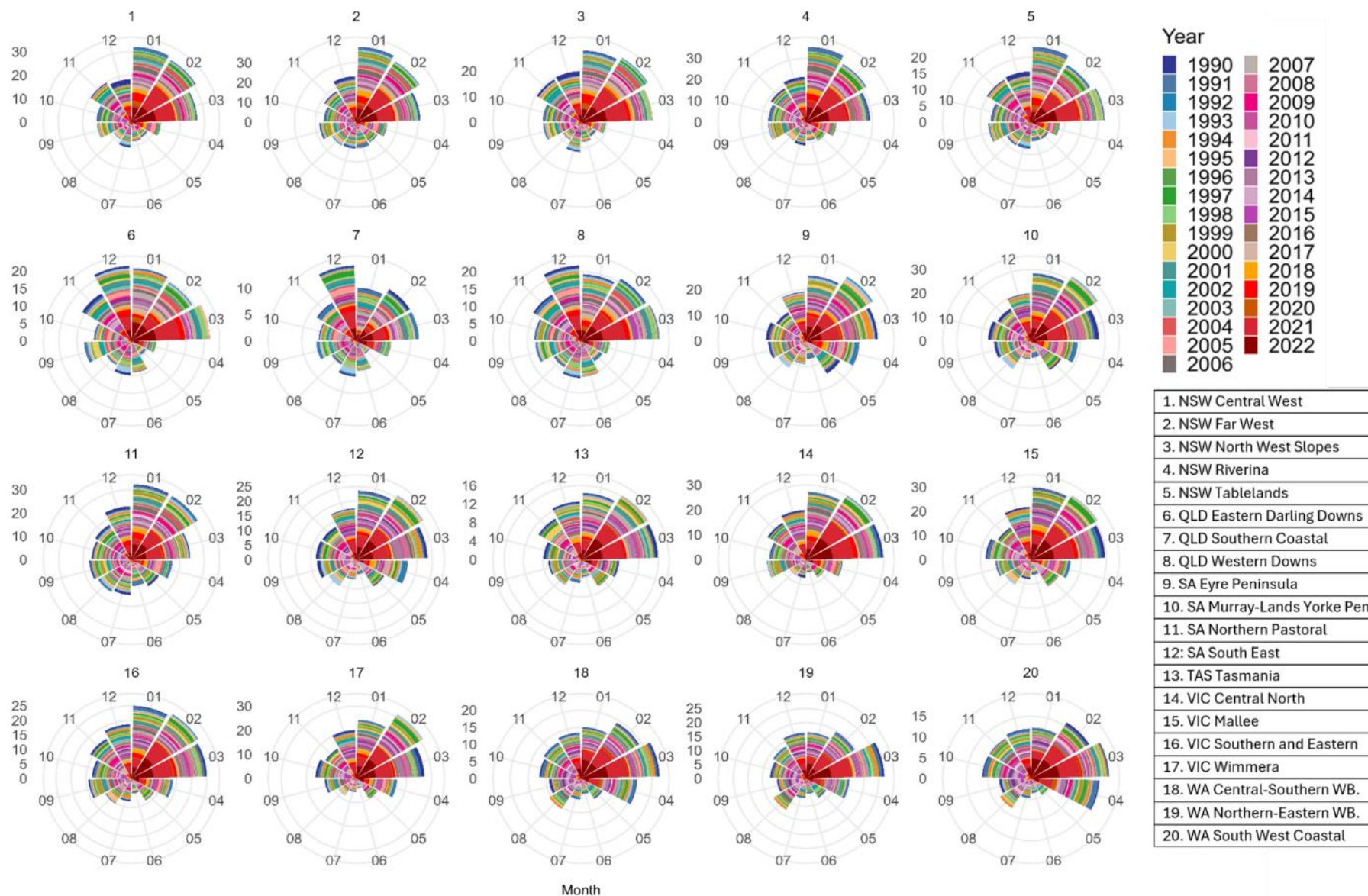
Fig. 21 Polar Chart Low-Intense Monthly Heatwave Severity by ABARES Region

Each polar chart represents a different ABARES region (1 to 20), The quadrants are divided by months, with January (01) at the top, progressing clockwise through December (12). The radial axis shows the low-intense spell severity (°C²/ha). Colours represent different years, ranging from 1990 to 2022, as shown in the legend.
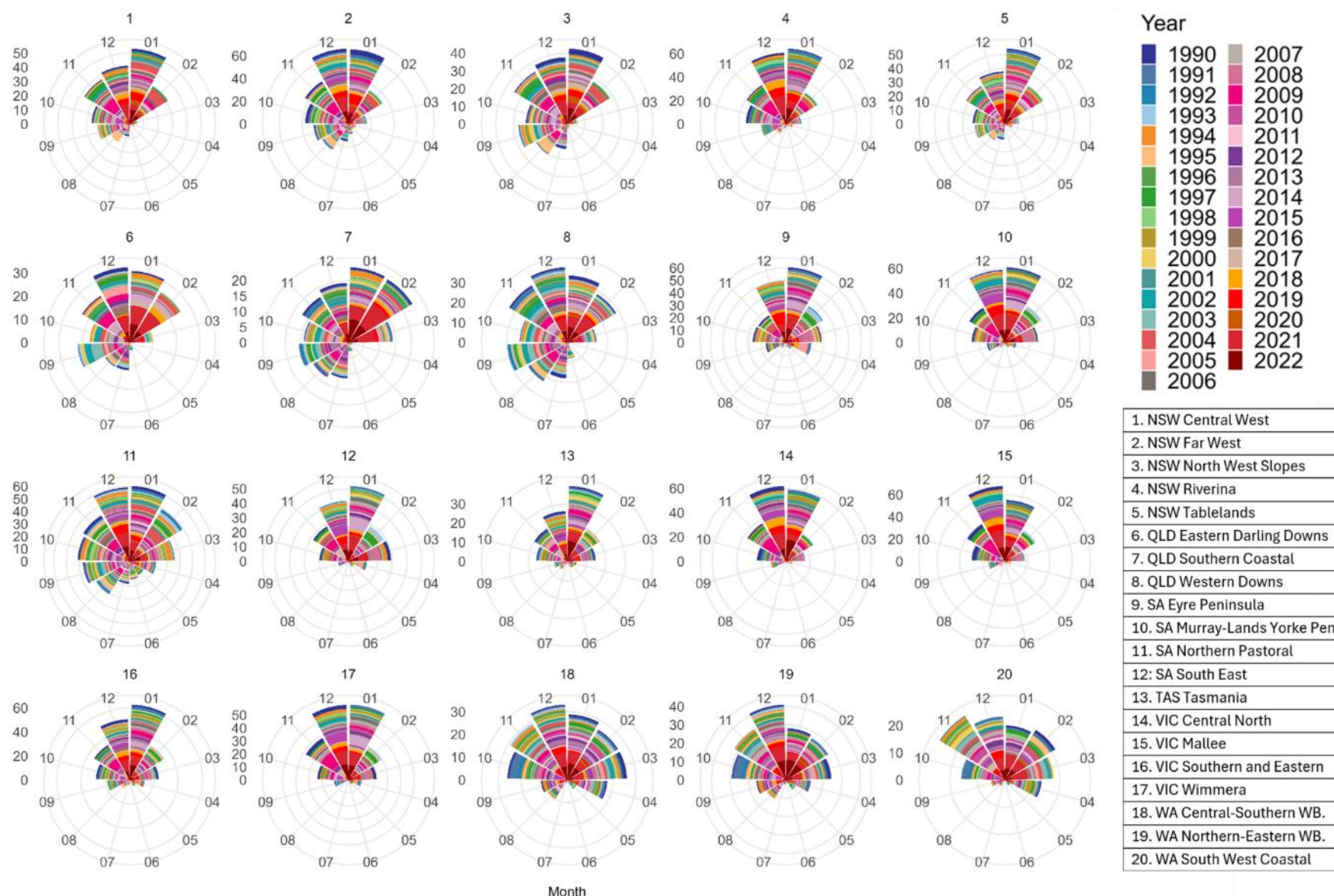
Fig. 22 Polar Chart Severe Monthly Heatwave Severity by ABARES Region

Each polar chart represents a different ABARES region (1 to 20), The quadrants are divided by months, with January (01) at the top, progressing clockwise through December (12). The radial axis shows the severe heatwave severity (°C²/ha). Colours represent different years, ranging from 1990 to 2022, as shown in the legend.
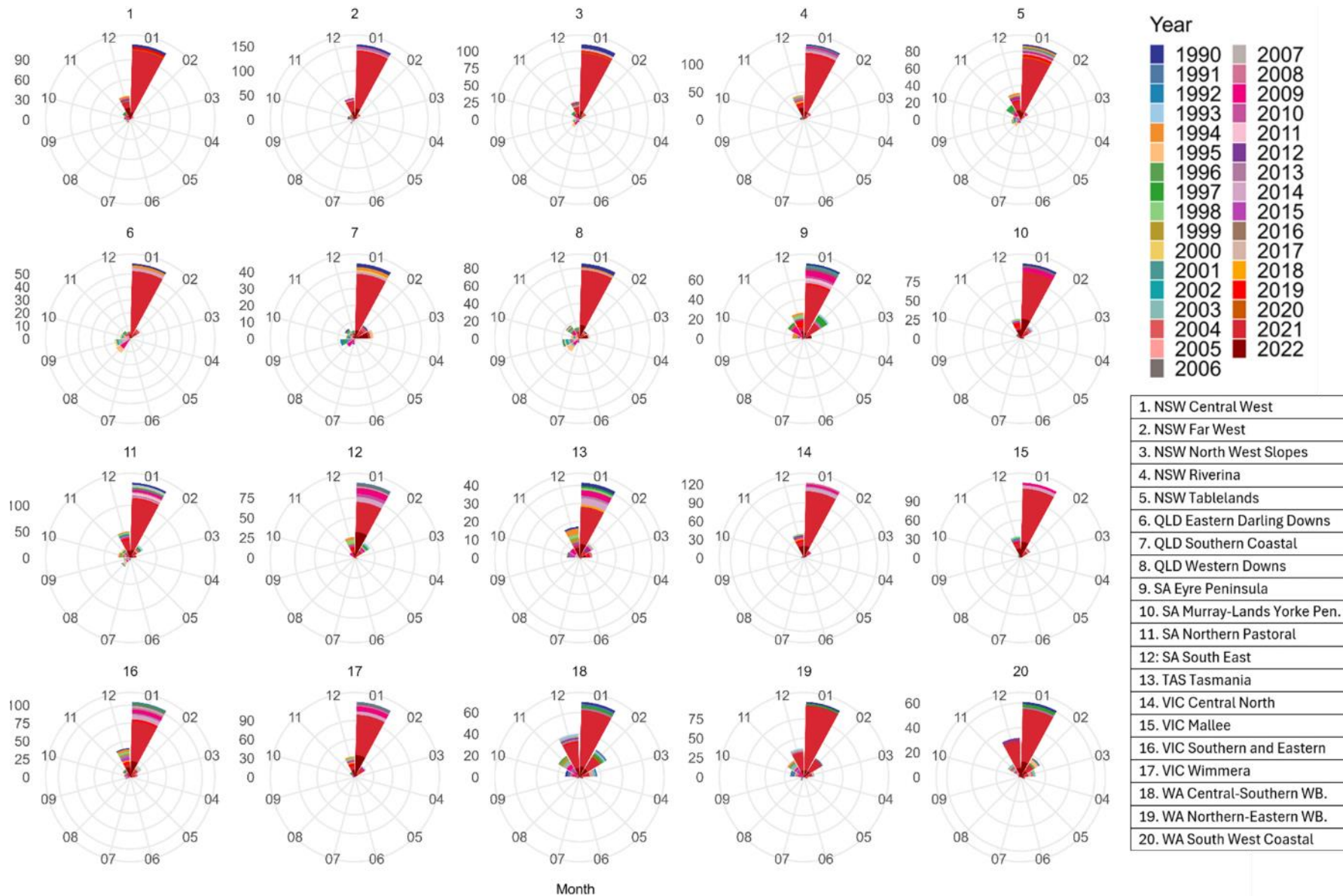
Fig. 23 Polar Chart Monthly Extreme Heatwave Severity by ABARES Region

Each polar chart represents a different ABARES region (1 to 20), The quadrants are divided by months, with January (01) at the top, progressing clockwise through December (12). The radial axis shows the extreme heatwave severity (°C²/ha). Colours represent different years, ranging from 1990 to 2022, as shown in the legend

The linear regression trends for the seasonality of the first heatwave events of the year (HWT) are summarised in Fig. 24. Overall, the trends show an earlier onset of severe and extreme heatwaves across multiple regions, while low-intense spells remain stable starting in July. Notable backward shifts for severe heatwaves include 13: TAS by 55 days (mid-November to late September), 18-19: WA Northern-Eastern and Central-Southern WB by 46 days, and 16: VIC Southern and Eastern by 44 days. For extreme heatwaves, prominent shifts include region 9: SA Eyre Peninsula by 43 days (mid-January to late-November), 16: VIC Southern and Eastern by 38 days (from mid-December to mid-November), and 11: SA Northern Pastoral by 35 days (late November to mid-October).
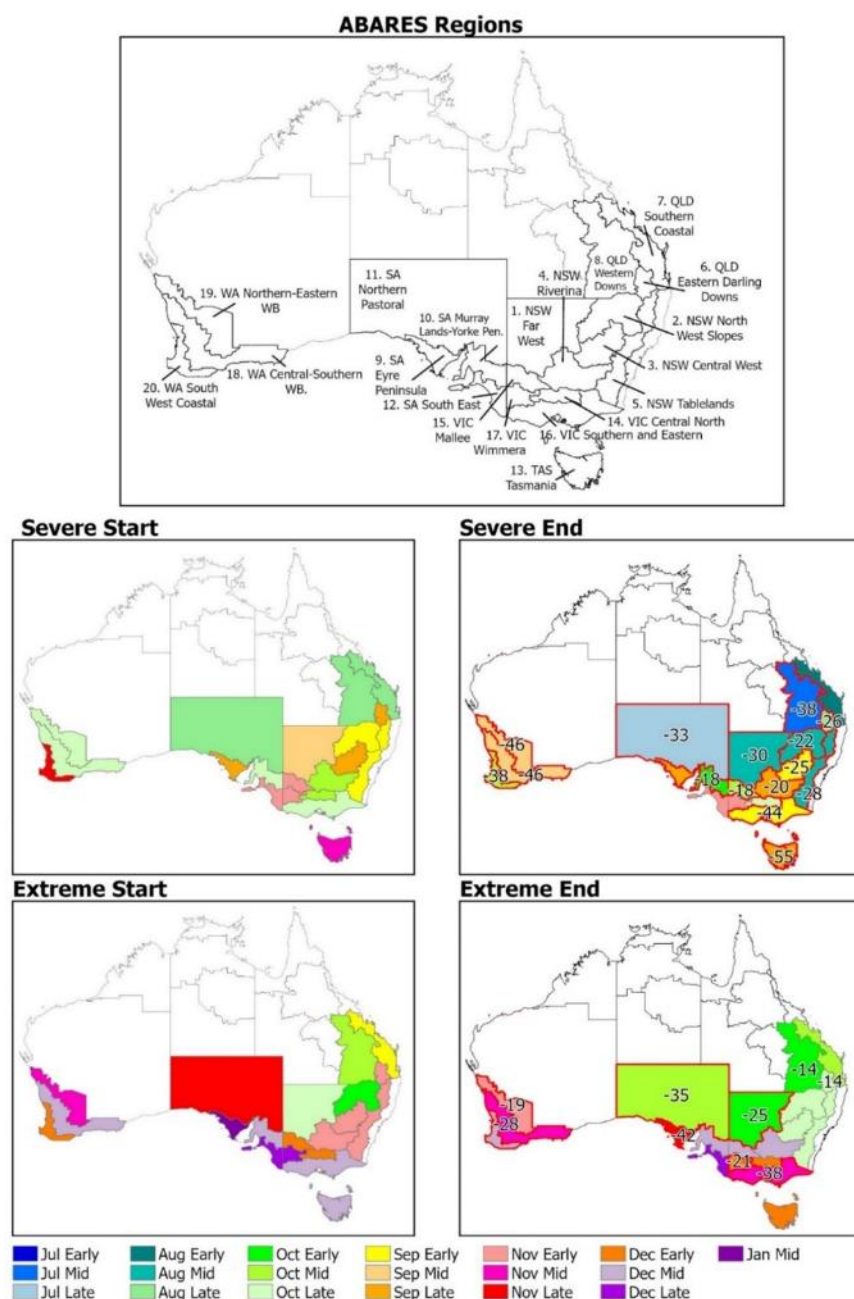
Fig. 24 HWT Linear Regression Trends

The map shows trends in the timing of the first heatwave of the year (HWT) centred from July to June. ABARES regions are colour-coded by the mid, and late thirds of each month with changes above 14 days outlined in red.

Chapter 4 Results Part 2: Spatio-temporal Trends in CDHEs

In this chapter, the focus shifts to the spatio-temporal patterns of CDHEs.

4.1 CDHE Trends and Statistics Australia-Wide

In this section the variability in frequency and magnitude of CDHE events is analysed for different drought and heatwave levels. Duration is first analysed separately for each drought and heatwave pairing, with the total event percentage presented in Table 8. This table reveals that low-intense warm spells under mild to moderate drought conditions account for the majority of CDHEs in Australia (61%), with short events (1–3 days) being the most frequent (82.6%). In contrast, CDHEs associated with severe and extreme heatwaves, especially under severe and extreme drought conditions, are much less common.

Table 7. Group Percentages of CDHE Event Counts

CDHE Category	1 day	2 days	3 days	4 days	5 days	6 days	>= 7 days	Total
Low-Intense Spell – Mild D	11.952	7.732	4.426	2.115	1.199	0.717	1.452	29.593
Low-Intense Spell – Moderate D	12.807	8.421	4.881	2.409	1.325	0.791	1.549	32.183
Low-Intense Spell – Severe D	7.004	4.590	2.679	1.321	0.717	0.438	0.832	17.581
Low-Intense Spell – Extreme D	1.922	1.279	0.747	0.353	0.203	0.131	0.242	4.878
Severe HW – Mild D	2.586	1.580	0.725	0.274	0.121	0.052	0.111	5.448
Severe HW – Moderate D	2.555	1.602	0.768	0.292	0.114	0.050	0.053	5.435
Severe HW – Severe D	1.340	0.829	0.415	0.153	0.061	0.019	0.017	2.833
Severe HW – Extreme D	0.334	0.203	0.095	0.037	0.014	0.005	0.006	0.693
Extreme HW – Mild D	0.240	0.146	0.085	0.045	0.022	0.017	0.044	0.599
Extreme HW – Moderate D	0.216	0.119	0.065	0.025	0.016	0.010	0.018	0.469
Extreme HW – Severe D	0.106	0.064	0.027	0.014	0.007	0.004	0.010	0.232
Extreme HW – Extreme D	0.024	0.013	0.010	0.005	0.001	0.001	0.003	0.056
Total	41.085	26.579	14.924	7.043	3.797	2.234	4.338	100

Fig. 25 presents the percentage breakdown of the total CDHE event durations. When drought and heatwave categories are combined, there is an increased presence of longer CDHEs, though shorter events still dominate. This variability reflects the episodic nature of heatwaves, where periods of low-intense spells may be a precursor to severe and extreme heatwaves, while there are also rare episodes of prolonged severe and extreme heatwaves aligning with drought.
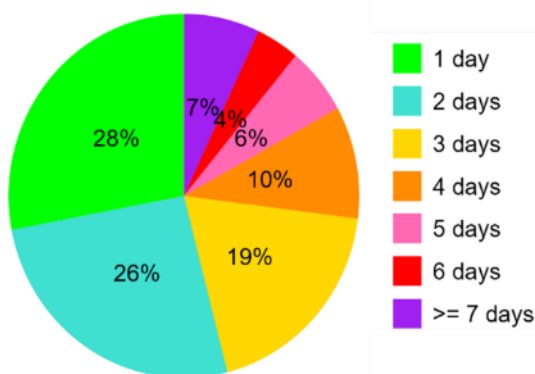
Fig. 25 Pie Chart of Total CDHE Events by Duration

The violin plot in Fig. 26 shows daily CDHE magnitudes also vary by heatwave and drought severity and duration. Panel A indicates CDHEs with low-intense spells have lower overall magnitudes with limited variability, whereas severe and extreme categories show much higher overall CDHE magnitudes and variability. Collectively this shows that combinations of extreme heatwave and drought hazards result in more intense CDHE days. In Panel B, magnitudes are observed to increase with longer durations, particularly those lasting 7 days or more, reaching significantly higher magnitudes. Viewing the duration of each heatwave and drought severity component separately, it can also be observed that the spread of high CDHE magnitudes is greater for prolonged severe and extreme hazard spells (see supplementary Fig. vi). This highlights both the severity and duration of heatwaves and drought strongly influence the magnitude of CDHEs.
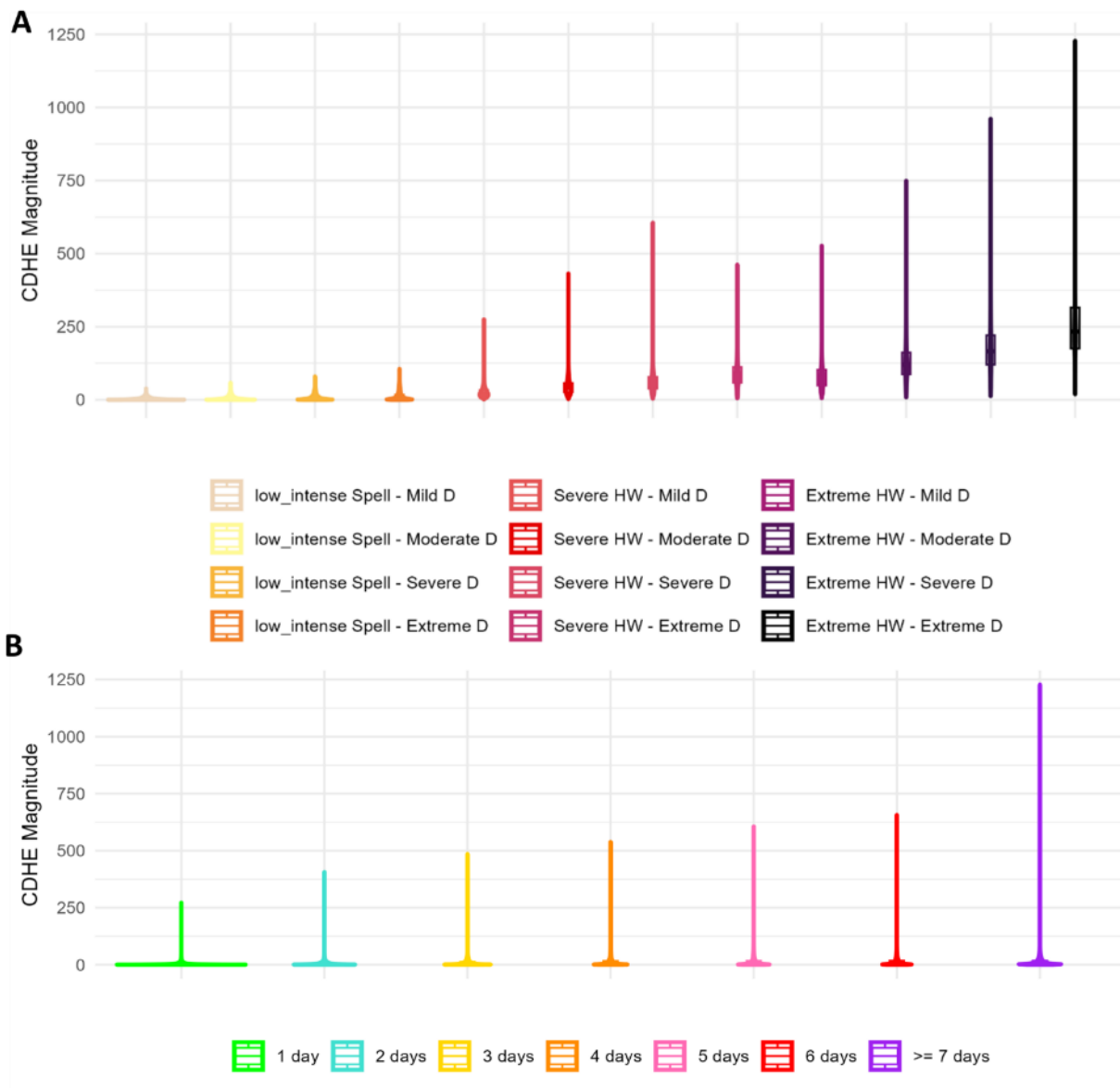
Fig. 26 Violins for CDHE daily Magnitude by A: Heatwave and Drought Category and B: Duration

Panel A shows a violin plot of daily CDHE magnitude ($-EHF \times scPDSI$) in $°C^2$ on the y axis and the heatwave and drought combinations on the x-axis. Panel B shows a violin plot of CDHE magnitude on the y axis and duration (1 to ≥7 days) on the x axis.

43

Fig. 27 illustrates the mean yearly CDHE frequency across Australia during the periods 1910–1999 and 2000–2022. The map shows that CDHE frequency varies widely, from 0 days on average (no colour) to over 50 days on average per year. CDHEs with mild, moderate, and severe drought occur across all of Australia, while extreme drought CDHEs are constrained to Eastern Australia and South West WA during the most recent period only (2000–2022). CDHEs with low-intense warm spells show the largest frequency increases over the last two decades, particularly in South West and East WA (around Perth and arid regions), NT (North and South), TAS, and southeastern Australia (QLD, VIC, Northern SA, and West NSW), with increases of 15–30 days per year. Severe heatwave CDHEs have also increased in these areas but are more spatially constrained, with rises of 4–20 days per year. Extreme heatwave CDHEs show increased frequency in WA and Northern NT, with SW WA emerging as a high-frequency area for extreme drought and heatwaves (30-37 days per year). Overall, the national average frequency increase between 1910–1999 and 2000–2022 include low-intense spells with severe drought (+8 days), low-intense spells with extreme drought (+16 days), severe heatwaves with mild drought (+9 days), and extreme heatwaves with moderate drought (+14 days).

Fig. 28 shows the spatial distribution of mean CDHE severity for each drought and heatwave combination across Australia from 1910–1999 and 2000–2022. CDHE severity ranges from 0 °C² to over 600 °C² per cell, following similar spatial trends to CDHE frequency. Nationally, CDHE severity has increased in the last two decades for all types, with the largest rises for extreme heatwave CDHEs, particularly those with extreme drought (+1104°C²), mild drought (+521°C²), moderate drought (+345°C²), and severe drought (+291°C²). Severe heatwave CDHEs have seen average severity increases of 81–153°C², and low-intense CDHEs with moderate and extreme drought have risen by 102–110°C². The severity map highlights that southeast, southern, and western Australia experience the most intense CDHEs, with severity hotspots expanding further west in Southeast Australia and east in Western Australia.
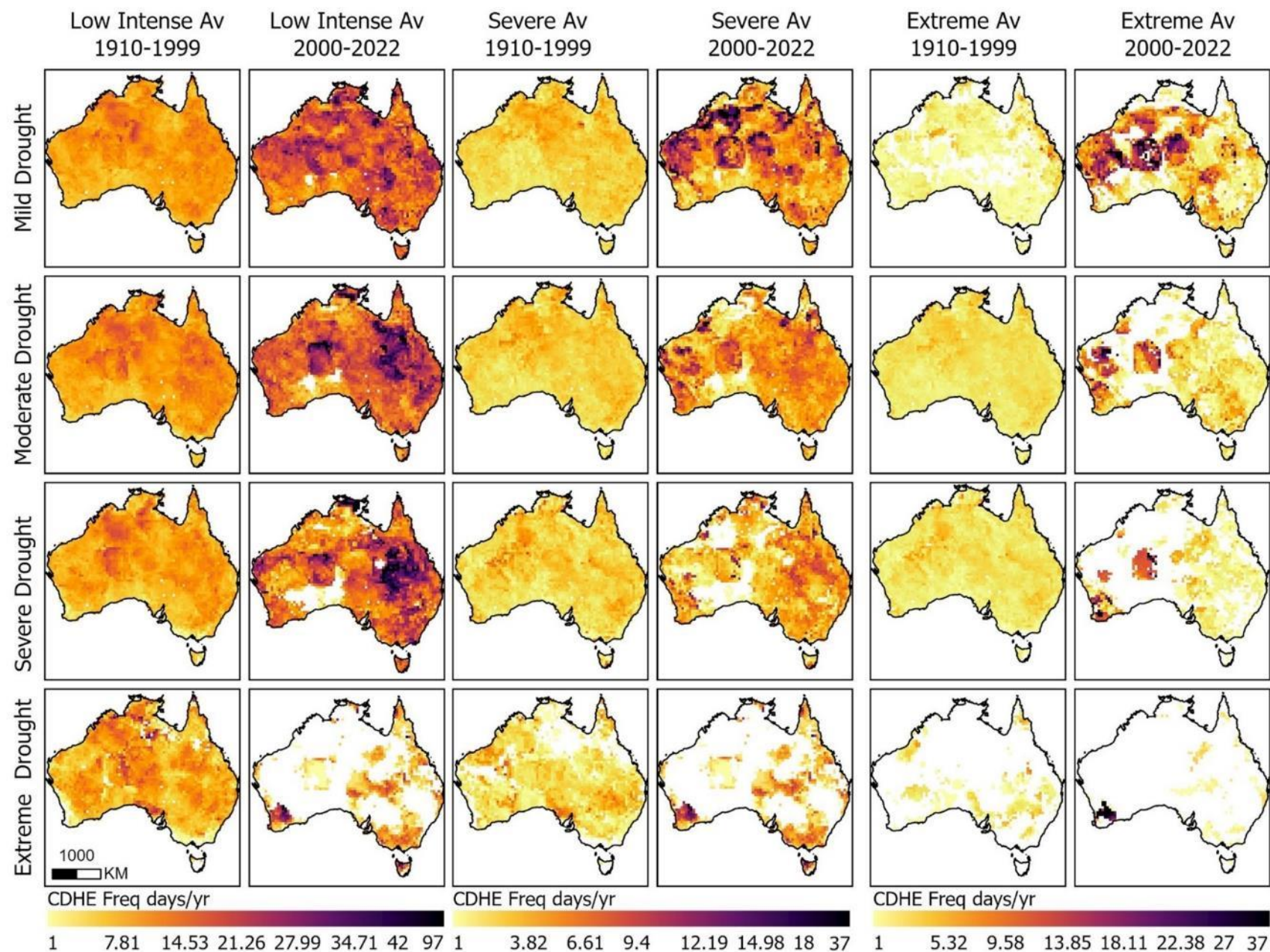
Fig. 27 Average CDHE Gridded Frequency by Heatwave Severity and Drought Class

45
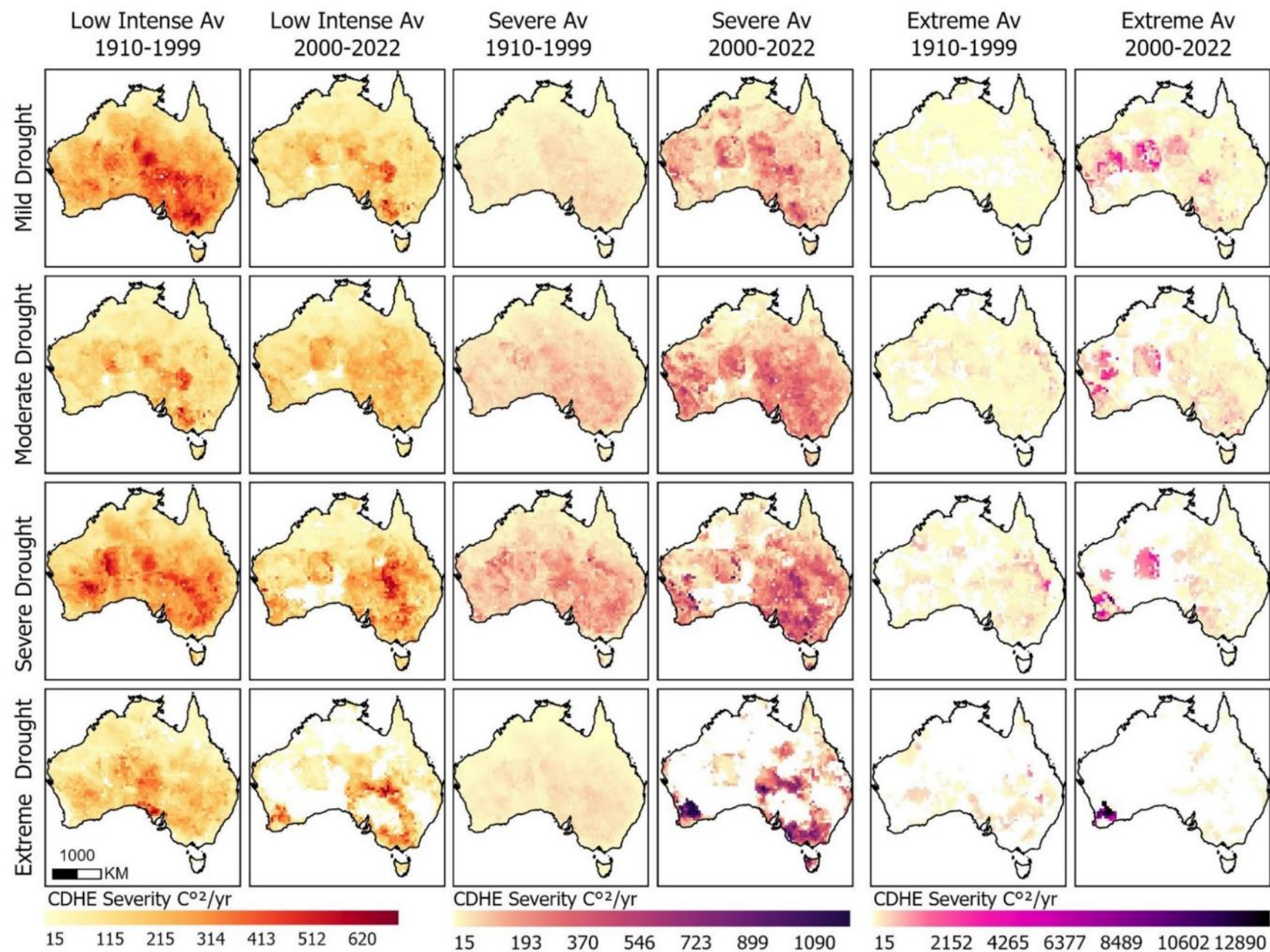
Fig. 28 Average CDHE Gridded Severity by Heatwave Severity and Drought Class

46

Fig. 29 summarises the percentage of the Australian landmass affected by CDHEs each year, exhibiting a marked rise across over time. Peak CDHE coverage occurred in years 2022–2021, 2019–2012, 2009, 2005–2002, 1998, 1996–1995, 1990, 1981, 1973, 1958, 1942, 1939–1940, and 1928. Panel A shows all CDHEs peaked in 2022 including 12% from low-intense spells, 6% severe heatwaves, and 2.29% extreme heatwaves. Panel B displays the yearly mean (blue) and maximum (black) single-day coverage of CDHEs. The mean CDHE coverage and maximum single-day coverage have steadily increased. The most widespread single CDHE days surpass 50% of Australia's area. This includes days in December 2022 (72.8%), May 2014 (66.8%), June 1995 (58.38%), March 2016 (57.2%), July 1975 (54.3%), March 2017 (52.2%), and August 1973 (51.1%). Panel C combines all CDHE categories, illustrating an overall increase the scale of area impacted over time. Recent years have also reached record 10-20% coverage (769,000-1,530,000 sqkm), highlighting CDHEs have become more widespread compared to historical patterns.
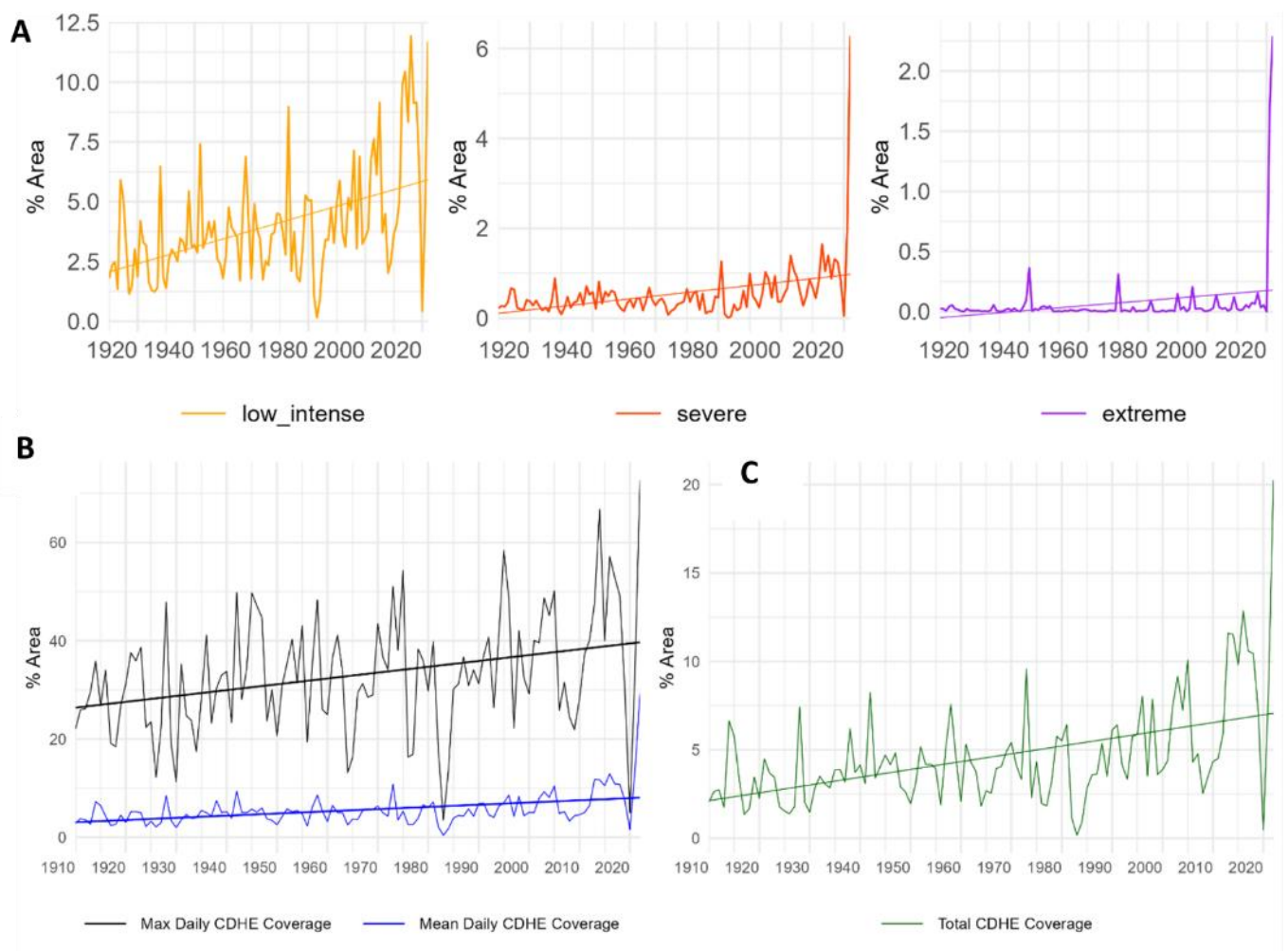
Fig. 29 Yearly CDHE Coverage (A: Coverage % by Heatwave Severity, B: Max and Mean Daily Coverage %, C: Total Coverage %)

Panel A shows the annual area percentage covered by CDHEs separated by heatwave severity on the y-axis, calculated as total CDHE days divided by the total number of grid cells Australia-wide. Panel B illustrates the daily area percentage affected by all CDHE events on the y-axis, with the black line representing the maximum percentage area of a single day and the blue line showing the mean percentage area across all days. Panel C contains the total annual area covered by all CDHEs. Linear trend lines are also displayed on each time series.

Fig. 30 presents a heatmap displaying the distribution of yearly CDHE severity of each drought and heatwave combination across Australia. This chart highlights that CDHE combinations involving mild, moderate, and severe droughts dominate. Extreme droughts and heatwaves, while capable of producing highly severe events, are much rarer and thus contribute less to the overall total severity. The chart also shows the spread of extreme CDHEs (those in the darkest tiles) have increased in frequency since the 2000s.
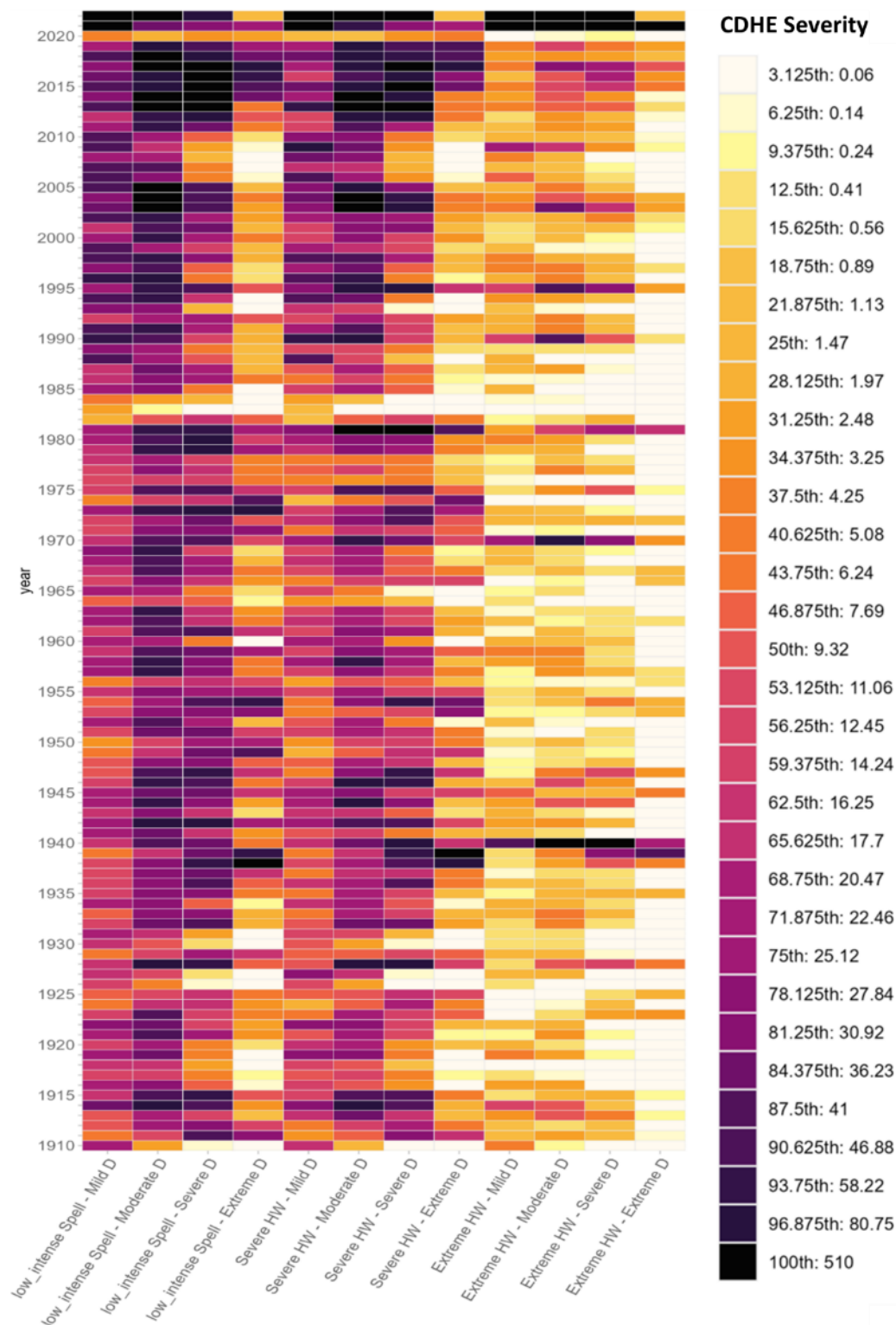
Fig. 30 Heat map of Yearly CDHE Severity by Category and Year

The x-axis represents the CDHE category while the y-axis shows the calendar years. Tile colours correspond to the yearly CDHE severity Australia-wide, measured in °C²/Area (no. cells), divided into thirty-two quantiles.

Fig. 31 presents the trends in CDHE frequency and severity across Australia, covering all events. The first two columns illustrate increases in mean annual frequency and severity between 1910–1999 and 2000–2022. During these periods, annual frequency rose from 18 to 35 days (+17 days), and severity increased from 195 to 515 °C² (+320 °C²). High CDHE frequency is most concentrated in southeastern and western Australia, as well as northern NT and QLD. CDHE severity is most concentrated in southeastern and western Australia. Hotspots of CDHE frequency and severity are also found to overlap with ABARES growing regions outlined in black. The third column in Figure 31 displays the Sen Slope trends, revealing statistically significant positive trends in CDHE frequency (0.05–1.57 days/year) and severity (0.14–23.36 °C²/year) across most of Australia, except in parts of WA, NT, and NSW. Regions where CDHE frequency trends exceed two standard deviations (0.38–1.57 days/year) include South West and East WA, and northern QLD. For severity, trends higher than 2 standard deviations (4.08–23.36 °C²/year) appear in WA (South West and arid regions), SA and southern VIC.
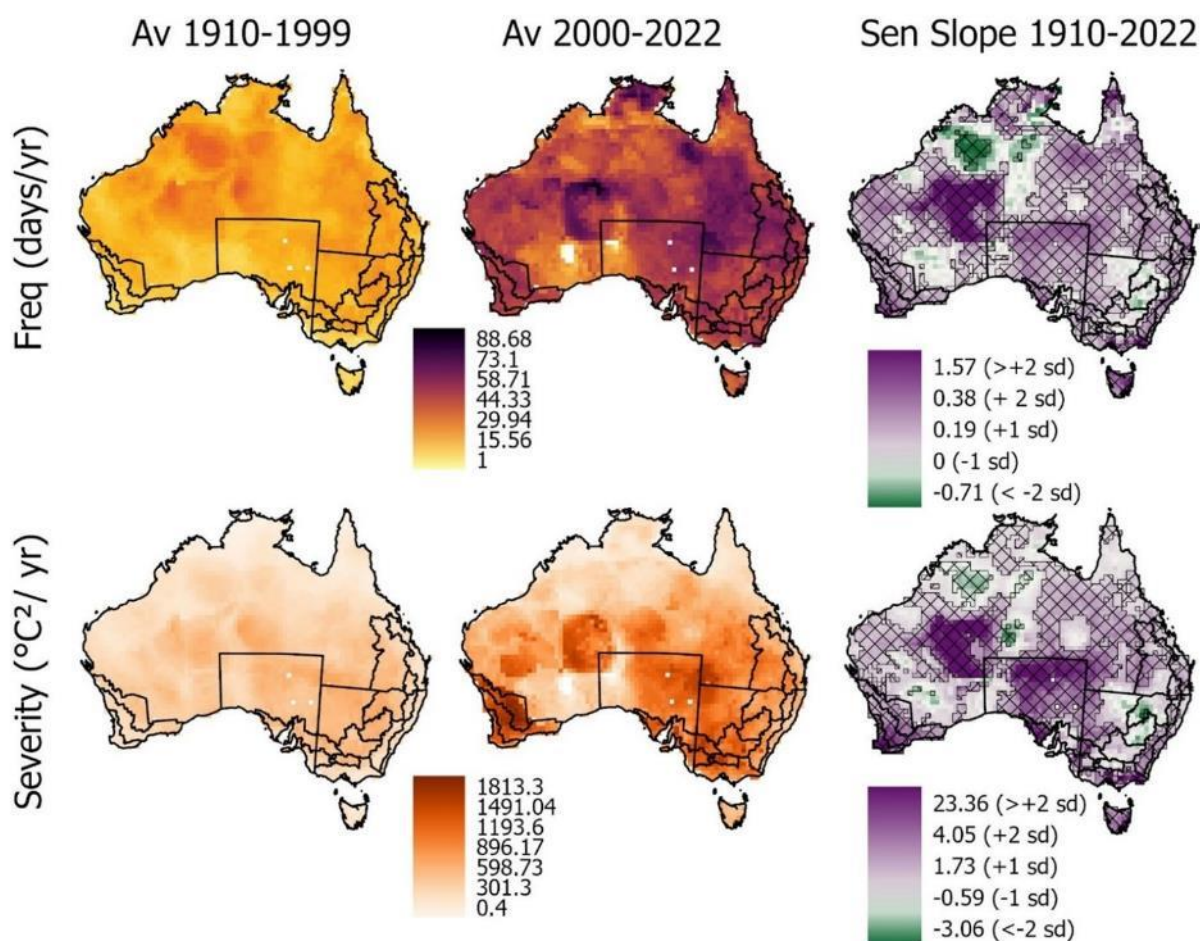
Fig. 31 CDHE Frequency and Severity Trends

The first two columns show the average gridded CDHE frequency (days/year) and CDHE severity (°C²/year) for the periods 1910–1999 and 2000–2022, with a separate colour scale for each metric. The third column displays the Sen Slope trend, with the Mann-Kendall significance ($p < 0.05$) overlaid as a mesh. The trend is represented using a purple-green diverging colour scale, where white indicates changes within ±1 standard deviation, purples indicate increases of more than +1 standard deviation, and greens represent decreases of more than -1 standard deviation.

4.2 CDHE Trends and Statistics by Growing Region

This section examines CDHE variability across growing regions, one of the foci of this thesis. Fig. 32 shows that CDHE magnitude differs by growing region and heatwave and drought category. Some regions, like 19: WA Northern-Eastern WB, exhibit much higher CDHE magnitudes overall, with events exceeding 1000, whereas other regions, like 13: TAS Tasmania or 5: NSW Tablelands, show generally lower magnitudes. The pattern of increasing CDHE magnitude with the severity of heatwaves and droughts is consistent across all regions, but the absolute values vary. There are also regional differences in CDHE magnitudes within the same category, partly due to differences in the EHF (this can be viewed in supplementary Fig, vi).
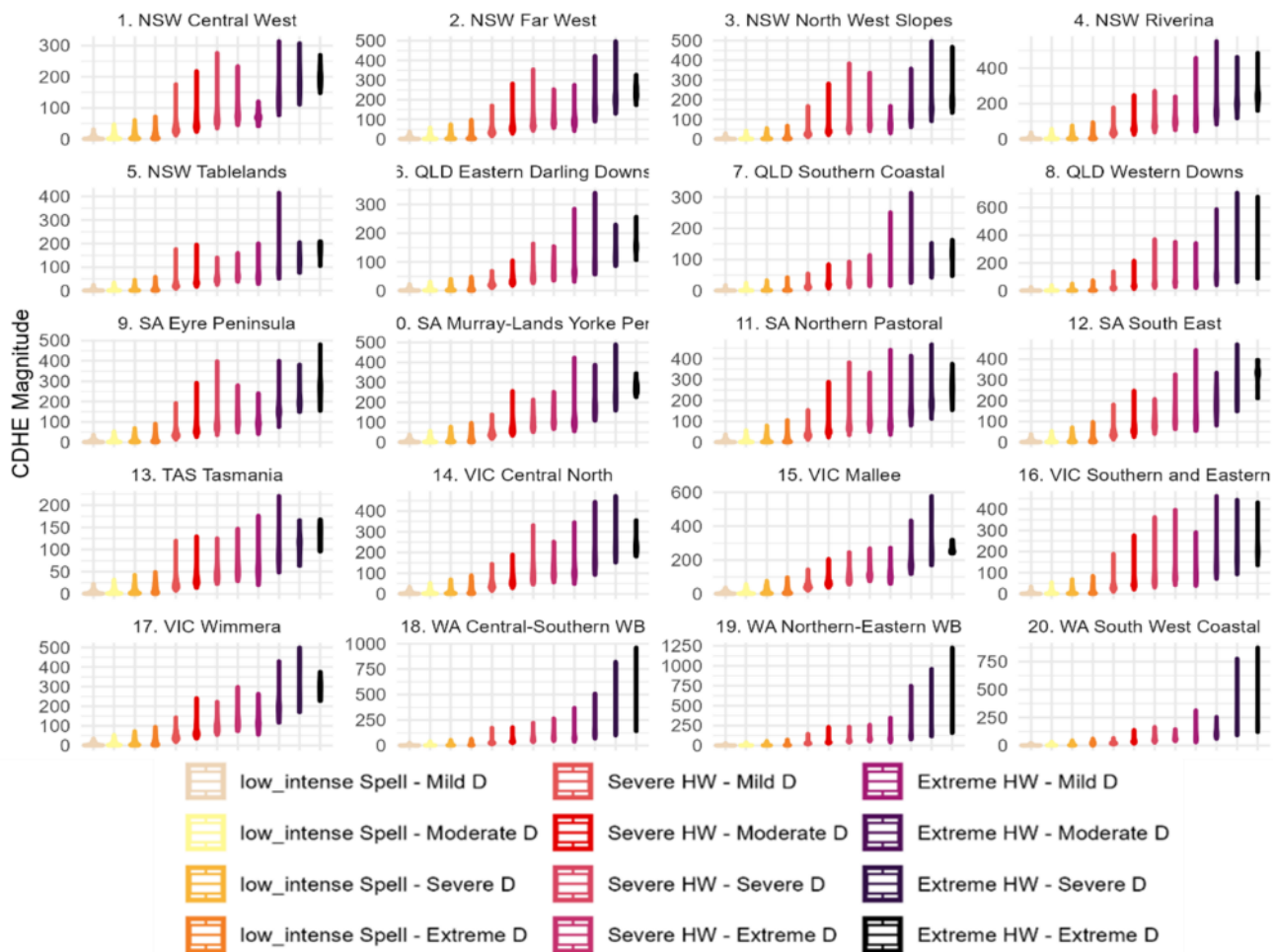
Fig. 32 Violins for CDHE Daily Magnitude by Heatwave and Drought Category and ABARES Region

The y-axis shows CDHE magnitude ($-EHF \times scPDSI$) in °C^2, colour represents combined CDHE categories, and each panel corresponds to an ABARES region.

Fig. 33 shows the average yearly regional frequency of CDHEs across ABARES regions for 1910-1999 and 2000-2022. CDHE frequency increased across all regions in 2000-2022, also shifting to more severe and extreme heatwaves and drought. Low-intense spell CDHEs rose from 3.92-16.84 days per cell in 1910-1999 to 15.65-33.5 days per cell in 2000-2022. Severe heatwave CDHEs increased from 0.49-2.2 to 2.91-6.7 days per cell, and extreme CDHEs rose from 0.04-0.17 to 0.22-1.65 days per cell, reflecting a trend toward more frequent and severe CDHEs in the recent period.
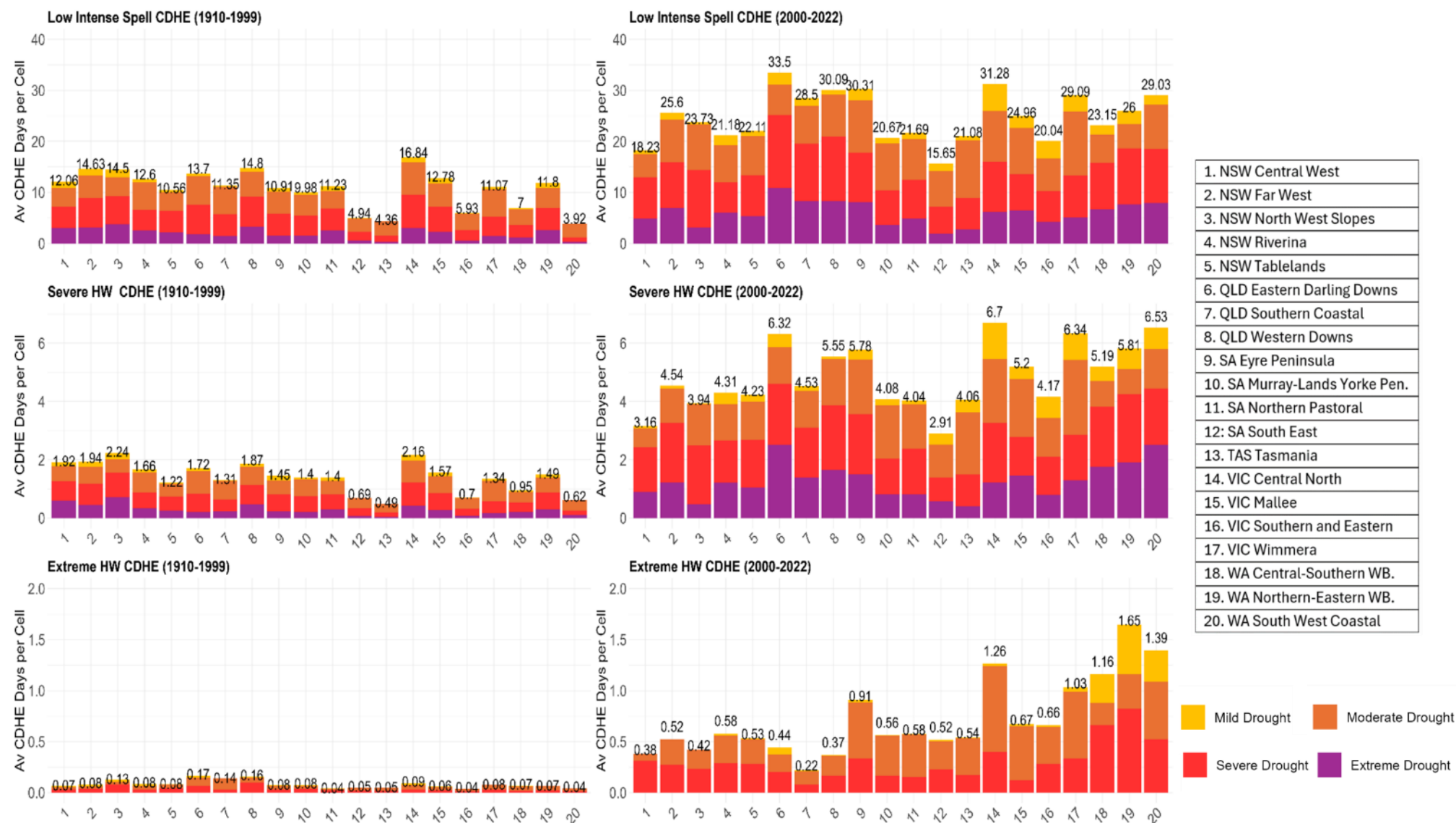
Fig. 33 Bar Chart of CDHE Regional Frequency by Heatwave and Drought Category

The x-axis labels ABARES Regions (1-20), displaying average regional CDHE frequency (days per cell) for 1910-1999 (left) and 2000-2022 (right). Heatwave severity is distinguished by panels, while drought severity is represented by bar colours.

Fig. 34 presents ABARES regional boxplots of daily CDHE magnitude in Panel A and yearly regional CDHE frequency in Panel B for all combined CDHEs. For daily CDHE magnitude, growing regions 2: NSW Far West, 8: Queensland Western Downs, 11: SA Northern Pastoral, and 18-19: WA Central and Northern WB display the highest CDHE magnitudes, marked by extreme outliers. Fig. 34, Panel B shows substantial variation in CDHE occurrence across regions. CDHEs have occurred in most years (averaging 109 years in the 113-year record) and generally range from 0 to 30 days per cell, though they can reach up to 60-172 days per cell in years of frequent CDHEs. Regions in NSW, QLD, SA (9,10,11), VIC (14,15), and WA exhibit the highest CDHE frequency, as reflected by the taller boxes and outliers.
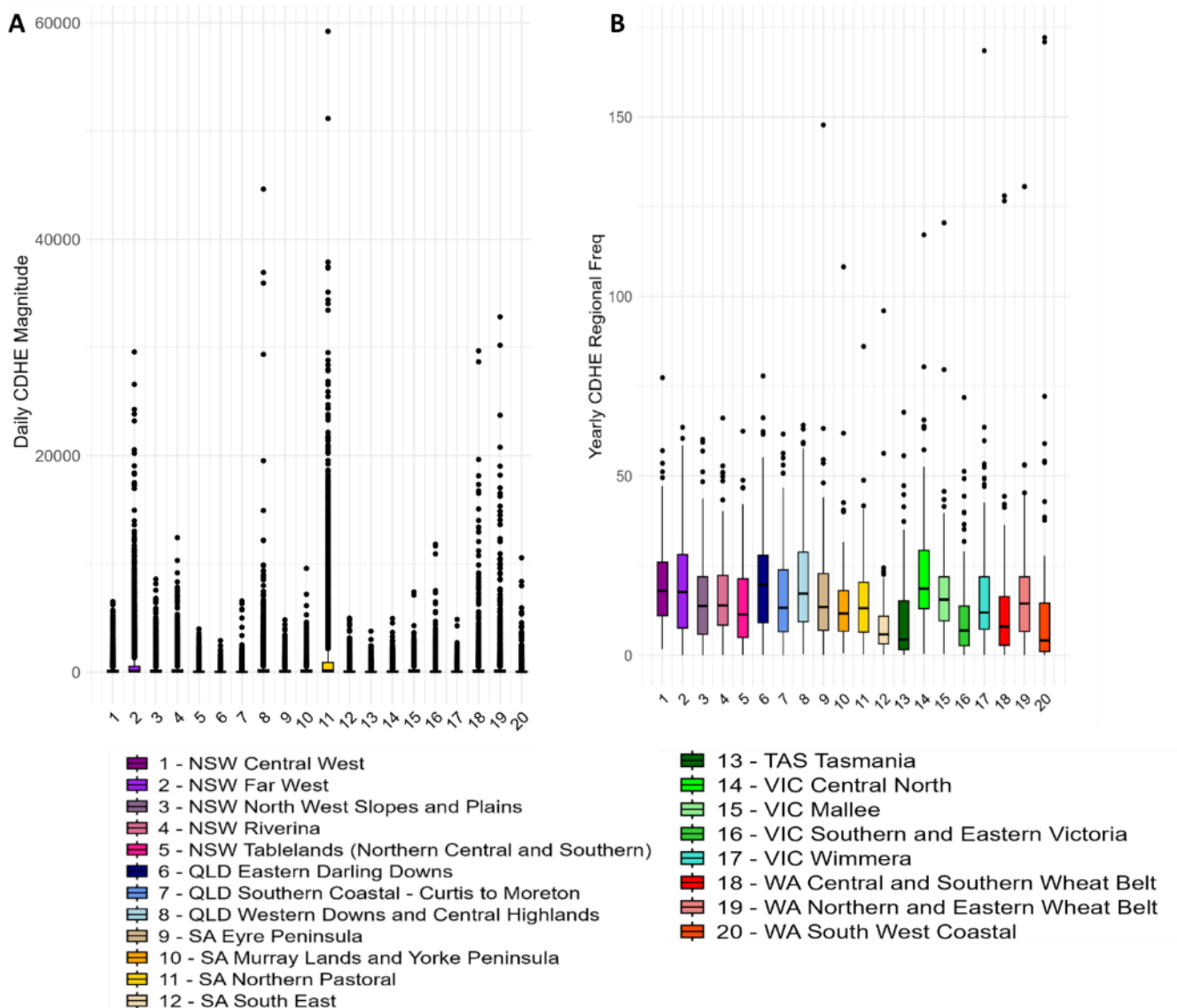
Fig. 34 ABARES Boxplots of A: Daily CDHE Magnitude and B: Yearly CDHE Regional Frequency

The x-axis lists the regions (numbered 1 to 20), while the y-axis indicates the CDHE daily magnitude

($-EHF \times scPDSI$) in °C² (A) and yearly CDHE regional frequency (days / area (no. cells))

Fig. 35 displays ABARES regional boxplots of CDHE duration in Panel A and yearly regional CDHE severity in Panel B for all combined CDHEs. Most CDHEs last between 1 and 4 days but can extend between four and five months (120-150 days), except in Queensland (6,7,8) and NSW Central West (1), where they last up to 3 months. Regions in WA, SA, and NSW (2,4,5) show frequent extreme duration CDHEs between 3-4 months. Fig. 35, Panel

B shows variability in yearly regional CDHE severity across regions. Most regions experience CDHEs between 0-300°C² per cell, with peaks between 800-13,600°C² per cell. Regions in WA, VIC (14,15,17), and SA reach the highest yearly regional severity. Periods of extreme yearly CDHE severity reflects years with the most intense and frequent CDHEs, which vary by region and are influenced by heatwave and drought behaviour.
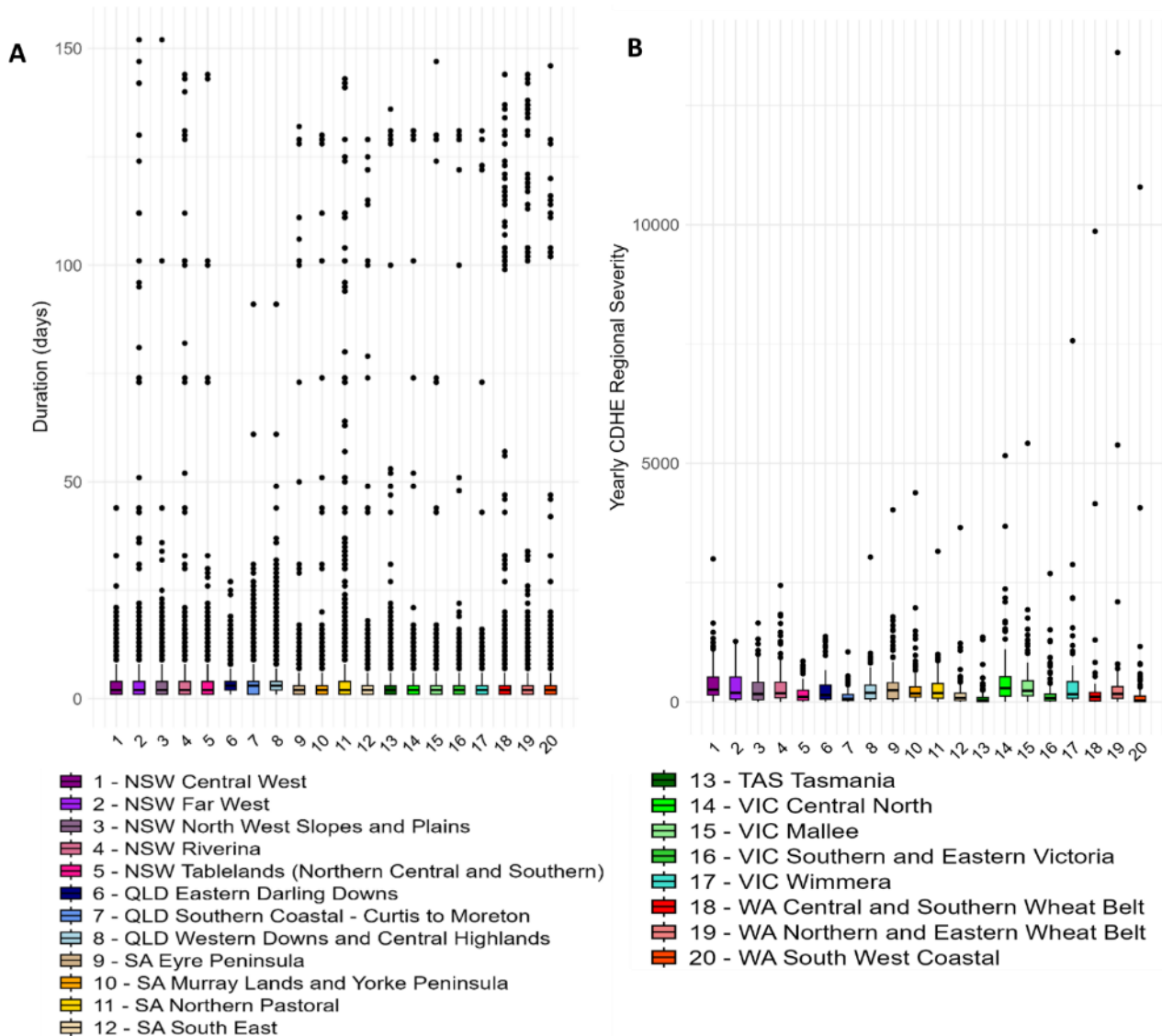
Fig. 35 ABARES Boxplots of A: Daily CDHE Duration and B: Yearly CDHE Regional Severity

The x-axis lists the regions (numbered 1 to 20), while the y-axis indicates the CDHE duration in days (A) and yearly CDHE regional severity ($°C^2/area$ ($no.cells$))

4.3 CDHE Trends and Statistics by Seasonality and Growing Region

This section explores CDHE seasonality by monthly regional heatwave severity. Fig. 36 illustrate in the years available for the ABARES data (1990-2022), CDHEs have occurred every month of the year, and are most concentrated in the summer months. CDHEs emerge from August to October, and peak in January for most regions, except for Queensland (6-8) which are more active over winter and spring. CDHEs are less active from March to July. Compared to earlier years, CDHEs have increased in Feburary to April across eastern Australia (QLD, NSW, SA, VIC, TAS) (refer to Supplementary Data Table V).
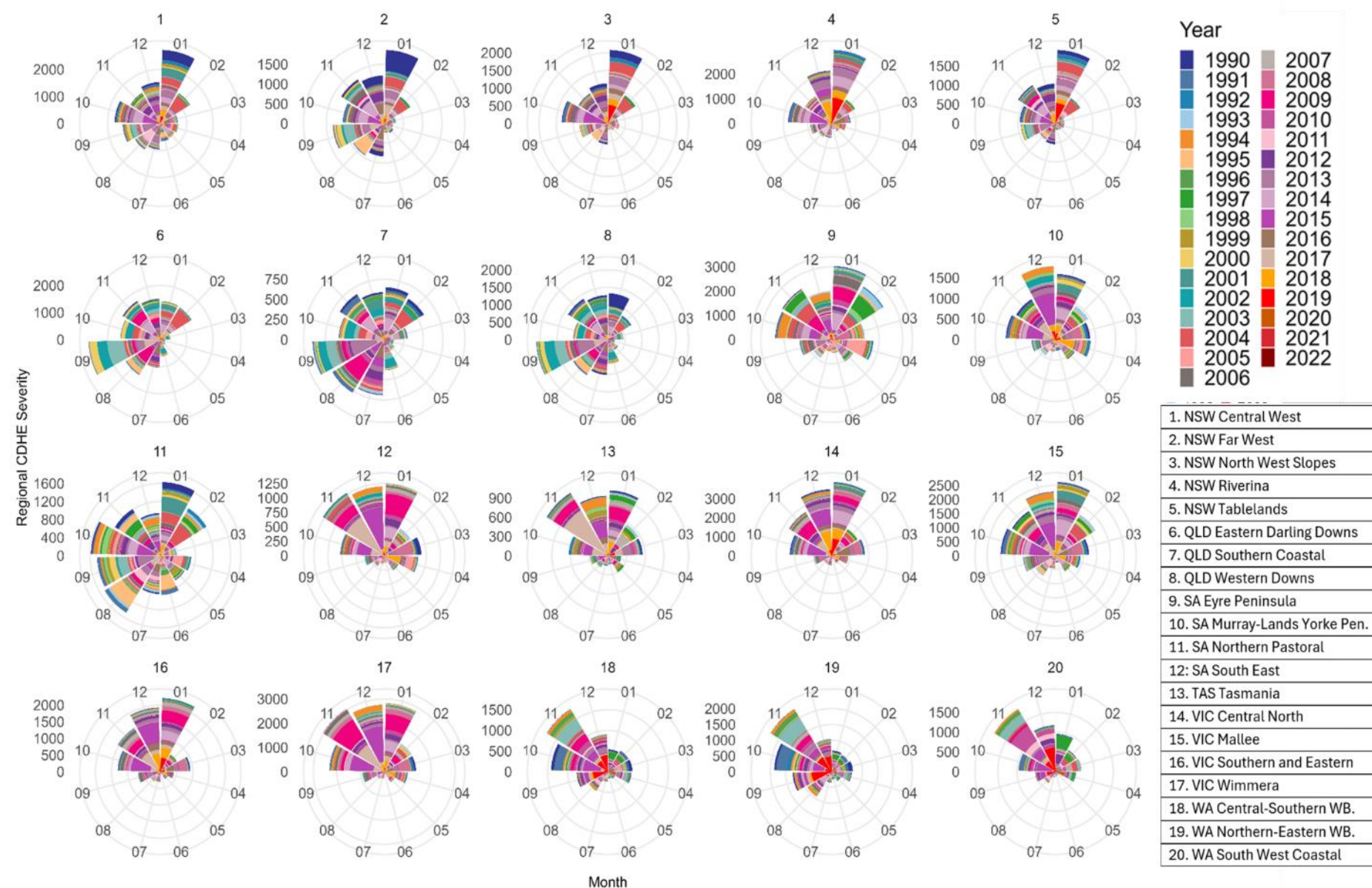
Fig. 36 Polar Chart Monthly CDHE Severity by ABARES Regio

Each polar chart represents a different ABARES region (1 to 20). The quadrants are divided by months, with January (01) at the top, progressing clockwise through

December (12). The radial axis shows CDHE Regional Severity (°C²/Area (no. cells). Colours represent years, ranging from 1990 to 2022, as shown in the legend.

Chapter 5 Results Part 3: Impact of CDHEs on Crop Yield

This chapter presents the final results, examining the relationship between CDHEs and cereal crop yield (part 3). Figure 37 shows ABARES regional boxplots of detrended yield data by crop. The boxplots indicate a mean of zero across all growing regions, demonstrating that the detrending process successfully standardised the data, allowing for meaningful comparisons across different regions. Wheat and barley yields show higher variability at lower values in NSW and VIC, and TAS than in QLD, SA, and WA, where values are more stable. In contrast, wheat and barley exhibit the lowest yields in SA and WA. Oats display the largest lower variability in SA and VIC, and TAS. The most extreme low wheat yields occurred in region 1: NSW Central West (1995), 12: SA South East (2007-2008), and 18: WA Central-Southern WB (2011, 2013, and 2020). For barley, record low yield occurred in region 9: SA Eyre Peninsula (2007-2008), 10: SA Murray Lands (2007), 12: SA South East (2007), and 18-19: WA Central-Southern and Northern-Eastern WB (2001, 2003, 2011). In oats, lowest yields were found in region 20: WA South West Coastal (1991, 2019, and 2020). Low sorghum yield anomalies also include QLD Southern Coastal (2016, 2020).
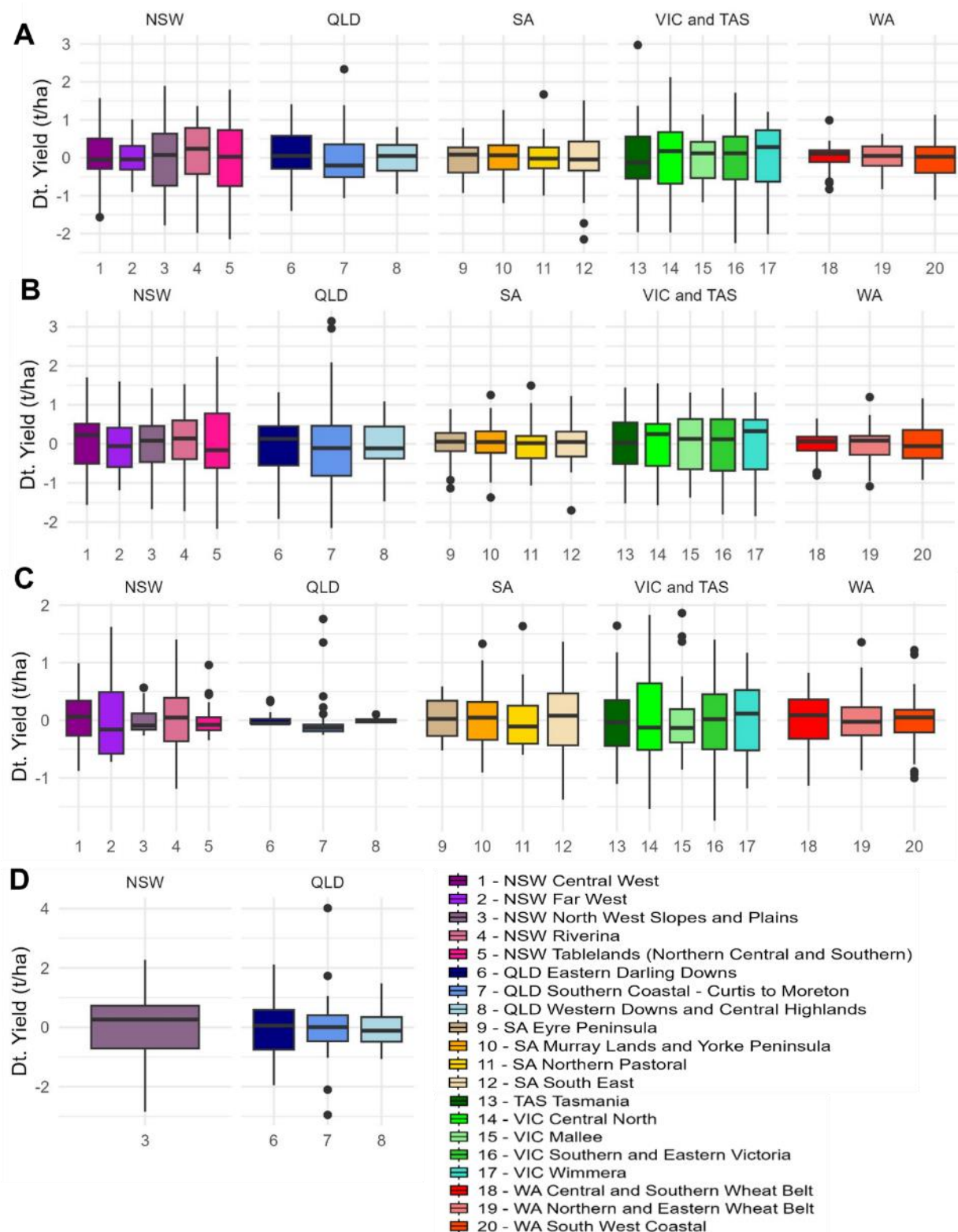
Fig. 37 ABARES Boxplots of Detrended Yield for A: Wheat, B: Barley, C: Oats and D: Sorghum

The x-axis lists the regions (numbered 1 to 20), while the y-axis indicates the yield anomalies (tons/ha) by cereal crop, calculated by subtracting the linear trend from yield.

Fig. 38 illustrates yield anomalies frequently co-occur across multiple crops and regions, with the most widespread anomalies observed in 1995, 2003, 2007-2008, and 2019-2020. The bubble chart highlights combined wheat, oats and barley yield anomalies is very frequent combination, followed by wheat and barley. The regions which have the largest yield anomalies include region 4: NSW Riverina, 6: QLD Eastern Darling Downs, 17: VIC Wimmera, 14: VIC Central North, 1: NSW Central West and 16: VIC Southern and Eastern (see Supplementary Fig. vii). The frequency of anomalies is greatest in region 6: QLD Eastern Darling Downs, 13: Tasmania, 8: QLD Western Downs, 16: VIC Southern and Eastern, and 20: WA South West Coastal.

Region	Name
1.	NSW Central West
2.	NSW Far West
3.	NSW North West Slopes
4.	NSW Riverina
5.	NSW Tablelands
6.	QLD Eastern Darling Downs
7.	QLD Southern Coastal
8.	QLD Western Downs
9.	SA Eyre Peninsula
10.	SA Murray-Lands Yorke Pen.
11.	SA Northern Pastoral
12.	SA South East
13.	TAS Tasmania
14.	VIC Central North
15.	VIC Mallee
16.	VIC Southern and Eastern
17.	VIC Wimmera
18.	WA Central-Southern WB.
19.	WA Northern-Eastern WB.
20.	WA South West Coastal

Type

- barley
- barley-oats
- barley-sorghum
- oats
- sorghum
- wheat
- wheat-barley
- wheat-barley-oats
- wheat-barley-sorghum
- wheat-oats

Type	Count
barley	18
barley-oats	6
barley-sorghum	2
oats	23
sorghum	10
wheat	21
wheat-barley	40
wheat-barley-oats	49
wheat-barley-sorghum	5
wheat-oats	5

Fig. 38 Bubble Chart of Combined Crop Loss Yield Anomalies by ABARES Region and Year

The x-axis represents ABARES regions (numbered 1 to 20), while the y-axis shows the years from 1990 to 2022. Bubble size indicates the magnitude of the combined yield loss anomalies (in tons/ha) for cereal crops grown. Blank spaces mean no loss anomalies for any crop occurred in that region and year. Colours correspond to different crop types, as listed in the legend. The table at the bottom right displays the count of each crop type affected by anomalies across all regions.

Fig. 39-40 examine the annual area percentage and regional severity of CDHEs across ABARES regions during wheat growing months (April-August), marking years with high CDHE frequency or severity. These charts show significant year-to-year variability in CDHE impact, with regions experiencing either high frequency and/or severity. However, yield anomalies do not always align with CDHE peaks, suggesting other factors also influence yield outcomes.
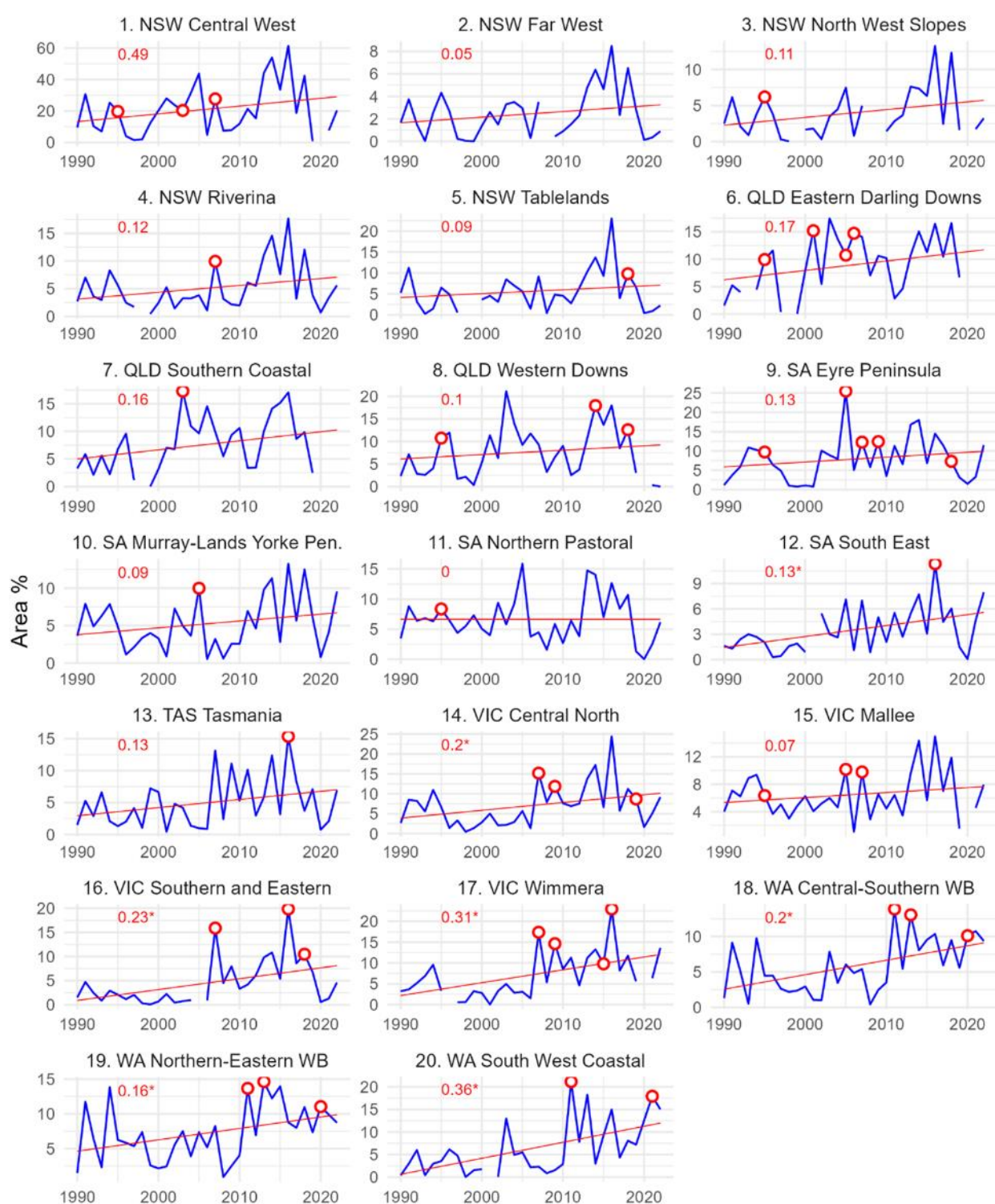
Fig. 39 Time Series Total Regional CDHE Coverage for Wheat Growing Months

The y-axis represents the percentage of area covered by CDHEs during wheat growing months (April-August), calculated as the total CDHE days divided by the area grid cells. Red circles mark yield anomalies (>1 Sd) and CDHEs above the 75th percentile in frequency or severity.
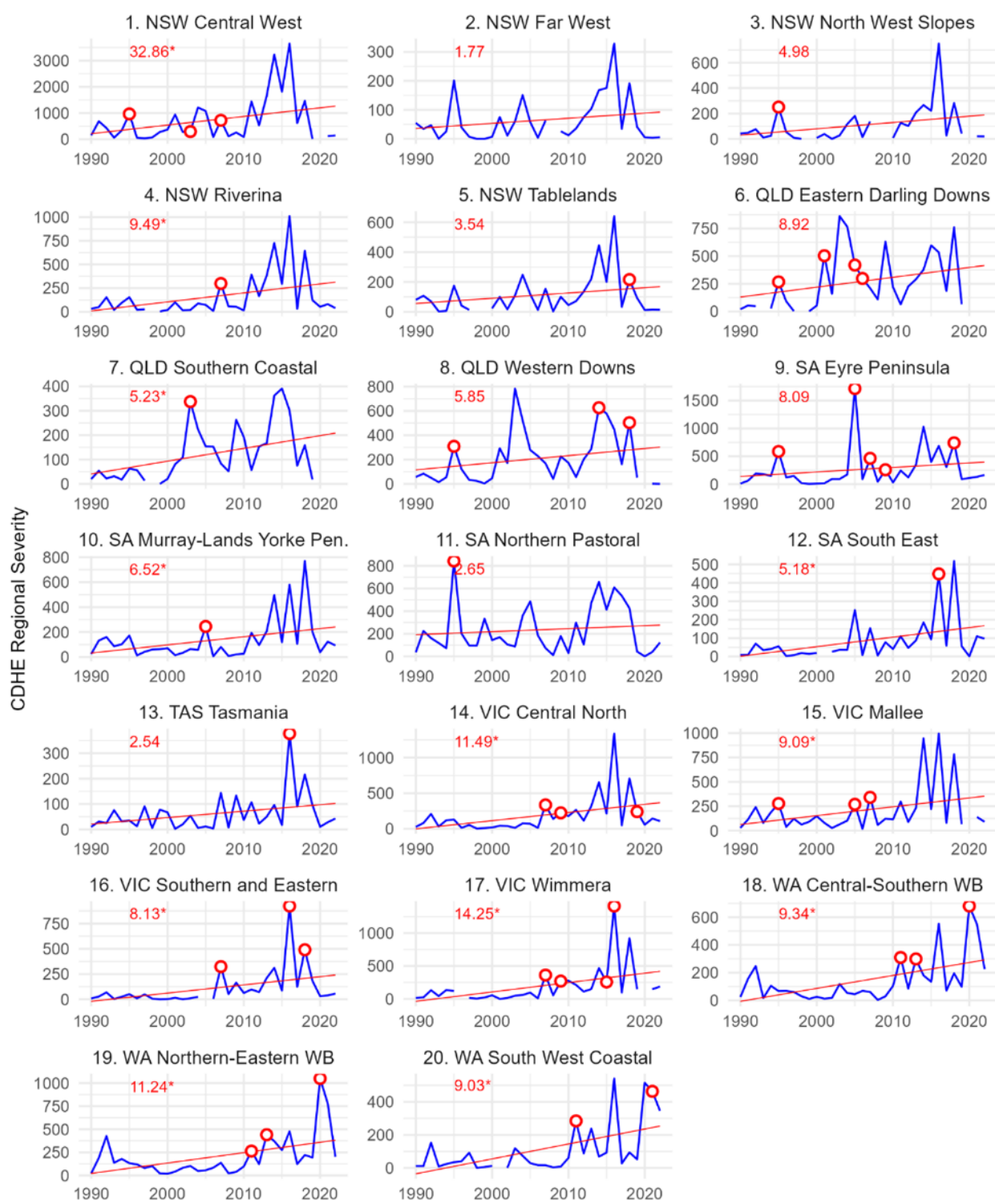
Fig. 40 Time Series Regional CDHE Severity for Wheat Growing Months

The y-axis represents the regional CDHE severity ($°C^2$/$area$ ($no.cells$)) during wheat growing months (April-August). Red circles mark yield anomalies (>1 Sd) and CDHEs above the 75th percentile in frequency or severity.

Fig. 41-44 present the detrended yield time series for each cereal crop (wheat, barley, oats, and sorghum), showing both positive and negative anomalies in yield from 1990 to 2022. Red bars indicate years with yield loss anomalies, while red circles mark years when these losses coincide with high CDHE frequency or severity. These charts highlight some regions have particularly severe yield loss associated with CDHEs across wheat, barley, oats and sorghum. It is also apparent the frequency of yield anomalies differs by region and crop. Notably, certain regions, such as VIC (16, 17), WA (19, 20), and SA and TAS (9, 11-13), show clear and recurrent patterns of yield anomalies linked to CDHEs. Other regions also have yield anomalies co-inciting with CDHEs; however, it may have only occurred infrequently or inconsistently with CDHE area and severity. This variability in the overlap between yield anomalies and CDHE events suggests differing levels of sensitivity across regions. This also underscores the need to refine the identification of CDHE events that specifically impact yield, as not all recorded CDHE events may affect crop performance.
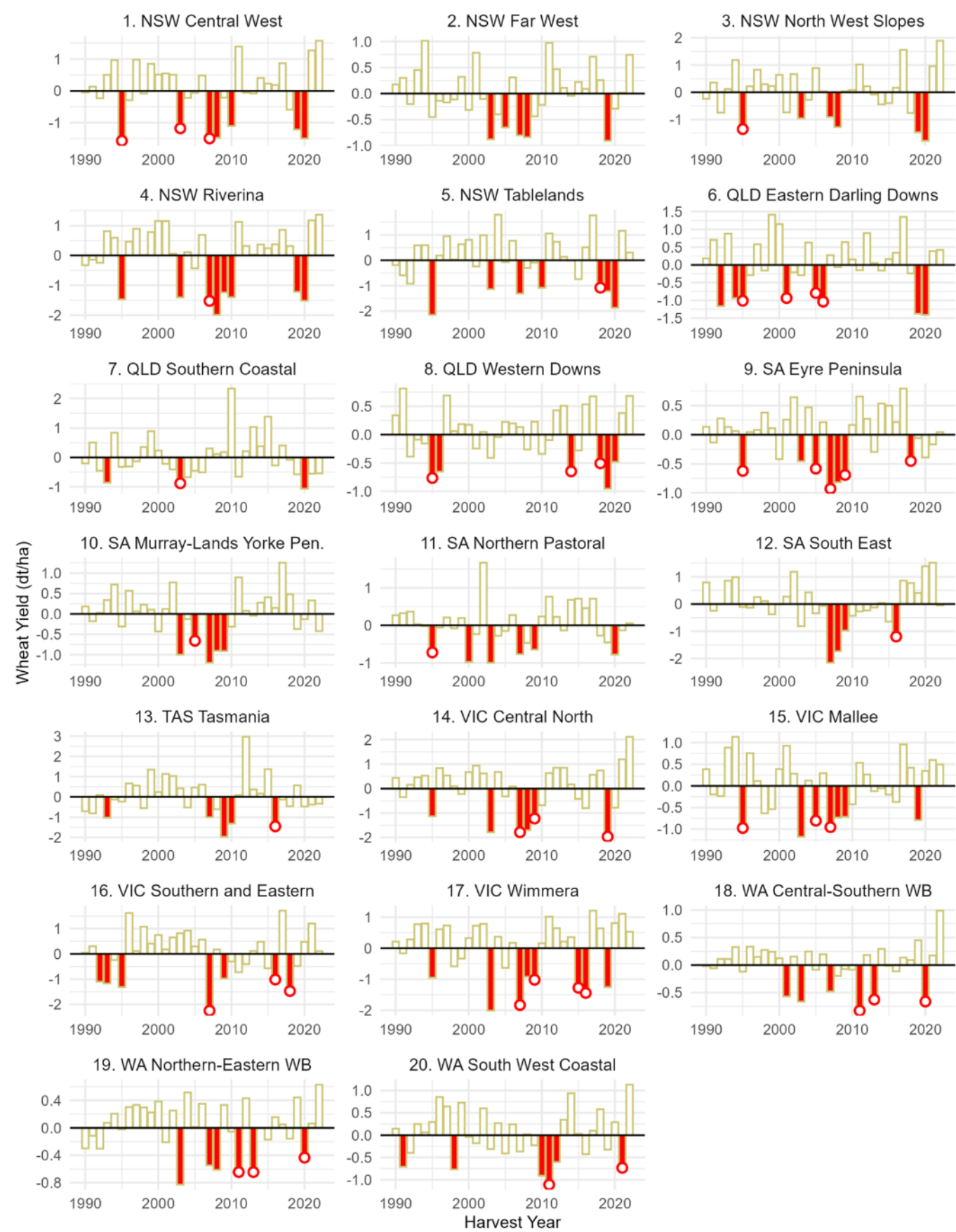
Fig. 41 Wheat Yield Anomalies for ABARES Regions Obtained by Linear Detrending

The y-axis represents wheat yield anomalies (tons/ha), calculated by subtracting the linear trend from yield. The x-axis represents harvest years (1990-2022). Red bars highlight yield anomalies (>1 Sd), while red circles indicate years when these anomalies coincide with CDHE events exceeding the 75th percentile in frequency or severity.
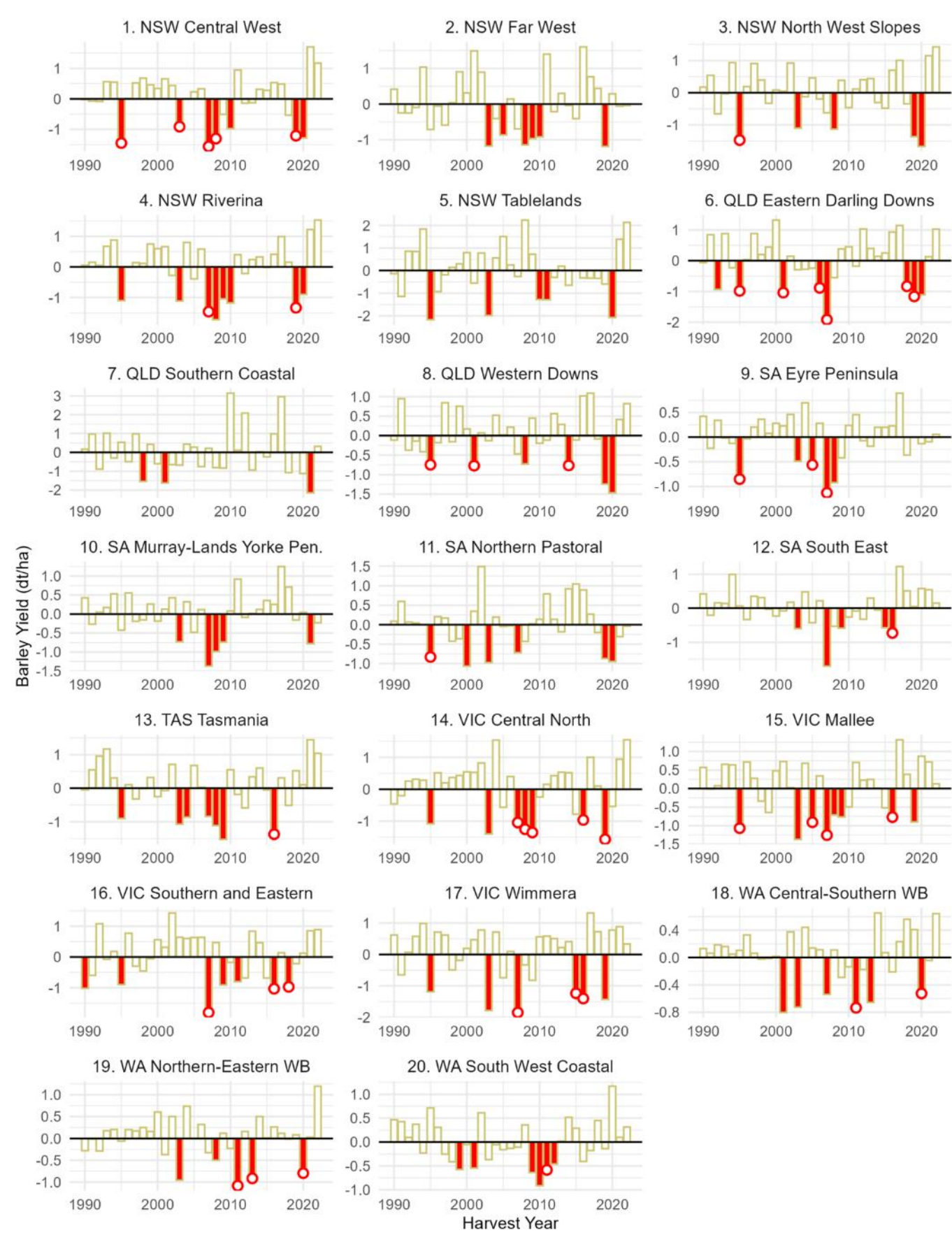
Fig. 42 Barley Yield Anomalies for ABARES Regions Obtained by Linear Detrending

The y-axis represents barley yield anomalies (tons/ha), calculated by subtracting the linear trend from yield. The x-axis represents harvest years (1990-2022). Red bars highlight yield anomalies (>1 Sd), while red circles indicate years when these anomalies coincide with CDHE events exceeding the 75th percentile in frequency or severity.

62
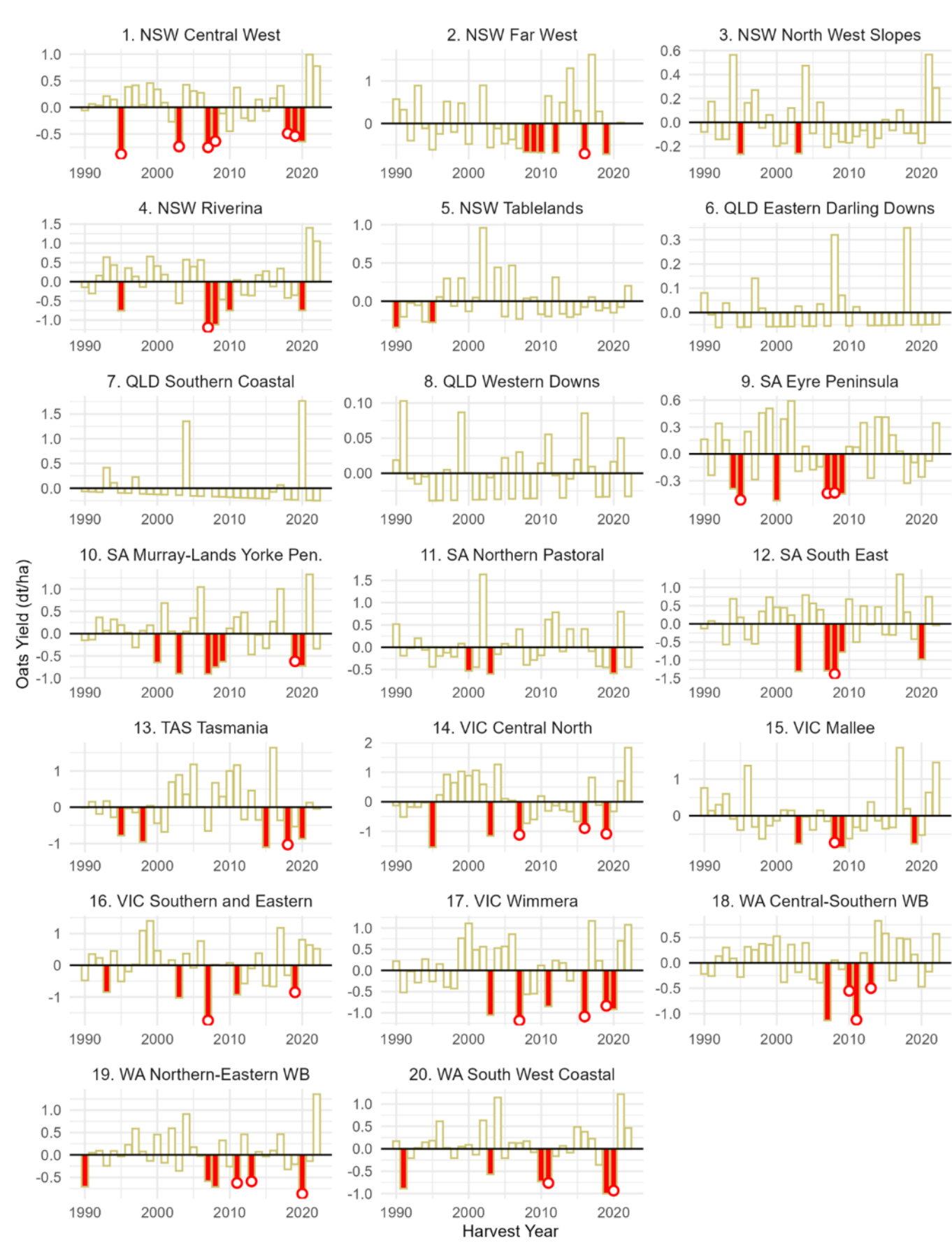
Fig. 43 Oat Yield Anomalies for ABARES Regions Obtained by Linear Detrending

The y-axis represents oat yield anomalies (tons/ha), calculated by subtracting the linear trend from yield. The x-axis represents harvest years (1990-2022). Red bars highlight yield anomalies (>1 Sd), while red circles indicate years when these anomalies coincide with CDHE events exceeding the 75th percentile in frequency or severity.
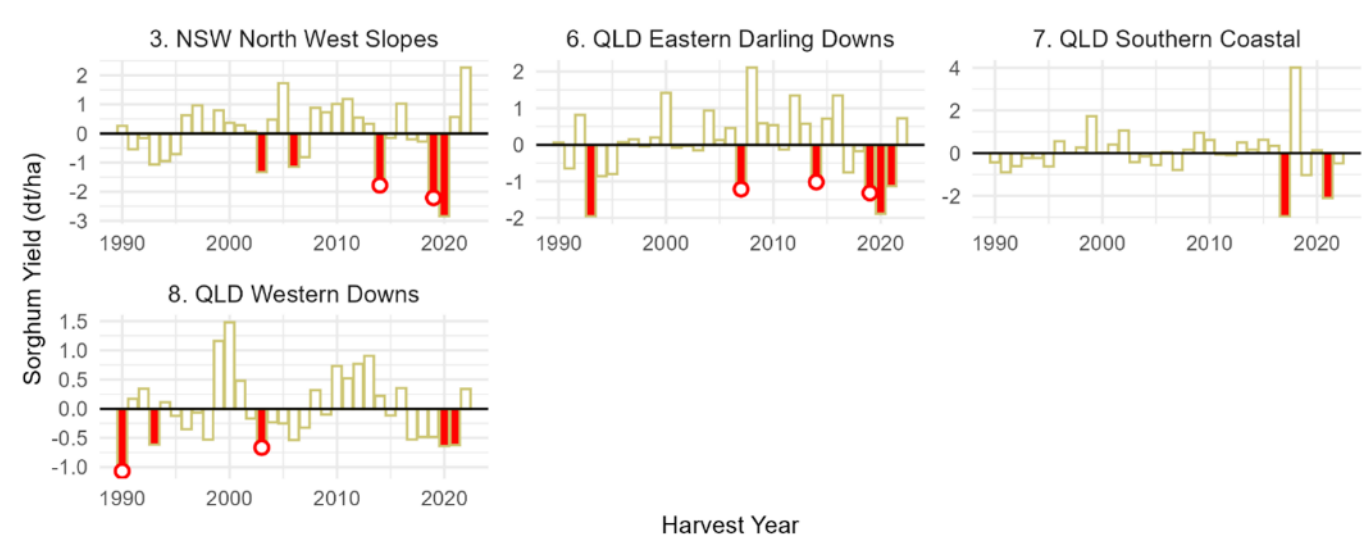
Fig. 44 Sorghum Yield Anomalies for ABARES Regions Obtained by Linear Detrending

The y-axis represents sorghum yield anomalies (tons/ha), calculated by subtracting the linear trend from yield. The x-axis represents harvest years (1990-2022). Red bars highlight yield anomalies (>1 Sd), while red circles indicate years when these anomalies coincide with CDHE events exceeding the 75th percentile in frequency or severity.

To assess the level of statistical significance of the observed CDHE and yield relationships a simple Pearson correlation was applied (Tables 9 and 10). In examining the correlation between CDHE area and severity with detrended yield in Tables 9 and 10, most regions show weak negative correlations, while a few exhibit moderate negative correlations. In particular, region 16: VIC Southern and Eastern has the strongest statistically significant negative correlations (i.e. yield decreases when CDHEs increases) for both wheat (-0.49*, -0.45*) and barley (-0.52*, -0.45*). Statistically significant negative correlations are also seen in region 13: Tasmania wheat (-0.37*), 5: NSW Tablelands barley (-0.39*) and 14: VIC Central North barley (-0.41*). Other prominent negative correlations (not statistically significant) between CDHE area and yield were found in wheat regions 8: QLD Western Downs (-0.29), 13: Tasmania (-0.33), and 19: WA Northern-Eastern WB (-0.27). The same negative correlations were also observed in oats regions 16: VIC Southern and Eastern (-0.34), barley regions 12: SA South East (-0.29), 13: Tasmania (-0.33), and 17: VIC Wimmera (-0.29) as well as sorghum regions 3: NSW North West Slopes (-0.34) and 6,8: QLD Eastern and Western Downs (-0.31 each). Similar patterns are also observed in the severity correlations, although the values tend to be slightly weaker. Overall, the results highlight regional differences in correlation strength between CDHE area and severity, as well as variations across crops, suggesting there are varied responses to CDHEs.

Table 8. Pearson's Correlation between Growing Season CDHE Area and Detrended Yield

ABARES Region	Wheat	Oats	Barley	Sorghum
1. NSW Central West	0.04	0.01	-0.02	NA
2. NSW Far West	-0.08	-0.03	-0.03	NA
3. NSW North West Slopes	-0.21	-0.12	-0.12	-0.34
4. NSW Riverina	0.09	-0.08	-0.08	NA
5. NSW Tablelands	-0.17	-0.23	**-0.39***	NA
6. QLD Eastern Darling Downs	-0.22	-0.1	-0.22	-0.31
7. QLD Southern Coastal	0.07	0.05	0.14	-0.16
8. QLD Western Downs	-0.29	0	-0.05	-0.31
9. SA Eyre Peninsula	-0.1	-0.03	-0.2	NA
10. SA Murray-Lands Yorke Pen.	0.21	0.1	0.3	NA
11. SA Northern Pastoral	0.3	0.11	0.34	NA
12. SA South East	-0.22	0.09	-0.29	NA
13. TAS Tasmania	-0.33	0.25	-0.33	NA
14. VIC Central North	-0.19	-0.26	**-0.41***	NA
15. VIC Mallee	0	0.31	-0.26	NA
16. VIC Southern and Eastern	**-0.49***	-0.34	**-0.52***	NA
17. VIC Wimmera	-0.25	-0.15	-0.29	NA
18. WA Central-Southern WB	-0.23	-0.17	-0.2	NA
19. WA Northern-Eastern WB	-0.27	0.09	-0.23	NA
20. WA South West Coastal	-0.17	0.11	-0.14	NA

Table 9 Pearson's Correlation between Growing Season CDHE Severity and Detrended Yield

ABARES Region	Wheat	Oats	Barley	Sorghum
1. NSW Central West	0.05	-0.01	0.09	NA
2. NSW Far West	-0.08	-0.09	0.01	NA
3. NSW North West Slopes	-0.23	-0.2	-0.07	-0.24
4. NSW Riverina	0.09	-0.16	-0.03	NA
5. NSW Tablelands	-0.06	-0.21	-0.27	NA
6. QLD Eastern Darling Downs	-0.07	0.02	-0.13	-0.1
7. QLD Southern Coastal	0.19	0	0.13	-0.11
8. QLD Western Downs	-0.31	-0.05	-0.04	-0.31
9. SA Eyre Peninsula	-0.19	-0.06	-0.19	NA
10. SA Murray-Lands Yorke Pen.	0.19	0.02	0.25	NA
11. SA Northern Pastoral	0.17	-0.09	0.2	NA
12. SA South East	-0.13	0.05	-0.06	NA
13. TAS Tasmania	**-0.37***	-0.06	-0.25	NA
14. VIC Central North	-0.15	-0.28	-0.31	NA
15. VIC Mallee	-0.1	-0.04	-0.27	NA
16. VIC Southern and Eastern	**-0.45***	-0.29	**-0.45***	NA
17. VIC Wimmera	-0.23	-0.16	-0.11	NA
18. WA Central-Southern WB	-0.25	-0.13	-0.16	NA
19. WA Northern-Eastern WB	-0.26	0.02	-0.19	NA
20. WA South West Coastal	-0.1	0.31	-0.04	NA

Chapter 6 Discussion and Conclusions

6.1 Summary of Key Findings

A summary and interpretation of the results from heatwaves (Results part 1), CDHEs (Results part 2) and yield (Results part 3) with regard to literature forms the first part of the discussion.

6.11 Heatwaves

This study independently developed a new heatwave dataset for Australia and subsequently analysed their historical trends and variability, as detailed in Chapter 3. The heatwave severity classification from Nairn and Fawcett (2015) was applied to partition events by increasing intensity while accounting for regional climate differences. Being able to identify episodes of severe and extreme heatwave events is essential. since these events pose the greatest risks to communities and industries and often necessitate more substantial adaptive responses (Nairn et al., 2018; Trancoso et al., 2020). It was found that longer duration of heatwaves intensifies the EHF magnitude, attesting to Australia's record-breaking heatwaves all exhibiting extreme intensity and duration. The rarest, most intense events are also the ones that exceed critical adaptation thresholds, resulting in heightened vulnerability (Nairn & Fawcett, 2015).

This study has quantified the spatio-temporal variability of heatwaves across Australia and individual growing regions on several timescales, including by days, multi-day events, and aggregated years and months. By analysing the yearly frequency of each heatwave category using the non-parametric Sen Slope with Mann Kendal trend significance, it has been identified that the frequency of all heatwave categories has increased over much of Australia. Increases in heatwave frequency were most evident in low-intensity and severe categories across the long-term record, while extreme heatwaves transitioned from rare, localised events occurring decades apart to widespread events separated by only a few years. The spatial pattern of heatwave frequency Sen Slope trends is consistent with findings by Perkins and Alexander (2013) and Reddy et al. (2021), although this study has higher trend values due to the inclusion of all heatwave durations.

Time series analysis showed heatwave behaviour varies considerably from year to year, with periods of low activity alternating with periods marked by intense, frequent heatwaves. The mean area and total coverage of heatwave events across Australia have shown substantial increases over time. Additionally, years with severe and extreme heatwaves have evolved from sparse small-scale events emerging into years with the most extreme and widespread heatwave disastrous on record, affecting several regions at the same time.

Australia's sensitivity to experiencing heatwave days covering nearly the entire continent has also risen across all types of heatwaves. In January 2021, an extreme heatwave day set the record for widespread impact, affecting nearly the whole continent, and similar patterns were observed for severe heatwaves and

low-intense spells between 2021-2022. This may be considered unusual given that January 2021 occurred during a La Nina phase, whereas most heatwaves have previously occurred under El Nino conditions (Reddy et al., 2022). The La Nina phase in 2022 contributed to cooler conditions and extreme rainfall over Eastern Australia; however, despite this, Western Australia experienced record-breaking temperatures and heatwaves in January 2021 (Macadam et al., 2022). Previous heatwave studies that only consider 3-day events may overlook these widespread occurrences. Short-duration extreme heatwaves are also associated with other types of CEs, including compound heatwaves and extreme rainfall events. The dynamics of daily heatwaves have been shown to influence precipitation extremes, potentially preconditioning extreme rainfall (Sauter et al., 2023). Extreme heatwaves may also be further evidence of the increasing fingerprint of climate change on heatwaves in Australia outside of natural variability (Lane et al., 2023).

Regional analysis affirms the most extreme heatwave impacts in terms of severity and duration coincide with ABARES growing regions. Statistical analysis found that some of the highest EHF magnitudes and longest events have overlapped with growing regions. This has also been observed on a yearly timescale, with the regional heatmap of extreme heatwave severity showing a clear clustering of extreme events since the 2000s. The total area coverage of the yearly regional heatwaves has also been found to increase across growing regions. The timing of severe and extreme heatwave impacts has also shifted earlier, with the heatwave season extending into late summer. This overarching analysis confirms that new heatwave extremes have emerged, placing unprecedented pressures on Australian agriculture, as also discussed in earlier research (He et al., 2022; Ridder, Pitman, & Ukkola, 2022).

6.12 CDHEs

The study then moved on to an analysis of CDHEs across Australia, as detailed in Chapter 4. A new Australia-wide data set of CDHEs was developed based on the intersection of both droughts (defined by the PDSI) and heaves (from the EHF). The analysis confirmed that CDHEs have expanded in area, frequency, and severity over the past two decades, with abrupt increases in South East Australia, Queensland, and both South West and East Western Australia. These findings align with prior studies by Laz et al. (2023), Reddy et al. (2022), and Ridder, Pitman and Ukkola (2022). Previous Australian CDHE research has focused on summer-season CDHEs from November to March, targeting human impacts (Laz et al., 2023; Reddy et al., 2022), whereas this study targets agricultural impacts, considering a broader heatwave definition to identify heatwaves year around for all durations as well as the sc-PDSI index for improved recognition of agricultural drought. Since this study used a different approach, there were small differences between the spatial patterns; however, the overarching trends were still consistent. Additionally, heatwave severity categories are included alongside drought levels, which previous studies did not examine.

Somewhat counterintuitive was the finding that CDHEs are most prevalent during mild droughts, becoming less widespread as drought severity increases. However, this is consistent with previous findings and is reflective of the decrease in the occurrence of extreme droughts compared to mild as defined by the PDSI (Laz et al., 2023). As expected, CDHEs affect less area than heatwaves, with most CDHEs associated with low-intense spells. Low-intense spell CDHEs of all drought levels have shown the largest increases in frequency and area, contributing most to the recent rises from 2000 to 2022. Mapping the average area affected by each drought-heatwave combination further identifies the constraints of each combination; those involving extreme drought from 2000 to 2022 are largely limited to eastern Australia and central and southwest parts of WA. CDHE severity is also dependent on location, exhibiting higher levels in southeast, southern, and western Australia. Of concern is that new hotspots in both frequency and severity have been identified in South West WA, also aligning with WA's wheat belt growing regions.

Severe and extreme CDHEs are rare, averaging six days per year, with longer-duration severe and extreme events even less frequent. Despite their rarity, there is evidence that the severity and duration of both heatwaves and droughts influence CDHE daily magnitude, with the most extreme events occurring in severe and extreme drought and heatwave CDHEs. This is consistent with previous findings of Geirinhas et al. (2021), who identified the most intense CDHE magnitudes corresponded to extreme and long-lasting heatwave classes during severe drought.

Time series analysis revealed that CDHE behaviour varies greatly between years and across seasons yet shows a clear increasing trend in mean area and total annual coverage. Years with severe and extreme heatwave CDHEs were found to contribute less to total severity; however, the spread and severity contribution of these occurrences spiked in recent years, including 2019, 2021, and 2022, also aligning with broader heatwave trends. Sen Slope trends of CDHE frequency and severity identify southeastern and western Australia, particularly ABARES growing regions, as the areas most exposed to CDHEs over the long term. While these trends differ from AWAP data analysed by Reddy et al. (2022) due to CDHE definition differences, both studies have found an intensification and expansion of CDHE hotspots in southeastern and western Australia since the 2000s.

The regional CDHE analysis confirms that the most severe and extreme CDHE events are closely aligned with Australian growing areas and occur during growing months. A shift toward higher frequency CDHEs within growing regions, including more severe and extreme heatwaves and droughts was identified in the 2000-2022 period. The limited number of observations for some heatwave and drought combinations means that not all categories occur every year and are confined to specific areas. Since historical records are constrained, the potential variability within some categories could not be fully captured, leading the analysis to focus on broader CDHE categories. Statistical analysis of regional CDHE metrics revealed substantial variation in CDHE daily magnitude, regional frequency and severity, as well as event duration across

regions. Regions with the highest daily CDHE magnitudes include 11: SA Northern Pastoral, 8: Queensland Western Downs, and 18-20: WA. Most CDHE events lasted between 1 and 4 days, with rare instances extending three to five months across growing regions. Monthly CDHE severity exhibited interannual variability; however, the applied definition effectively captured year-round CDHE events. Most regional CDHE activity was identified between August and February, with additional detection of critical autumn and winter events that impact crop yield.

This study has successfully created both a heatwave and CDHE dataset and explored spatio-temporal trends in frequency, severity, duration, area and seasonality Australia-wide and by growing regions. Further, the final datasets have successfully applied the methodology from previous studies while refining to be suitable for analysis of the agricultural impacts of CDHEs on cereal crop yield.

6.13 Yield

Chapter 5 has looked into the variability of cereal crop yield anomalies and how they are linked to CDHEs. Previous climate yield studies in Australia have only considered individual hazards and are limited to just wheat. The long-term, state-wide production records for wheat, available since 1900, have supported previous hazard yield assessments of Hague et al. (2016) over a longer historical timeline. An assessment of climate hazards on NSW shire-level wheat data available from 1922 has also been conducted by Wang et al. (2015). However, Australia-wide regional analysis, including other cereal crops presented in this study, has extended the results of previous findings while also identifying the impact of CDHEs. This study has identified that yield anomalies frequently occur together, particularly across wheat, oats and barley. The largest combined yield anomalies have also been identified in NSW and VIC growing regions.

Time series analysis identified significant signals from regional CDHE area and severity that aligned with several yield anomalies for wheat, barley, and oats, mainly in VIC: Southern and Eastern and Wimmera, SA: Eyre Peninsula, Northern Pastoral, South East, WA wheat belts and Tasmania. A similar trend was observed for sorghum in NSW North West Slopes and QLD Eastern and Western Downs. These patterns were also reflected in Pearson's correlations, showing negative relationships between CDHE activity and detrended yield in growing months. Statistically significant negative correlations were found in Southern and Eastern Victoria for wheat and barley (-0.49, -0.45), Tasmania for wheat (-0.37), NSW Tablelands for barley (-0.39), and Central North Victoria for barley (-0.41). These findings align with broader observations by Hague et al. (2016), which reported negative correlations between heatwave days and detrended wheat yield from 1911 to 2012, including -0.51 in Southeast Australia and -0.31 in Southwest Western Australia. The difference in values is attributable to the study's smaller regional focus and shorter timeframe. This study also links yield anomalies to CDHE events, highlighting their potential to reduce crop yield, with varying impacts across regions.

The recent shift towards unprecedented severe and extreme heatwaves and CDHEs is expected to intensify under climate change, as droughts increase the intensity of heatwaves, shifting previously rare events to a new normal (He et al., 2022). This shift also means a greater overlap of these events with critical growing periods, posing significant challenges for agriculture (Afroz et al., 2023). However, crop yields are influenced by not only heat and drought but also a variety of other extreme weather events and natural hazards, which together pose significant food security risks. These include seasonal rainfall deficiencies, frost days, floods, cold waves, flash droughts, extreme humidity, and other CEs (Hague et al., 2016; Malik et al., 2022; Sauter et al., 2023). In a warming world, the variability, intensity and frequency of extreme weather and climatic extremes are expected to increase, creating further challenges for agriculture (Bevacqua et al., 2021). Climate change is also expected to reduce winter and spring rainfall across large areas of Australia and increase heatwaves, particularly during the spring, which will expose crops to more droughts, heatwaves, and CDHEs (Wang et al., 2015). Climate change also accelerates crop phenology, leading to shorter growing seasons (Lamaoui et al., 2018).

Adapting to these agricultural impacts of extreme weather presents substantial challenges. In drought years, farmers have responded by delaying sowing to reduce the risk of heat stress around flowering but may be at the expense of frost risk (Lamaoui et al., 2018; Wang et al., 2015). Irrigation is also employed to mitigate heatwave impacts by cooling surface temperatures, though this approach is limited by water availability. Farmers have also adapted to sow only in areas with adequate water, as well as by planting crop varieties that mature earlier or later (Lamaoui et al., 2018).

This study has successfully linked cereal crop yield anomalies to CDHEs across growing regions, revealing that some regions have distinct responses to these events. Insights from this work provide a solid foundation for future research, which could further explore the seasonal impacts of CDHEs on yield, assess potential future impacts of CDHEs and other hazards under climate change, and explore farmers' adaptation measures. Investigating the effects of climate variability on yield will be essential for managing crop cultivation under future climate conditions.

6.2 Summary of Future Work

Although the findings reported here are based on observational data and available analytical methods, certain limitations remain that should be addressed in future studies. This section discusses improvements and additional directions for future work, including methodology enhancements, and additional analyses.

6.21 Methodology Enhancements

The heatwave data in this study is derived from the Australian Gridded Climate Data, which interpolates temperature from observational records. However, uncertainty arises in gridded datasets, particularly in sparsely monitored regions like central-west Australia (Jones et al., 2009). To mitigate this, Reddy et al. (2022) suggest masking data beyond a 2° radius from a station to minimise interpolation errors. Laz et al. (2023) also further refined CDHE detection by using ground-based weather stations in southeastern Australia, achieving a finer 30 km resolution. Although the Mann-Kendall test is employed in this study, its trend magnitudes are susceptible to random noise, potentially inflating trends. To counter this, Reddy et al. (2021) apply a Savitzky-Golay third-order polynomial filter to smooth random noise. Additionally, the Mann-Kendall test may falsely indicate trends due to data autocorrelation. Previous studies have employed pre-whitening techniques to remove autocorrelation to further improve trend attribution (Reddy et al., 2021). To further strengthen the trends presented in this study, future work could consider refinement of the data and trend analysis using the above techniques.

In addition, the modelling to detect relationships between climate variables and yield impacts could be further expanded on. This study has been limited by the extremes available in the observational record of CDHEs, which did not occur enough to be able to test each heatwave and drought category. This limitation has been addressed in other CDHE studies through the use of climate model simulations (e.g. CIMP6, CORDEX); however, it has not been linked to yield in Australia (Zengchao. Hao et al., 2022; Reddy et al., 2022; Ridder, Pitman, & Ukkola, 2022). There is also the ability to conduct crop model simulations for various extreme conditions, successfully employed by Vogel et al. (2021).

There are also other methods for attributing relationships between yield and CDHEs, including machine learning and multivariate statistical models. Machine learning methods such as Random Forest (RF) models have been highly regarded for detecting relationships between climate variables and impacts (Beillouin et al., 2020). For instance, Zhang et al. (2024) applied RF models with both mean and extreme climate predictors to explain yield variability in China, highlighting precipitation and the number of CDHE days as key constraints to maize production.

Multivariate techniques have been used to evaluate the additional impact of CDHEs compared to individual hazards using joint probabilities. One prominent approach, the meta-Gaussian model (also known as the Gaussian copula), has been used to test the probability of crop yield reduction from droughts, heatwaves and their combination (Afroz et al., 2023; Feng et al., 2019; Hao et al., 2018). Afroz et al. (2023) used this method in the top five maize producing countries, finding that in the USA, the probability of yield reduction increased by 31% during CDHEs, compared to 4% for heatwaves and 7% for droughts alone.

6.22 Identifying CDHE Drivers

A better understanding of the underlying physical mechanisms and drivers of heatwaves, droughts, and CDHEs can help improve their predictability. Driver analysis also helps determine how these events will evolve under climate change and natural variability (Zengchao. Hao et al., 2022; Ndayiragije & Li, 2022). Several Australian studies have investigated the driving mechanisms behind intense and prolonged heatwaves. At the synoptic scale, heatwaves and CDHEs are driven by low-pressure systems that can recirculate hot air masses, lasting for days and, in rare cases, several weeks (Nairn, 2022; Reddy et al., 2022). During CDHEs, dry soils further exacerbate heatwave intensity by reducing evaporative cooling (Zengchao. Hao et al., 2022). Both extreme heatwaves and CDHEs are also associated with delayed seasonal rainfall and elevated nighttime temperatures (Zengchao. Hao et al., 2022).

On a global scale, both high temperatures and droughts are driven by circulation patterns and modes of climate variability, including the El Niño-Southern Oscillation (ENSO), Indian Ocean Dipole (IOD), Interdecadal Pacific Oscillation (IPO), Madden-Julian Oscillation (MJO), and Southern Annular Mode (SAM) (Reddy et al., 2022; Verdon-Kidd & Kiem, 2009). High-intensity and widespread heatwaves and CDHEs in Australia have been linked to co-occurring El Niño and positive IOD phases (Reddy et al., 2022). Future research could consider the roles of other climate drivers (such as IPO, MJO, and SAM) and their interactions across different types of heatwaves, CDHEs, and other CEs like heatwaves and intense rainfall. Additionally, assessing global drivers of CDHEs and potential teleconnections could clarify how drivers may trigger simultaneous yield impacts in multiple countries (Zengchao. Hao et al., 2022). Such insights could improve the seasonal-scale predictability of various CEs, supporting agricultural risk reduction efforts to protect crop yields.

Due to the temporal limitations of Australia's instrumental rainfall records (120 years at most) and the complex drivers behind drought, past research has leveraged paleoclimate data to provide a broader historical context. Indeed, the Millennium drought marked the lowest 13-year rainfall record since 1865; however, historically, droughts have been longer, more widespread, and more severe (BOM, 2020; Verdon-Kidd & Kiem, 2009) For example, 'megadroughts' lasting over 30 years have been identified in southwestern Australia (1755–1785 CE), and the most severe drought period in terms of rainfall deficit in the last seven centuries was identified between 1876-1888 (O'Donnell et al., 2021). Multiple studies have shown that the instrumental rain record is insufficient for estimating drought risk (Verdon-Kidd et al., 2017). Given these paleoclimate reconstructions, the risk of prolonged and more severe droughts and CDHEs in Australia may be greater than previously understood, with potentially more extreme impacts. Thus, future research could expand driver analysis to evaluate past drought variability, offering insights that support more agricultural risk reduction.

6.24 Creating Other Impact-based Models for Different CDHEs

The impact of historical climate hazards (heatwaves, droughts, floods, and CE) on crop yields can be assessed using impact-based metrics that do not rely on hazard thresholds. This is because yields may also be affected by the cumulative frequency and intensity of milder events as well as the lead and lag effects (Brás et al., 2021). One impact-based approach, Superimposed Epoch Analysis (SEA) composites multiple events into a signal to isolate impacts relative to the years preceding, during, and following the hazard. Brás et al. (2021) applied SEA to examine the impacts of extreme weather on crop yields during two periods, 1961-1990 and 1991-2015. Their findings indicate that heatwaves and droughts roughly tripled production losses, increasing from -3.6% to -9.8%, while yield losses doubled from -4.4% to -8.9%. This method could also be applied to CDHEs, providing insights into the sensitivity of yield impacts to various categories of heatwaves and droughts within CDHEs. This also opens up opportunities for future research on the complex interactions between CEs and crop production.

6.3 Significance of Findings and Conclusion

The significance of findings in this study includes the applicability of understanding historical CDHE spatio-temporal variability in growing regions, and the impacts of CDHEs on cereal crop yield. Insights into CDHEs and their potential to negatively affect crop yield are pivotal for assessing Australia's exposure and risks of CDHEs. Understanding climate vulnerabilities and the impacts of natural hazards on yield is also important for enabling agricultural stakeholders to anticipate, prepare for, and mitigate adverse climate impacts more effectively as well as for improving climate governance. The Environmental, Social, and Governance (ESG) framework highlights the broader significance of this research, as shown in Table 10.

Table 10 Environmental, Social and Governance (ESG) for CDHEs

Category	Subcategory	Key Points
Environment	Water Resource Management	• CDHEs have cascading effects on water supply and ecosystems. • This study provides insights into the spatio-temporal trends in CDHEs
	Climate Risk	• CDHEs are expected to intensify under climate change. • This study assesses climate risk by identifying the most impacted regions
Social	Food Security	• CDHEs pose threats to global food security. • Crop yield impacts are studied. • A foundation for a risk assessment for policymakers and agricultural stakeholders.
	Livelihoods and Economic Stability	• CDHEs have significant economic and livelihood impacts. • Quantification of CDHE impacts aids decision-making for governments and businesses. • Enhances resilience.
Governance Considerations	Risk Assessment Framework	• A risk framework for CDHEs is vital for climate governance. • Assists policymakers and organisations in making informed decisions for climate change adaptation and mitigation.

The impacts of CDHEs are complex, highlighting the need for multidisciplinary collaboration among scientists, agricultural experts, health professionals, and government agencies. There is scope for future studies to explore mitigation and adaptation strategies for CDHEs to increase resilience. Future research could also assess the impact of CDHEs on food supply systems, health, agriculture, and humans.

This study provides novel insights into Australian CDHEs, introducing a refined definition of CDHEs that considers their impact on crop yield. The findings enhance the recognition of agricultural droughts alongside seasonal heatwaves, revealing that both have occurred widely across Australia, with an abrupt increase in frequency since the 2000s. This trend is particularly pronounced for extreme heatwaves and CDHEs involving severe and extreme drought conditions. Additionally, CDHEs have been linked to yield anomalies in key cereal crops, including wheat, oats, barley, and sorghum. The high sensitivity of cereal crop yields in growing regions including Southern and Eastern and Wimmera Victoria, SA Eyre Peninsula, Northern Pastoral, and South East, WA wheat belts and Tasmania to CDHEs also raises concerns for the future, as CDHEs are expected to further increase in frequency and severity under climate change. This study also articulates the vulnerability of Australian cereal crops to climate-related hazards and extreme weather events, which pose a major threat to food security.

References

Afroz, M., Chen, G., & Anandhi, A. (2023). Drought- and heatwave-associated compound extremes: A review of hotspots, variables, parameters, drivers, impacts, and analysis frameworks [Systematic Review]. *Frontiers in Earth Science, 10*. https://doi.org/10.3389/feart.2022.914437

Argüeso, D. (2024). *dargueso/EHF: v2.1 (v2.1)*. Retrieved Feburary 29, 2024 from https://github.com/dargueso/EHF?tab=readme-ov-file

Argüeso, D., Di Luca, A., Evans, J. P., Parry, M., Gross, M., Alexander, L. V., & Perkins-Kirkpatrick, S. E. (2015). *NARCliM Technical Note 5 Heatwaves affecting NSW and the ACT: recent trends, future projections and associated impacts on human health*. Sydney, Australia Retrieved from https://www.climatechange.environment.nsw.gov.au/sites/default/files/2021-06/Heatwaves%20NARCliM%20Technical%20Note%205.pdf

Aubrecht, C., Fuchs, S., & Neuhold, C. (2013). Spatio-temporal aspects and dimensions in integrated disaster risk management. *Natural Hazards, 68*(3), 1205-1216. https://doi.org/10.1007/s11069-013-0619-9

Australian Bureau of Agricultural and Resource Economics and Sciences (ABARES - DAFF). (2023b). *Farm surveys definitions and methods*. https://www.agriculture.gov.au/abares/research-topics/surveys/farm-definitions-methods#regions

Australian Bureau of Meteorology (BOM). (2019). *Special Climate Statement 68—widespread heatwaves during December 2018 and January 2019*. http://www.bom.gov.au/climate/current/statements/scs68.pdf

Australian Bureau of Meteorology (BOM). (2020). *Previous droughts*. Retrieved March 11th, 2024 from http://www.bom.gov.au/climate/drought/knowledge-centre/previous-droughts.shtml#:~:text=The%20Millennium%20drought%3A%201997%20to%202009,-%5Bback%20to%20top&text=Between%201997%20and%202009%20much,cropping%20zones%20were%20severely%20affected

Australian Bureau of Meteorology (BOM). (2023). *Australian Gridded Climate Data (AGCD) / AWAP ; v1.0.1 Snapshot (1900-01-01 to 2022-12-31). Downloaded from NCI*. Retrieved March 2nd, 2024 from https://doi.org/10.25914/hjqj-0x55

Australian Bureau of Statistics (ABS). (2022). *Value of Agricultural Commodities Produced, Australia*. Retrieved february 29, 2024 from https://www.abs.gov.au/statistics/industry/agriculture/value-agricultural-commodities-produced-australia/latest-release#value-of-crops

Beillouin, D., Schauberger, B., Bastos, A., Ciais, P., & Makowski, D. (2020). Impact of extreme weather conditions on European crop production in 2018. *Philosophical Transactions of the Royal Society B: Biological Sciences, 375*(1810), Article 20190510. https://doi.org/10.1098/rstb.2019.0510

Bevacqua, E., De Michele, C., Manning, C., Couasnon, A., Ribeiro, A. F. S., Ramos, A. M., Vignotto, E., Bastos, A., Blesić, S., Durante, F., Hillier, J., Oliveira, S. C., Pinto, J. G., Ragno, E., Rivoire, P., Saunders, K., van der Wiel, K., Wu, W., Zhang, T., & Zscheischler, J. (2021). Guidelines for Studying Diverse Types of Compound Weather and Climate Events. *Earth's Future, 9*(11), Article e2021EF002340. https://doi.org/10.1029/2021EF002340

Brás, T., Seixas, J., Carvalhais, N., & Jägermeyr, J. (2021). Severity of drought and heatwave crop losses tripled over the last five decades in Europe. *Environmental Research Letters, 16*(6), Article 065012. https://doi.org/10.1088/1748-9326/abf004

Breshears, D. D., Fontaine, J. B., Ruthrof, K. X., Field, J. P., Feng, X., Burger, J. R., Law, D. J., Kala, J., & Hardy, G. E. S. J. (2021). Underappreciated plant vulnerabilities to heat waves. *New Phytologist, 231*(1), 32-39. https://doi.org/https://doi.org/10.1111/nph.17348

Cheng, W., Li, D., Liu, Z., & Brown, R. D. (2021). Approaches for identifying heat-vulnerable populations and locations: A systematic review. *Science of The Total Environment, 799*, Article 149417. https://doi.org/10.1016/j.scitotenv.2021.149417

Climate Council. (2015). *Thirsty country: climate change and drought in Australia* [Report]. https://www.climatecouncil.org.au/droughtreport2015

Climatic Research Unit, U. o. E. A. (2021). *DROUGHT INDICES Self-calibrating Palmer Drought Severity Index (scPDSI)*. https://crudata.uea.ac.uk/cru/data/drought/

Cui, P., Peng, J., Shi, P., Tang, H., Ouyang, C., Zou, Q., Liu, L., Li, C., & Lei, Y. (2021). Scientific challenges of research on natural hazards and disaster risk. *Geography and Sustainability, 2*(3), 216-223. https://doi.org/https://doi.org/10.1016/j.geosus.2021.09.001

Devanand, A., Falster, G. M., Gillett, Z. E., Hobeichi, S., Holgate, C. M., Jin, C., Mu, M., Parker, T., Rifai, S. W., Rome, K. S., Stojanovic, M., Vogel, E., Abram, N. J., Abramowitz, G., Coats, S., Evans, J.

P., Gallant, A. J. E., Pitman, A. J., Power, S. B., . . . Ukkola, A. M. (2024). Australia's Tinderbox Drought: An extreme natural event likely worsened by human-caused climate change. *Science Advances*, *10*(10), eadj3460. https://doi.org/doi:10.1126/sciadv.adj3460

Ding, Y., Hayes, M. J., & Widhalm, M. (2011). Measuring economic impacts of drought: a review and discussion. *Disaster Prevention and Management: An International Journal*, *20*(4), 434-446. https://doi.org/10.1108/09653561111161752

Feng, S., Hao, Z., Zhang, X., & Hao, F. (2019). Probabilistic evaluation of the impact of compound dry-hot events on global maize yields. *Science of The Total Environment*, *689*, 1228-1234. https://doi.org/10.1016/j.scitotenv.2019.06.373

Gallic, E., & Vermandel, G. (2020). Weather shocks. *European Economic Review*, *124*, 103409. https://doi.org/https://doi.org/10.1016/j.euroecorev.2020.103409

Geirinhas, J., Russo, A., Libonati, R., Sousa, P., Miralles, D., & Trigo, R. (2021). Recent increasing frequency of compound summer drought and heatwaves in Southeast Brazil. *Environmental Research Letters*, *16*(3), Article 034036. https://doi.org/10.1088/1748-9326/abe0eb

Gibson, A. J., Verdon-Kidd, D. C., & Hancock, G. R. (2022). Characterising the seasonal nature of meteorological drought onset and termination across Australia. *Journal of Southern Hemisphere Earth Systems Science*, *72*(1), 38-51. https://doi.org/10.1071/ES21009

Hague, B., Braganza, K., & Jones, D. (2016). Effects of heat extremes on wheat yields in Australia. *Journal of Southern Hemisphere Earth System Science*, *66*, 314-341. https://doi.org/10.22499/3.6603.005

Hao, Z., Hao, F., Singh, V. P., Xia, Y., Shi, C., & Zhang, X. (2018). A multivariate approach for statistical assessments of compound extremes. *Journal of Hydrology*, *565*, 87-94. https://doi.org/10.1016/j.jhydrol.2018.08.025

Hao, Z., Hao, F., Xia, Y., Feng, S., Sun, C., Zhang, X., Fu, Y., Hao, Y., Zhang, Y., & Meng, Y. (2022). Compound droughts and hot extremes: Characteristics, drivers, changes, and impacts. *Earth-Science Reviews*, *235*, 104241. https://doi.org/https://doi.org/10.1016/j.earscirev.2022.104241

Hao, Z., Hao, F., Xia, Y., Feng, S., Sun, C., Zhang, X., Fu, Y., Hao, Y., Zhang, Y., & Meng, Y. (2022). Compound droughts and hot extremes: Characteristics, drivers, changes, and impacts. *Earth-Science Reviews*, *235*, Article 104241. https://doi.org/10.1016/j.earscirev.2022.104241

He, Y., Fang, J., Xu, W., & Shi, P. (2022). Substantial increase of compound droughts and heatwaves in wheat growing seasons worldwide. *International Journal of Climatology*, *42*(10), 5038-5054. https://doi.org/https://doi.org/10.1002/joc.7518

IPCC. (2021). Summary for Policymakers. In V. Masson-Delmotte, P. Zhai, A. Pirani, S. L. Connors, C. Péan, S. Berger, N. Caud, Y. Chen, L. Goldfarb, M. I. Gomis, M. Huang, K. Leitzell, E. Lonnoy, J. B. R. Matthews, T. K. Maycock, T. Waterfield, O. Yelekçi, R. Yu, & B. Zhou (Eds.), *Climate Change 2021: The Physical Science Basis. Contribution of Working Group I to the Sixth Assessment Report of the Intergovernmental Panel on Climate Change* (pp. 3-32). Cambridge University Press. https://doi.org/10.1017/9781009157896.001

IPCC. (2022). Summary for Policymakers. In H.-O. Portner, D. Roberts, C. Trisos, N. Simpson, & V. Möller (Eds.), *Climate Change 2022: Impacts, Adaptation, and Vulnerability. Contribution of Working Group II to the Sixth Assessment Report of the Intergovernmental Panel on Climate Change*. Cambridge University Press. https://doi.org/10.1017/9781009325844.001

Jones, D., Wang, W., & Fawcett, R. J. B. (2009). High-quality spatial climate data-sets for Australia. *Australian Meteorological and Oceanographic Journal*, *58*, 233-248. https://doi.org/10.22499/2.5804.003

Kiem, A. S., Johnson, F., Westra, S., van Dijk, A., Evans, J. P., O'Donnell, A., Rouillard, A., Barr, C., Tyler, J., Thyer, M., Jakob, D., Woldemeskel, F., Sivakumar, B., & Mehrotra, R. (2016). Natural hazards in Australia: droughts. *Climatic Change*, *139*(1), 37-54. https://doi.org/10.1007/s10584-016-1798-7

Kingwell, R. (2019). *Australia's Grain Outlook 2030*. Grains Research & Development Corporation (GRDC) Retrieved from https://aegic.org.au/wp-content/uploads/2021/03/AEGIC-Australias-Grain-Outlook-2030.pdf

Lamaoui, M., Jemo, M., Datla, R., & Bekkaoui, F. (2018). Heat and Drought Stresses in Crops and Approaches for Their Mitigation [Review]. *Frontiers in Chemistry*, *6*, Article 26. https://doi.org/10.3389/fchem.2018.00026

Lane, T. P., King, A. D., Perkins-Kirkpatrick, S. E., Pitman, A. J., Alexander, L. V., Arblaster, J. M., Bindoff, N. L., Bishop, C. H., Black, M. T., Bradstock, R. A., Clarke, H. G., Gallant, A. J. E., Grose, M. R., Holbrook, N. J., Holland, G. J., Hope, P. K., Karoly, D. J., Raupach, T. H., & Ukkola, A. M. (2023). Attribution of extreme events to climate change in the Australian region – A review. *Weather and Climate Extremes*, *42*, 100622. https://doi.org/https://doi.org/10.1016/j.wace.2023.100622

Laz, O. U., Rahman, A., & Ouarda, T. B. M. J. (2023). Compound heatwave and drought hotspots and their trends in Southeast Australia. *Natural Hazards*, *119*(1), 357-386. https://doi.org/10.1007/s11069-023-06115-6

Leonard, M., Westra, S., Phatak, A., Lambert, M., van den Hurk, B., McInnes, K., Risbey, J., Schuster, S., Jakob, D., & Stafford-Smith, M. (2014). A compound event framework for understanding extreme impacts. *WIREs Climate Change*, *5*(1), 113-128. https://doi.org/https://doi.org/10.1002/wcc.252

Macadam, I., Crimp, A., Devanand, A., Gillett, Z., Kajtar, J., King, M., Parker, T., Patel, R., Purich, A., Reid, K., Shao, Y., & Brown, A. (2022). *The state of weather and climate extremes 2021*.

Malik, A., Li, M., Lenzen, M., Fry, J., Liyanapathirana, N., Beyer, K., Boylan, S., Lee, A., Raubenheimer, D., Geschke, A., & Prokopenko, M. (2022). Impacts of climate change and extreme weather on food supply chains cascade across sectors and regions in Australia. *Nature Food*, *3*(8), 631-643. https://doi.org/10.1038/s43016-022-00570-3

Mann, H. B. (1945). Nonparametric Tests Against Trend. *Econometrica*, *13*, 245.

Maughan, R. J. (2012). Hydration, morbidity, and mortality in vulnerable populations. *Nutrition Reviews*, *70*(s2), S152-S155. https://doi.org/10.1111/j.1753-4887.2012.00531.x

McArley, T. J., Morgenroth, D., Zena, L. A., Ekström, A. T., & Sandblom, E. (2022). Prevalence and mechanisms of environmental hyperoxia-induced thermal tolerance in fishes. *Proceedings of the Royal Society B: Biological Sciences*, *289*(1981), 20220840. https://doi.org/doi:10.1098/rspb.2022.0840

Mukherjee, S., Mishra, A., & Trenberth, K. E. (2018). Climate Change and Drought: a Perspective on Drought Indices. *Current Climate Change Reports*, *4*(2), 145-163. https://doi.org/10.1007/s40641-018-0098-x

Muleke, A., Harrison, M. T., Yanotti, M., & Battaglia, M. (2022). Yield gains of irrigated crops in Australia have stalled: the dire need for adaptation to increasingly volatile weather and market conditions. *Current Research in Environmental Sustainability*, *4*, Article 100192. https://doi.org/10.1016/j.crsust.2022.100192

Nairn, J. (2022). *Measurement, impact and mitigation of heatwaves* https://hdl.handle.net/2440/135484

Nairn, J., Ostendorf, B., & Bi, P. (2018). Performance of Excess Heat Factor Severity as a Global Heatwave Health Impact Index. *International Journal of Environmental Research and Public Health*, *15*(11), 2494. https://www.mdpi.com/1660-4601/15/11/2494

Nairn, J. R., Beaty, M., & Varghese, B. (2021). Australia's Black Summer heatwave impacts. *Australian Journal of Emergency Management*, *36*, 17-20. https://knowledge.aidr.org.au/resources/ajem-january-2021-australia-s-black-summer-heatwave-impacts/

Nairn, J. R., & Fawcett, R. J. B. (2015). The Excess Heat Factor: A Metric for Heatwave Intensity and Its Use in Classifying Heatwave Severity. *International Journal of Environmental Research and Public Health*, *12*(1), 227-253. https://www.mdpi.com/1660-4601/12/1/227

Ndayiragije, J. M., & Li, F. (2022). Effectiveness of Drought Indices in the Assessment of Different Types of Droughts, Managing and Mitigating Their Effects. *Climate*, *10*(9), Article 125. https://www.mdpi.com/2225-1154/10/9/125

O'Donnell, A. J., McCaw, W. L., Cook, E. R., & Grierson, P. F. (2021). Megadroughts and pluvials in southwest Australia: 1350–2017 CE. *Climate Dynamics*, *57*(7), 1817-1831. https://doi.org/10.1007/s00382-021-05782-0

Palmer, J. G., Verdon-Kidd, D., Allen, K. J., Higgins, P., Cook, B. I., Cook, E. R., Turney, C. S. M., & Baker, P. J. (2024). Drought and deluge: the recurrence of hydroclimate extremes during the past 600 years in eastern Australia's Natural Resource Management (NRM) clusters. *Natural Hazards*, *120*(4), 3565-3587. https://doi.org/10.1007/s11069-023-06288-0

Perkins-Kirkpatrick, S. E., Argüeso, D., & White, C. J. (2015). Relationships between climate variability, soil moisture, and Australian heatwaves. *Journal of Geophysical Research: Atmospheres*, *120*(16), 8144-8164. https://doi.org/10.1002/2015JD023592

Perkins-Kirkpatrick, S. E., White, C. J., Alexander, L. V., Argüeso, D., Boschat, G., Cowan, T., Evans, J. P., Ekström, M., Oliver, E. C. J., Phatak, A., & Purich, A. (2016). Natural hazards in Australia: heatwaves. *Climatic Change*, *139*(1), 101-114. https://doi.org/10.1007/s10584-016-1650-0

Perkins, S. E., & Alexander, L. V. (2013). On the Measurement of Heat Waves. *Journal of Climate*, *26*(13), 4500-4517. https://doi.org/10.1175/JCLI-D-12-00383.1

Qiu, J., Shen, Z., Leng, G., & Wei, G. (2021). Synergistic effect of drought and rainfall events of different patterns on watershed systems. *Scientific Reports*, *11*(1), Article 18957. https://doi.org/10.1038/s41598-021-97574-z

References

Reddy, P. J., Perkins-Kirkpatrick, S. E., Ridder, N. N., & Sharples, J. J. (2022). Combined role of ENSO and IOD on compound drought and heatwaves in Australia using two CMIP6 large ensembles. *Weather and Climate Extremes*, *37*, Article 100469. https://doi.org/10.1016/j.wace.2022.100469

Reddy, P. J., Perkins-Kirkpatrick, S. E., & Sharples, J. J. (2021). Intensifying Australian Heatwave Trends and Their Sensitivity to Observational Data. *Earth's Future*, *9*(4), 1-18. https://doi.org/10.1029/2020EF001924

Redmond, K. T. (2002). THE DEPICTION OF DROUGHT: A Commentary. *Bulletin of the American Meteorological Society*, *83*(8), 1143-1148. https://doi.org/https://doi.org/10.1175/1520-0477-83.8.1143

Reveiu, A., & Dardala, M. (2011). Techniques for Statistical Data Visualization in GIS. *Informatica Economica*, *15*, 72-79.

Ridder, N. N., Pitman, A. J., & Ukkola, A. M. (2022). High impact compound events in Australia. *Weather and Climate Extremes*, *36*, Article 100457. https://doi.org/10.1016/j.wace.2022.100457

Ridder, N. N., Pitman, A. J., Westra, S., Ukkola, A. M., Do, H. X., Bador, M., Hirsch, A. L., Evans, J. P., Di Luca, A., & Zscheischler, J. (2020). Global hotspots for the occurrence of compound events. *Nat Commun*, *11*(1), Article 5956. https://doi.org/10.1038/s41467-020-19639-3

Ridder, N. N., Ukkola, A. M., Pitman, A. J., & Perkins-Kirkpatrick, S. E. (2022). Increased occurrence of high impact compound events under climate change. *npj Climate and Atmospheric Science*, *5*, Article 3. https://doi.org/10.1038/s41612-021-00224-4

Sauter, C., Fowler, H. J., Westra, S., Ali, H., Peleg, N., & White, C. J. (2023). Compound extreme hourly rainfall preconditioned by heatwaves most likely in the mid-latitudes. *Weather and Climate Extremes*, *40*, 100563. https://doi.org/https://doi.org/10.1016/j.wace.2023.100563

Schneiderbauer, S., & Ehrlich, D. (2004). *Risk, Hazard and People's Vulnerability to Natural Hazards: a Review of Definitions, Concepts and Data*.

Sehgal, A., Sita, K., Siddique, K. H. M., Kumar, R., Bhogireddy, S., Varshney, R. K., HanumanthaRao, B., Nair, R. M., Prasad, P. V. V., & Nayyar, H. (2018). Drought or/and Heat-Stress Effects on Seed Filling in Food Crops: Impacts on Functional Biochemistry, Seed Yields, and Nutritional Quality [Review]. *Frontiers in Plant Science*, *9*, Article 1705. https://doi.org/10.3389/fpls.2018.01705

Sen, P. K. (1968). Estimates of the Regression Coefficient Based on Kendall's Tau. *Journal of the American Statistical Association*, *63*, 1379-1389.

Sherwood, S. C., & Huber, M. (2010). An adaptability limit to climate change due to heat stress. *Proceedings of the National Academy of Sciences*, *107*(21), 9552-9555. https://doi.org/10.1073/pnas.0913352107

Stanke, C., Kerac, M., Prudhomme, C., Medlock, J., & Murray, V. (2013). Health effects of drought: a systematic review of the evidence. *PLoS Curr*, *5*. https://doi.org/10.1371/currents.dis.7a2cee9e980f91ad7697b570bcc4b004

Tabari, H., & Willems, P. (2023). Global risk assessment of compound hot-dry events in the context of future climate change and socioeconomic factors. *npj Climate and Atmospheric Science*, *6*(1), Article 74. https://doi.org/10.1038/s41612-023-00401-7

Trancoso, R., Syktus, J., Toombs, N., Ahrens, D., Wong, K. K.-H., & Pozza, R. D. (2020). Heatwaves intensification in Australia: A consistent trajectory across past, present and future. *Science of The Total Environment*, *742*, Article 140521. https://doi.org/10.1016/j.scitotenv.2020.140521

Tripathy, K. P., Mukherjee, S., Mishra, A. K., Mann, M. E., & Williams, A. P. (2023). Climate change will accelerate the high-end risk of compound drought and heatwave events. *Proceedings of the National Academy of Sciences*, *120*(28), Article e2219825120. https://doi.org/10.1073/pnas.2219825120

Verdon-Kidd, D. C., Hancock, G. R., & Lowry, J. B. (2017). A 507-year rainfall and runoff reconstruction for the Monsoonal North West, Australia derived from remote paleoclimate archives. *Global and Planetary Change*, *158*, 21-35. https://doi.org/10.1016/j.gloplacha.2017.09.003

Verdon-Kidd, D. C., & Kiem, A. S. (2009). Nature and causes of protracted droughts in southeast Australia: Comparison between the Federation, WWII, and Big Dry droughts. *Geophysical Research Letters*, *36*(22), Article L22707. https://doi.org/10.1029/2009GL041067

Vogel, J., Rivoire, P., Deidda, C., Rahimi, L., Sauter, C. A., Tschumi, E., van der Wiel, K., Zhang, T., & Zscheischler, J. (2021). Identifying meteorological drivers of extreme impacts: an application to simulated crop yields. *Earth Syst. Dynam.*, *12*(1), 151-172. https://doi.org/10.5194/esd-12-151-2021

Wang, B., Chen, C., Asseng, S., Yu, Q., & Yang, X. (2015). Effects of climate trends and variability on wheat yields in eastern Australia. *Climate Research*, *64*(2), 173-186. https://doi.org/10.3354/cr01307

Webb, L. (2013). Impacts on agriculture. *Proceedings of the Royal Society of Victoria*, *125*(1), 24-30. https://doi.org/10.1071/RS13012

Welbergen, J. A., Klose, S. M., Markus, N., & Eby, P. (2008). Climate change and the effects of temperature extremes on Australian flying-foxes. *Proceedings of the Royal Society B: Biological Sciences*, *275*(1633), 419-425. https://doi.org/doi:10.1098/rspb.2007.1385

Wells., N., Goddard., S., & Hayes., M. J. A Self-Calibrating Palmer Drought Severity Index. *Journal of Climate*, *17*(12), 2335–2351. https://doi.org/10.1175/1520-0442(2004)017<2335:ASPDSI>2.0.CO;2

Zhang, C., Gao, J., Liu, L., & Wu, S. (2024). Compound drought and hot stresses projected to be key constraints on maize production in Northeast China under future climate. *Computers and Electronics in Agriculture*, *218*, Article 108688. https://doi.org/10.1016/j.compag.2024.108688

Zhang, Q., She, D., Zhang, L., Wang, G., Chen, J., & Hao, Z. (2022). High Sensitivity of Compound Drought and Heatwave Events to Global Warming in the Future. *Earth's Future*, *10*. https://doi.org/10.1029/2022EF002833

Zhang, Y., Beggs, P. J., McGushin, A., Bambrick, H., Trueck, S., Hanigan, I. C., Morgan, G. G., Berry, H. L., Linnenluecke, M. K., Johnston, F. H., Capon, A. G., & Watts, N. (2020). The 2020 special report of the MJA–Lancet Countdown on health and climate change: lessons learnt from Australia's 'Black Summer'. *Medical Journal of Australia*, *213*(11), 490-492.e410. https://doi.org/https://doi.org/10.5694/mja2.50869

Zhao, H., Gao, G., An, W., Zou, X., Li, H., & Hou, M. (2017). Timescale differences between SC-PDSI and SPEI for drought monitoring in China. *Physics and Chemistry of the Earth, Parts A/B/C*, *102*, 48-58. https://doi.org/https://doi.org/10.1016/j.pce.2015.10.022

Zscheischler, J., Martius, O., Westra, S., Bevacqua, E., Raymond, C., Horton, R. M., Van den Hurk, B. J. J. M., AghaKouchak, A., Jézéquel, A., Mahecha, M. D., Maraun, D., Ramos, A. M., Ridder, N. N., Thiery, W., & Vignotto, E. (2020). A typology of compound weather and climate events. *Nature Reviews Earth & Environment*, *1*(7), 333-347. https://doi.org/10.1038/s43017-020-0060-z

Appendix 1 Supplementary Figures
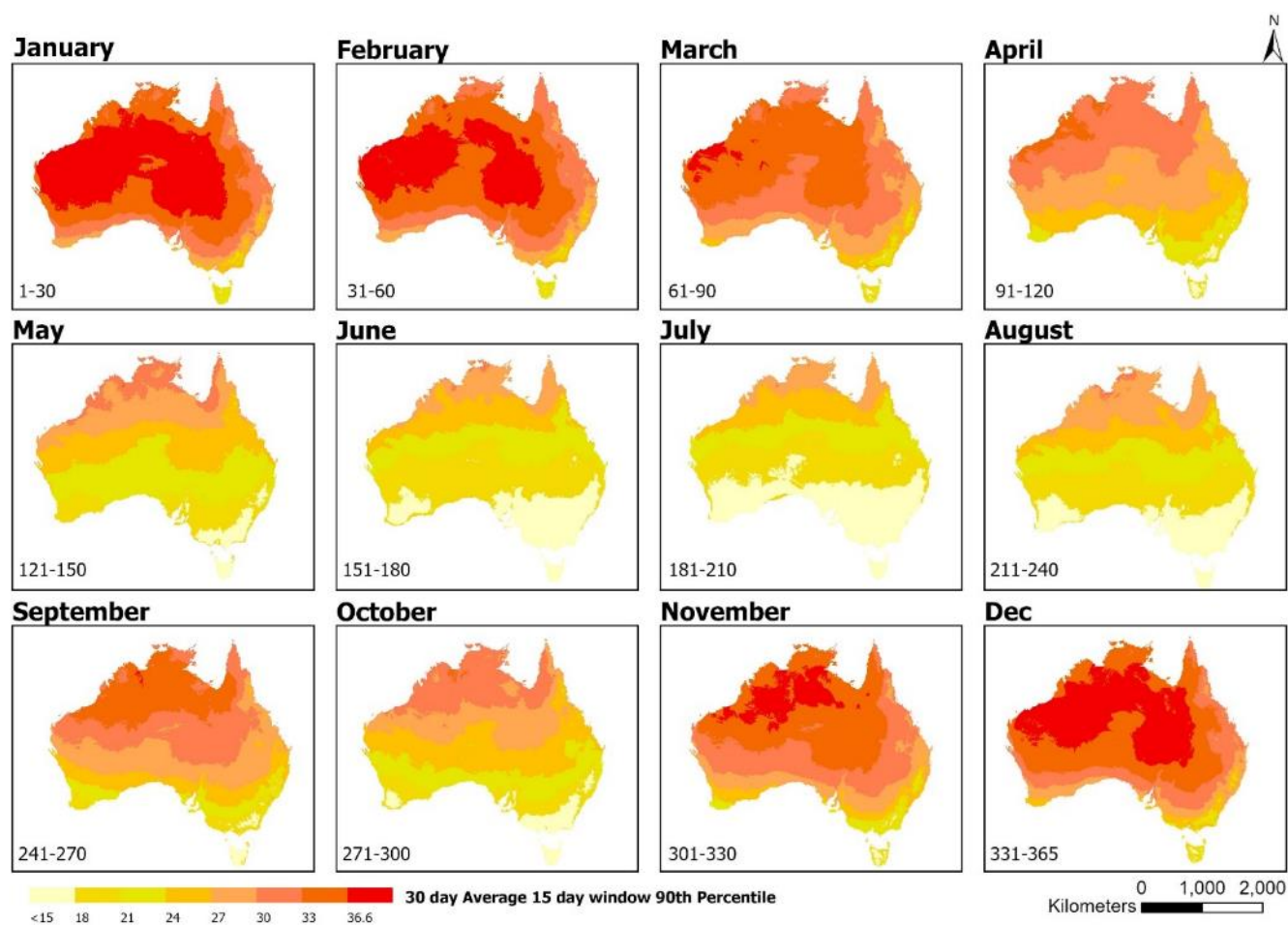
Fig. i PCT 15-day window Threshold for EHF Monthly Average
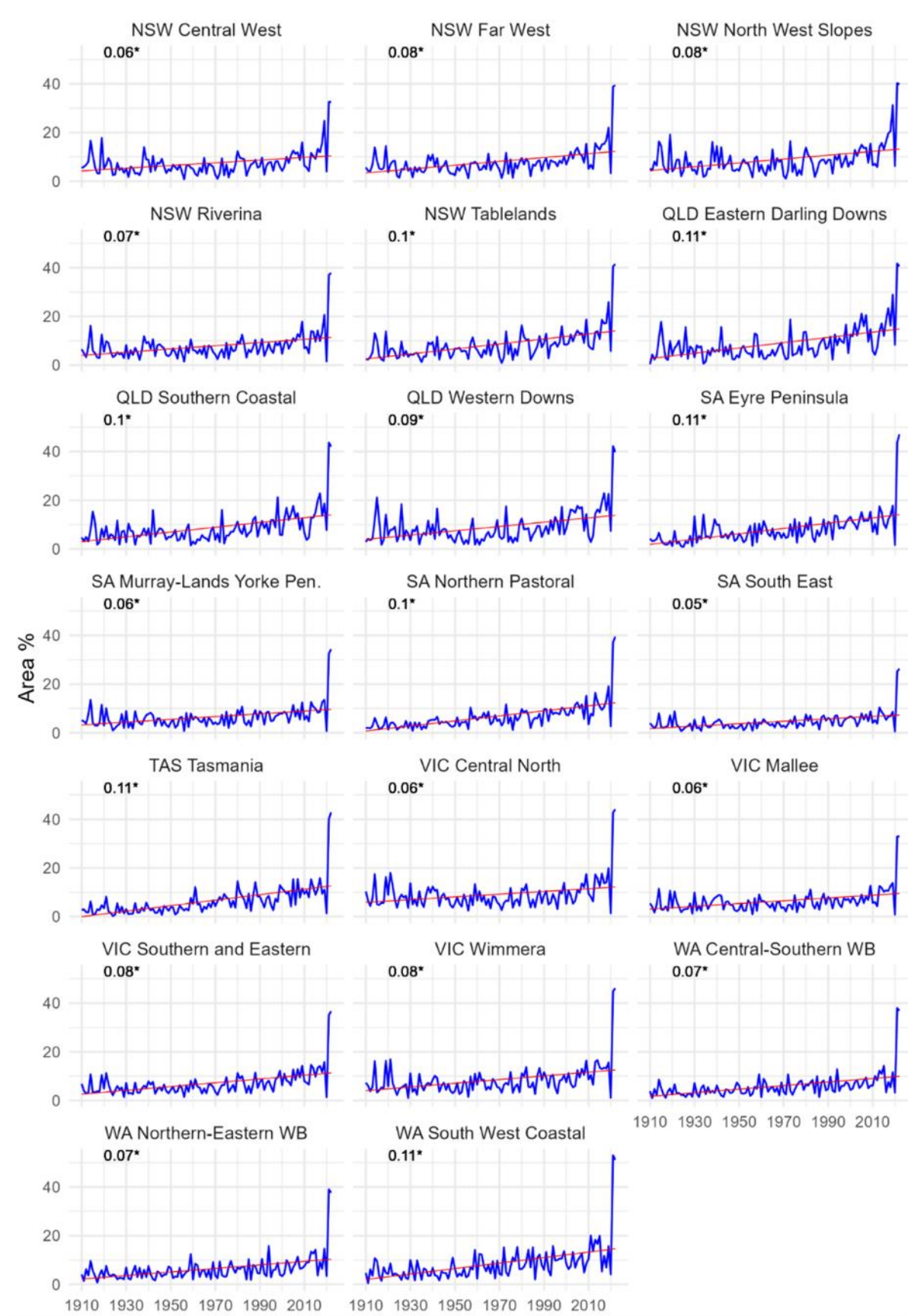
Fig. ii Yearly Total Heatwave Coverage Time series by ABARES Region

The y-axis shows the annual area percentage covered by heatwaves, calculated as total heatwave days divided by the total number of grid cells. Linear trend lines in red and labelled slopes are also displayed on each time series.
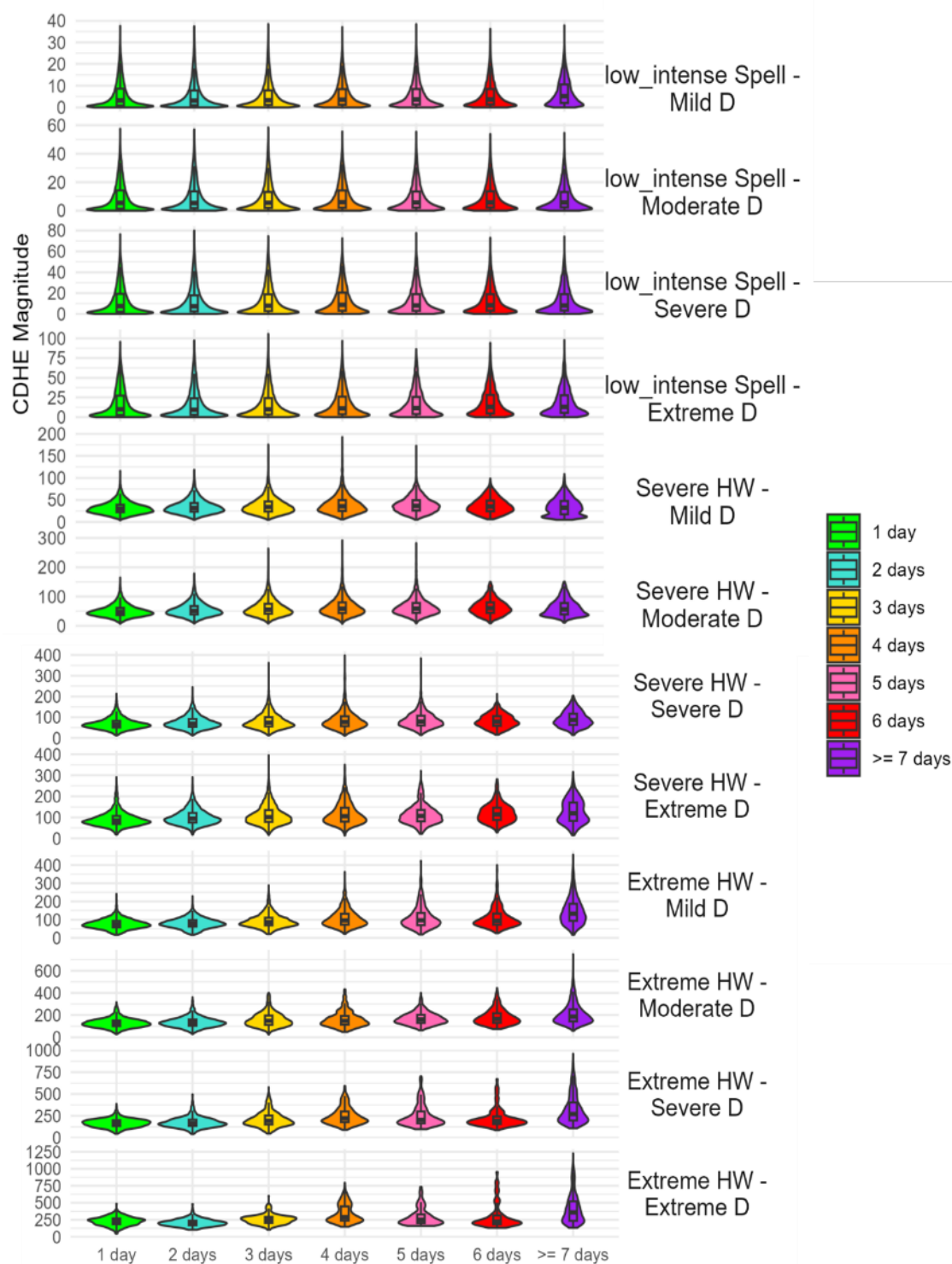
Fig. iii Violin plot of CDHE daily Magnitude by Duration and Severity
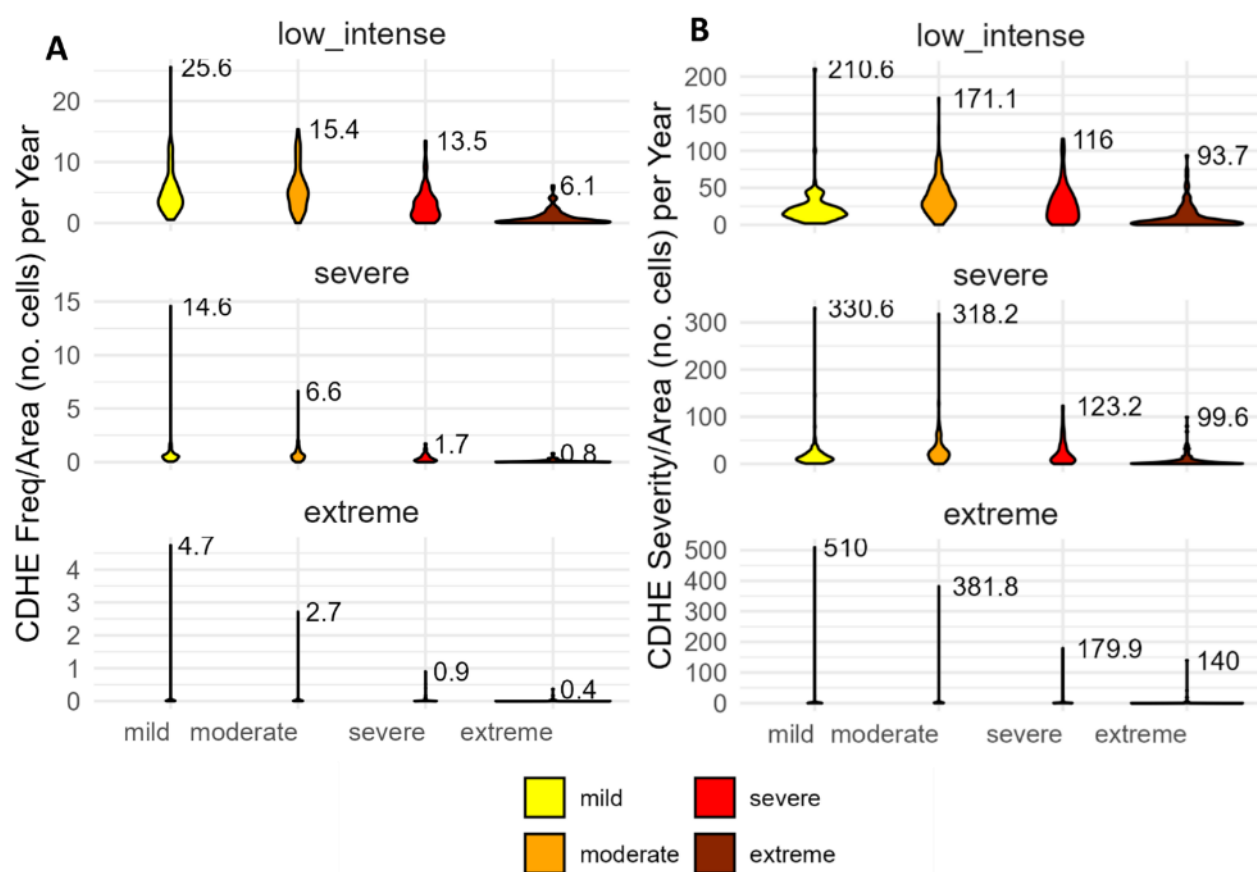
Fig. iv Violin Plots of Yearly CDHE Metrics per Cell Area by Drought and Heatwave Severity (A: CDHE Frequency, B: CDHE Severity)
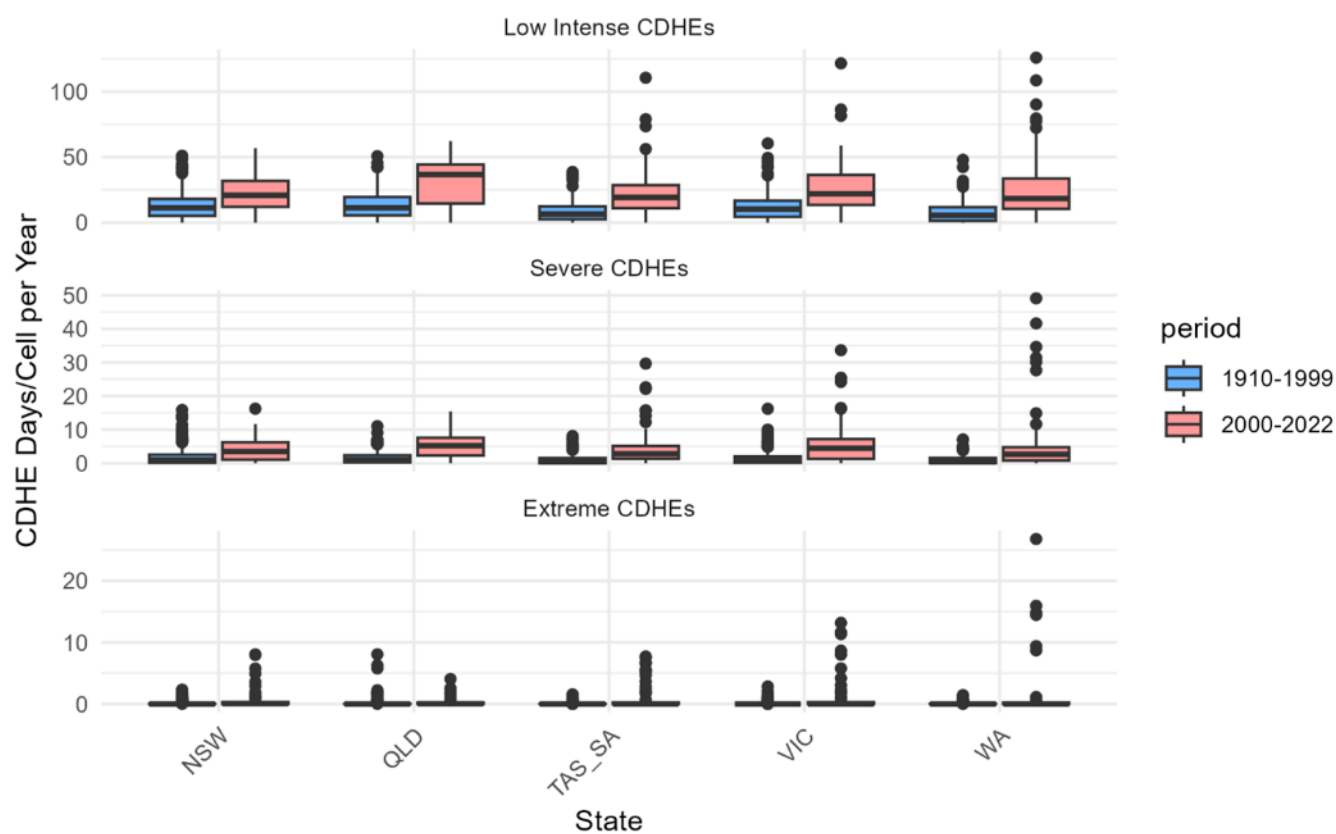
Fig. v Box Plot of the Regional CDHE Frequency (1910–1999 vs. 2000–2022) Across States and Territories
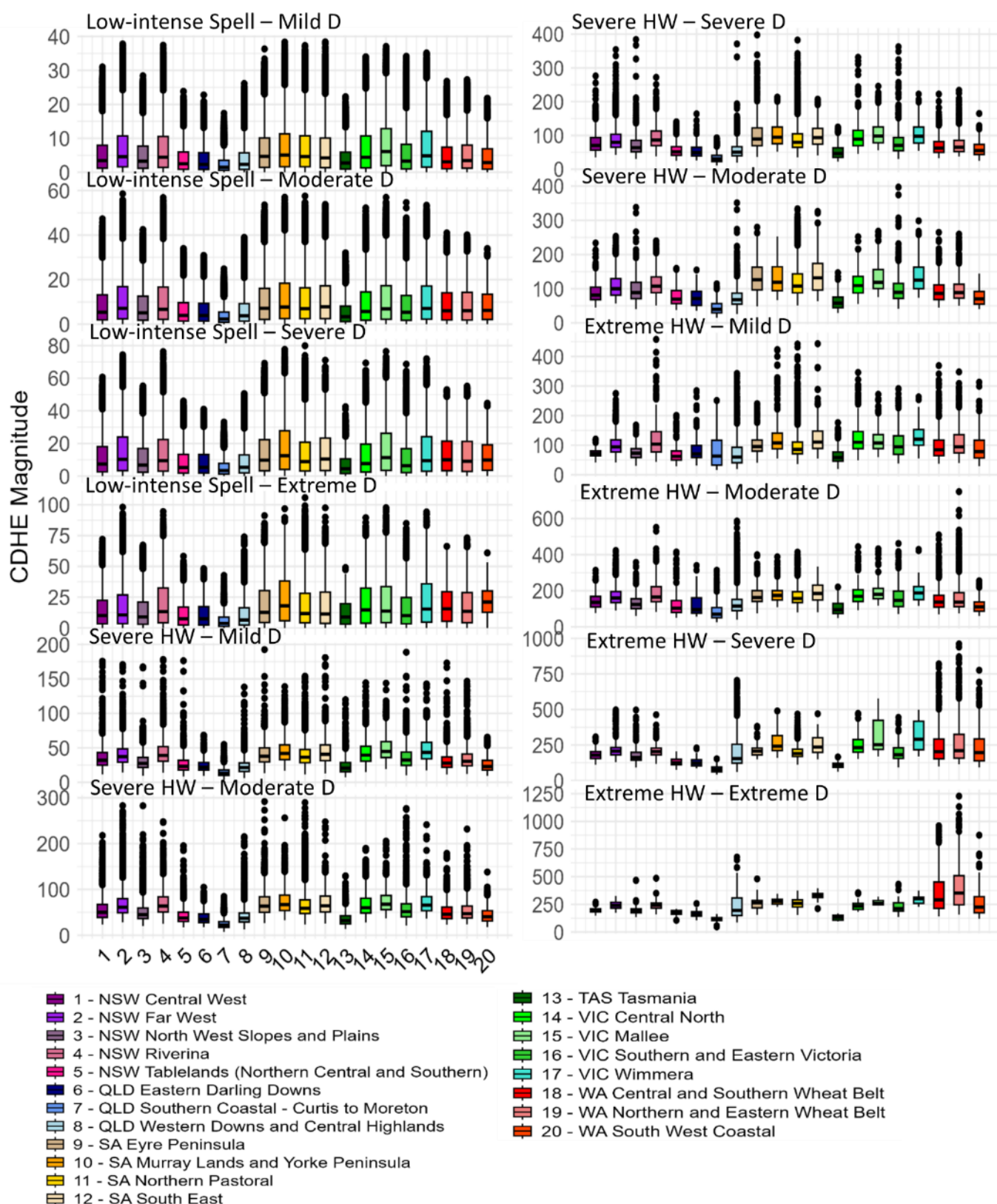
Fig. vi Box Plot CDHE Daily Magnitude by Severity and ABARES Growing Region
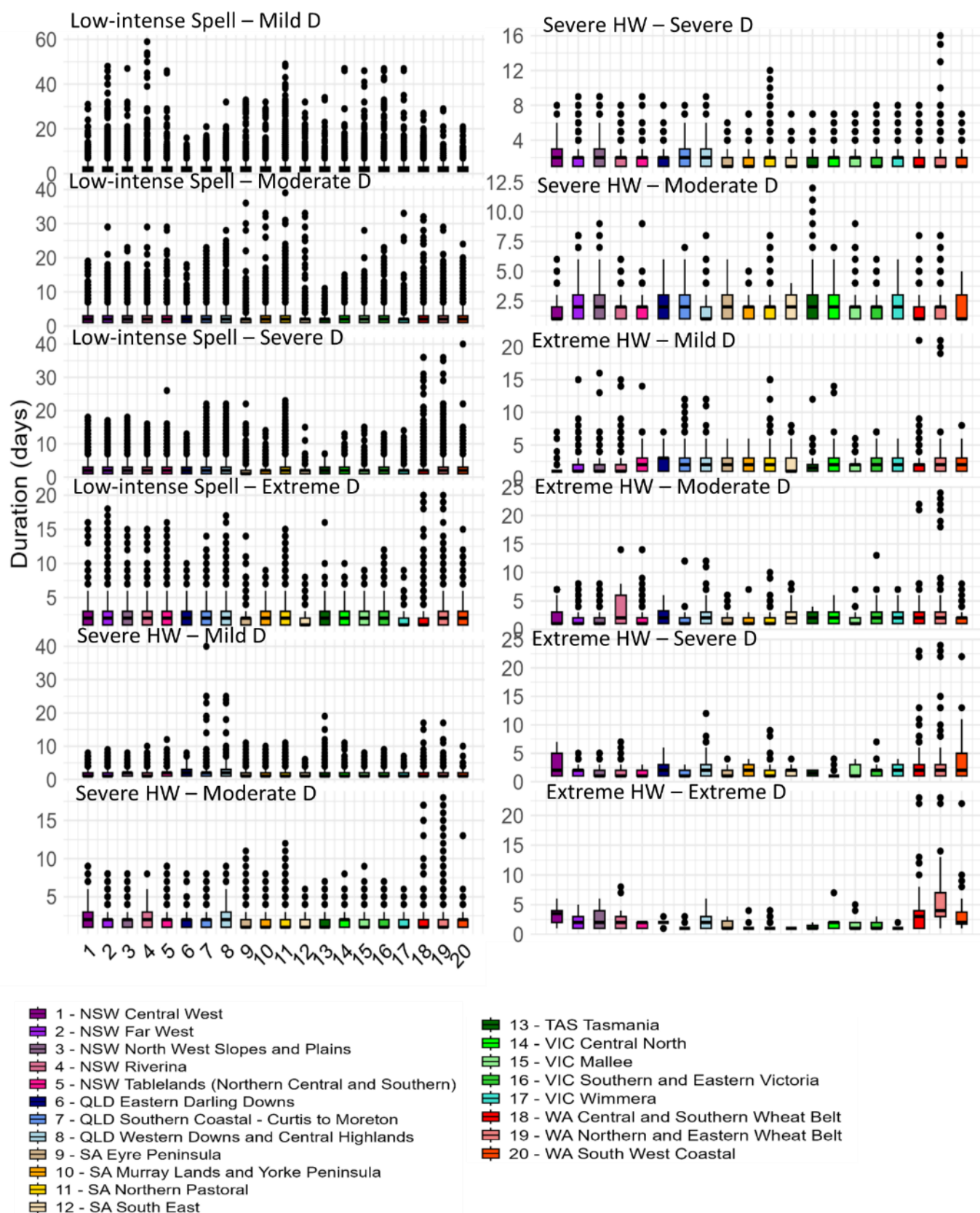
Fig. vii Box Plot CDHE Duration by Region and Severity
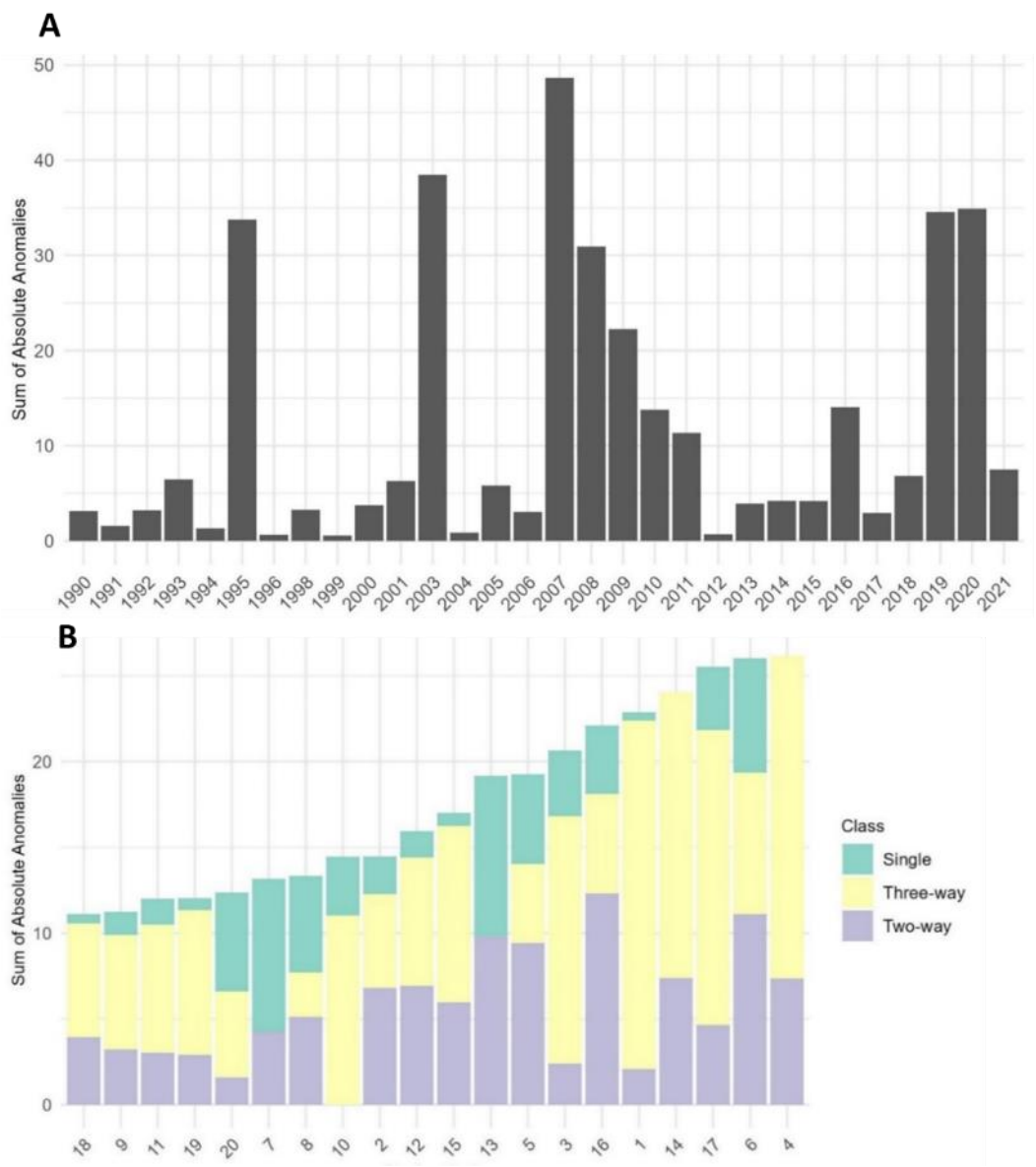
Fig. viii Bar Charts of Total Combined Crop Loss Anomalies by A: year and B: ABARES Region

Panel A displays the total combined crop loss anomalies aggregated by year across all ABARES regions, while Panel B shows the total crop loss anomalies aggregated by region across all years.

Appendix 2 Supplementary Data and Statistics

Table. i Heatwaves Max and Mean Daily Area Coverage Australia-Wide

Year	Mean Heatwave Area %	Max Heatwave Area %	Date of Max	Month of Max
2022	60.75	100.00	1/01/2022	January
2021	61.24	100.00	4/01/2021	January
1998	16.57	82.64	4/06/1998	June
2019	23.33	79.50	19/12/2019	December
2005	16.77	71.97	8/06/2005	June
1958	11.73	71.97	24/05/1958	May
1975	6.56	71.63	29/07/1975	July
2013	17.53	70.65	3/09/2013	September
2014	14.03	69.04	24/05/2014	May
2016	18.52	68.70	30/04/2016	April
1973	13.11	67.34	6/08/1973	August
2004	11.03	65.84	9/06/2004	June
1995	9.61	65.64	9/06/1995	June
1985	8.53	61.86	12/04/1985	April
2017	14.11	61.28	27/03/2017	March
2018	15.38	60.80	22/04/2018	April
1996	10.66	60.12	4/06/1996	June
1988	13.17	59.92	5/10/1988	October
2009	14.62	59.75	19/11/2009	November
1986	8.60	59.75	29/03/1986	March
2010	10.43	58.93	30/07/2010	July
1945	6.48	58.14	22/06/1945	June
2007	12.82	57.67	29/05/2007	May
1978	5.98	57.16	30/05/1978	May
2020	17.41	57.12	24/04/2020	April
1987	9.23	56.20	11/06/1987	June
1990	12.75	54.87	24/07/1990	July
2015	15.65	54.74	20/03/2015	March
1942	10.70	54.67	3/07/1942	July
2008	9.59	53.99	12/06/2008	June
1962	6.13	53.65	2/06/1962	June
2003	10.74	51.60	29/06/2003	June
1928	8.95	51.33	26/04/1928	April
1920	4.18	51.23	30/06/1920	June
1957	8.61	51.16	4/06/1957	June
2002	11.80	50.58	25/04/2002	April
1981	9.03	50.38	1/07/1981	July
1946	5.56	50.24	12/08/1946	August
1919	8.34	49.08	14/06/1919	June
1983	9.75	48.81	16/02/1983	February
1972	5.92	48.57	22/12/1972	December
1963	6.86	48.37	1/06/1963	June
1936	6.22	48.23	27/01/1936	January
1991	10.11	47.59	27/06/1991	June
1992	8.73	47.55	4/04/1992	April
2006	9.94	47.52	30/11/2006	November
1993	8.56	47.35	29/07/1993	July
1999	7.56	47.28	31/05/1999	May
2001	6.96	47.01	13/06/2001	June
1970	7.25	46.77	16/04/1970	April
1922	6.18	46.70	26/04/1922	April
1979	7.82	46.53	3/12/1979	December
1931	6.04	46.53	13/05/1931	May
1955	5.61	46.36	18/06/1955	June
1953	5.71	46.09	16/04/1953	April
1947	6.43	45.95	28/01/1947	January

2012	7.78	45.85	13/07/2012	July
1965	8.83	44.86	31/10/1965	October
1960	5.79	44.59	3/01/1960	January
1916	5.76	44.21	12/06/1916	June
1994	8.62	44.11	8/02/1994	February
1980	9.37	43.43	22/04/1980	April
1974	4.03	43.12	17/07/1974	July
1951	5.82	42.99	7/12/1951	December
1959	8.75	42.82	23/04/1959	April
1982	7.60	42.78	25/11/1982	November
1923	5.34	41.76	1/06/1923	June
1961	7.97	41.59	31/03/1961	March
1952	7.48	41.52	31/03/1952	March
1964	7.34	40.57	4/09/1964	September
2011	6.28	40.19	2/08/2011	August
1940	7.21	39.79	7/12/1940	December
1997	6.41	39.61	27/11/1997	November
1926	7.37	39.10	12/04/1926	April
1989	5.77	38.52	20/10/1989	October
1921	5.93	38.46	1/06/1921	June
1915	9.02	38.25	14/11/1915	November
1966	5.10	38.22	27/06/1966	June
1914	8.09	38.08	10/04/1914	April
1954	6.42	37.84	24/08/1954	August
1971	5.56	37.78	18/02/1971	February
1944	5.53	37.06	19/11/1944	November
1913	4.30	37.06	4/12/1913	December
1968	7.26	35.43	17/03/1968	March
1912	4.94	34.85	28/03/1912	March
2000	6.27	34.71	17/07/2000	July
1977	6.43	34.54	12/10/1977	October
1967	6.50	34.30	19/05/1967	May
1939	5.78	34.30	10/01/1939	January
1969	7.66	33.93	3/09/1969	September
1943	6.22	33.86	28/03/1943	March
1910	5.32	32.67	21/06/1910	June
1917	3.37	32.09	3/10/1917	October
1948	5.01	32.05	11/08/1948	August
1938	8.07	31.68	27/12/1938	December
1932	5.46	31.61	12/01/1932	January
1927	4.61	31.24	20/06/1927	June
1949	3.98	30.72	11/08/1949	August
1935	6.27	29.46	21/12/1935	December
1933	5.02	29.33	11/04/1933	April
1941	4.88	29.09	4/07/1941	July
1930	4.52	28.44	2/07/1930	July
1911	4.19	27.76	12/07/1911	July
1918	4.19	27.45	20/06/1918	June
1984	4.41	26.77	31/05/1984	May
1925	4.73	26.36	18/02/1925	February
1929	5.14	24.49	16/08/1929	August
1950	4.27	24.42	1/06/1950	June
1937	4.67	23.98	15/11/1937	November
1924	3.43	23.44	24/08/1924	August
1934	5.44	22.38	8/04/1934	April
1956	3.01	20.98	17/06/1956	June
1976	3.44	19.89	8/07/1976	July

Table. ii Monthly Heatwave Severity anomalies (≥1 σ)

| Severity | ABARES Region | Month | EHF Density | | | | | |
			Av. 1910-1955	Av. 1956-1989	Av. 1990-2022	+1956-1989	+1990-2022	std
Low-intense	1: NSW Central West	Feb	0.47	0.37	1.15	-0.09	0.77	0.71
	9: SA Eyre Peninsula	Feb	0.41	0.42	1.05	0.02	0.63	0.62
	16: VIC Southern and Eastern	Feb	0.38	0.32	0.87	-0.07	0.55	0.54
	17: VIC Wimmera	Feb	0.41	0.51	1.25	0.1	0.74	0.7
	1: NSW Central West	Mar	0.35	0.27	1.04	-0.08	0.77	0.71
	2: NSW Far West	Mar	0.36	0.33	1.07	-0.04	0.74	0.72
	3: NSW North West	Mar	0.25	0.22	0.9	-0.03	0.68	0.66
	5: NSW Tablelands	Mar	0.16	0.22	0.71	0.06	0.49	0.46
	6: QLD Eastern Darling Downs	Mar	0.16	0.19	0.86	0.03	0.68	0.55
	8: QLD Western Downs	Mar	0.22	0.18	0.68	-0.04	0.5	0.46
	14: VIC Central North	Mar	0.32	0.47	1.24	0.14	0.77	0.75
	7: QLD Southern Coastal	Dec	0.19	0.18	0.46	-0.01	0.29	0.25
Severe	3: NSW North West	Jan	1.59	0.94	2.13	-0.65	1.2	1.13
	1: NSW Central West	Feb	1.34	0.98	2.44	-0.36	1.46	1.42
	3: NSW North West	Feb	1.3	0.71	1.89	-0.59	1.18	1.13
	6: QLD Eastern Darling Downs	Feb	1.37	0.77	2.33	-0.6	1.57	1.22
	7: QLD Southern Coastal	Feb	0.51	0.46	1.32	-0.05	0.86	0.72
	8: QLD Western Downs	Feb	0.82	0.65	1.67	-0.18	1.03	0.93
	20: WA South West Coastal	Jun	0.5	1.59	NA	1.09	NA	0.79
	2: NSW Far West	Dec	1.75	1.25	3.01	-0.49	1.76	1.39
	4: NSW Riverina	Dec	1.44	1.31	3.38	-0.13	2.07	1.76
	10: SA Murray Lands-Yorke Pen	Dec	1.94	1.36	3.46	-0.58	2.1	1.79
	15: VIC Mallee	Dec	1.89	1.8	4.23	-0.09	2.43	2.04
Extreme	1: NSW Central West	Jan	6.8	1.6	22.62	-5.19	21.02	12.2
	2: NSW Far West	Jan	5.41	2.26	22.05	-3.14	19.79	13.6
	3: NSW North West	Jan	10.1	1.51	15.69	-8.59	14.17	9.8
	4: NSW Riverina	Jan	4.16	3.07	17.01	-1.08	13.94	13.4
	6: QLD Eastern Darling Downs	Jan	10.74	1.45	11.6	-9.3	10.15	7.99
	7: QLD Southern Coastal	Jan	7.8	0.88	7.5	-6.92	6.62	4.26
	8: QLD Western Downs	Jan	9.78	1.4	17.06	-8.38	15.66	6.95
	10: SA Murray Lands-Yorke Pen	Jan	4.97	2.26	19.79	-2.71	17.53	9.35
	12: SA South East	Jan	3.67	2.6	11.74	-1.07	9.14	6.36
	14: VIC Central North	Jan	4.71	4.1	20.48	-0.62	16.38	14
	15: VIC Mallee	Jan	5.77	2.53	29.85	-3.24	27.32	14.2
	16: VIC Southern and Eastern	Jan	3.98	2.79	9.51	-1.19	6.72	5.8
	17: VIC Wimmera	Jan	2.55	2.67	17.09	0.12	14.41	10.7
	18: WA Central-Southern WB.	Jan	2.33	2.78	11.64	0.45	8.85	5.54
	19: WA Northern-Eastern WB.	Jan	3.48	1.66	24.27	-1.82	22.61	10
	20: WA South West Coastal	Jan	1.7	2.35	12.2	0.65	9.85	5.87
	20: WA South West Coastal	Dec	2.11	1.19	10.62	-0.92	9.43	5.87

Table. iii HWT Regression Results (|diff|>14 days)

Earlier						
ABARES Region	**Day first**	**Day last**	**Date first**	**Date last**	**Diff**	**Severity**
1. NSW Central West	89	64	27/09/1911	2/09/2021	-25	severe
2. NSW Far West	74	44	12/09/1910	13/08/2021	-30	severe
2. NSW Far West	121	95	29/10/1913	3/10/2021	-25	extreme
3. NSW North West	65	43	3/09/1911	12/08/2021	-22	severe
4. NSW Riverina	103	83	11/10/1910	21/09/2021	-20	severe
5. NSW Tablelands	71	43	9/09/1911	12/08/2021	-28	severe
6. QLD Eastern Darling Downs	86	60	24/09/1911	29/08/2021	-26	severe
6. QLD Eastern Darling Downs	128	113	5/11/1913	21/10/2021	-15	extreme
8. QLD Western Downs	57	20	26/08/1911	20/07/2021	-38	severe
8. QLD Western Downs	112	98	20/10/1913	6/10/2021	-14	extreme
9. SA Eyre Peninsula	195	152	11/01/1928	29/11/2021	-43	extreme
10.SA Murray Lands-Yorke Pen	119	101	27/10/1910	9/10/2021	-18	severe
11. SA Northern Pastoral	62	29	31/08/1910	29/07/2021	-33	severe
11. SA Northern Pastoral	144	109	21/11/1912	17/10/2021	-35	extreme
13. TAS Tasmania	139	84	16/11/1912	22/09/2021	-55	severe
15. VIC Mallee	127	109	4/11/1910	17/10/2021	-18	severe
16. VIC Southern and Eastern	115	71	23/10/1910	9/09/2021	-44	severe
16. VIC Southern and Eastern	172	134	19/12/1912	11/11/2021	-38	extreme
17. VIC Wimmera	23	8	23/07/1910	8/07/2021	-15	low-intense
17. VIC Wimmera	183	162	30/12/1912	9/12/2021	-21	extreme
18. WA Central-Southern WB.	121	75	29/10/1910	13/09/2021	-46	severe
18. WA Central-Southern WB.	171	143	18/12/1913	20/11/2021	-28	extreme
19. WA Northern-Eastern WB	120	73	28/10/1910	11/09/2021	-46	severe
19. WA Northern-Eastern WB	143	124	20/11/1913	1/11/2021	-19	extreme
20. WA South West Coastal	144	106	21/11/1910	14/10/2021	-38	severe
Later						
ABARES Region	**Day first**	**Day last**	**Date first**	**Date last**	**Diff**	**Severity**
3. NSW North West	95	113	3/10/1913	21/10/2021	18	extreme
4. NSW Riverina	130	166	7/11/1913	13/12/2021	36	extreme
7. QLD Southern Coastal	71	106	9/09/1912	14/10/2021	36	extreme

Table. iv CDHEs Max and Mean Daily Area Coverage Australia-Wide

Year	Max CDHE Area %	Mean CDHE Area %	Date of Max	Month of Max
2022	72.8	29.2	25/12/2022	December
2014	66.8	11.7	24/05/2014	May
1995	58.4	7.0	9/06/1995	June
2016	57.2	12.9	4/03/2016	March
1975	54.3	5.3	29/07/1975	July
2017	52.9	10.9	27/03/2017	March
1973	51.1	10.8	6/08/1973	August
2005	50.1	10.4	8/06/2005	June
1942	49.8	9.3	5/05/1942	May
1945	49.8	5.7	22/06/1945	June
2018	49.2	10.8	2/11/2018	November
2003	48.7	9.2	29/06/2003	June
1996	48.6	8.6	5/06/1996	June
1958	48.3	8.6	23/05/1958	May
1928	47.9	8.5	26/04/1928	April
2013	47.7	11.8	3/09/2013	September
1946	47.1	5.1	12/08/1946	August
2004	45.2	8.1	9/06/2004	June
1947	44.8	6.0	28/01/1947	January
1970	43.5	6.3	15/04/1970	April
1955	43.1	4.7	18/06/1955	June
1998	42.1	8.3	22/03/1998	March
1962	41.1	5.0	2/06/1962	June
1936	41.1	5.0	28/01/1936	January
1994	41.0	6.3	10/07/1994	July
1992	40.8	4.6	22/02/1992	February
1953	40.3	5.2	16/04/1953	April
2012	40.1	6.4	13/07/2012	July
2001	40.1	5.0	13/06/2001	June
2015	40.0	10.5	20/03/2015	March
1981	39.9	7.2	19/09/1981	September
2002	39.6	8.0	25/04/2002	April
1923	38.7	5.0	1/06/1923	June
1978	38.3	3.8	30/05/1978	May
1974	38.0	3.5	17/07/1974	July
1921	37.6	5.2	1/06/1921	June
2011	37.3	5.0	2/08/2011	August
1991	37.0	6.9	27/06/1991	June
1987	36.7	4.3	13/05/1987	May
1971	36.7	5.0	18/02/1971	February
1961	36.5	6.5	1/04/1961	April
1979	35.9	6.6	3/12/1979	December
1922	35.9	5.2	26/04/1922	April
1914	35.9	7.2	10/04/1914	April
1952	35.5	5.8	31/03/1952	March
1957	35.3	6.1	19/06/1957	June
1931	35.3	3.5	13/05/1931	May
1944	34.5	5.0	19/11/1944	November
1972	34.1	4.3	28/12/1972	December
1989	34.1	4.3	19/10/1989	October
1916	34.0	4.3	12/06/1916	June
1940	33.8	5.2	7/12/1940	December
1963	33.6	5.0	1/06/1963	June
2021	33.2	13.3	29/12/2021	December
1939	33.0	5.0	10/01/1939	January
1999	32.4	4.4	20/05/1999	May
1954	31.6	5.4	24/04/1954	April
2007	31.5	5.2	4/03/2007	March
1967	31.3	5.4	19/05/1967	May

1990	31.3	6.8	17/07/1990	July
1920	31.2	3.0	30/06/1920	June
1986	31.2	4.4	4/04/1986	April
1988	30.9	5.8	1/11/1988	November
1951	30.9	4.2	6/03/1951	March
1938	30.3	7.4	27/12/1938	December
1985	30.2	3.9	5/08/1985	August
2019	30.1	7.4	23/01/2019	January
1949	30.0	3.4	11/08/1949	August
1980	29.8	6.0	22/04/1980	April
1913	29.6	2.6	3/12/1913	December
1966	29.4	3.6	27/06/1966	June
2000	29.2	5.1	17/07/2000	July
1969	29.0	5.7	3/09/1969	September
1968	28.5	5.8	17/03/1968	March
1935	28.4	5.5	19/02/1935	February
2010	28.1	4.6	31/07/2010	July
1943	28.1	5.1	28/03/1943	March
1919	26.9	4.5	1/05/1919	May
1915	26.8	6.4	20/07/1915	July
1993	26.4	4.0	29/07/1993	July
1912	26.2	3.5	28/03/1912	March
1959	26.0	5.3	23/04/1959	April
1911	26.0	3.8	12/07/1911	July
2006	25.9	4.8	30/11/2006	November
1960	25.0	3.2	30/07/1960	July
1932	24.8	4.6	12/01/1932	January
2008	24.5	3.3	12/06/2008	June
1933	23.8	3.9	11/04/1933	April
1948	23.6	3.7	10/08/1948	August
1925	23.5	3.2	18/02/1925	February
1941	23.4	3.9	20/12/1941	December
1937	23.2	4.3	15/11/1937	November
1924	22.4	2.2	24/08/1924	August
1927	22.3	3.0	19/10/1927	October
1997	22.2	4.2	27/11/1997	November
1910	22.0	2.8	26/05/1910	May
2009	21.9	4.4	14/08/2009	August
1950	20.6	2.5	21/07/1950	July
1956	19.4	2.3	16/06/1956	June
1917	19.1	2.4	4/10/1917	October
1929	18.9	3.4	17/02/1929	February
1918	18.4	2.6	19/06/1918	June
1982	17.7	2.1	1/01/1982	January
1934	17.4	3.9	8/04/1934	April
1977	16.9	2.6	18/06/1977	June
1976	16.3	2.6	10/12/1976	December
1965	16.3	3.7	30/12/1965	December
1984	13.5	1.7	31/05/1984	May
1964	13.1	2.5	6/03/1964	March
1926	12.2	2.1	12/04/1926	April
1930	11.3	2.0	20/10/1930	October
2020	5.0	1.6	13/04/2020	April
1983	3.5	0.4	25/12/1983	December

Table. v Monthly CDHE Severity anomalies (≥0.75σ)

ABARES Region	Month	Av_1910-1955	Av_1956-1989	Av_1990-2022	+1956-1989	+1990-2022	std
1. NSW Far West	Feb	27.7	24.1	55.0	-3.7	30.9	73.0
1. NSW Far West	Mar	24.4	11.4	34.3	-13.0	22.9	42.1
1. NSW Far West	Apr	14.5	7.0	27.3	-7.6	20.4	28.2
1. NSW Far West	Jun	15.1	13.3	24.5	-1.8	11.2	29.4
2. NSW North West Slopes	May	9.3	5.2	13.4	-4.1	8.1	17.7
2. NSW North West Slopes	Sep	33.4	21.2	60.7	-12.2	39.4	67.1
2. NSW North West Slopes	Dec	76.1	13.1	81.0	-63.0	67.9	107.4
3. NSW Central West	Apr	7.8	1.6	17.3	-6.2	15.7	19.2
3. NSW Central West	Sep	37.5	25.4	45.7	-12.1	20.3	59.0
3. NSW Central West	Oct	63.8	18.2	83.7	-45.7	65.6	107.0
3. NSW Central West	Dec	63.3	24.4	126.7	-39.0	102.3	154.3
4. NSW Riverina	Feb	42.3	25.1	60.3	-17.2	35.2	65.6
4. NSW Riverina	Apr	12.8	5.4	30.8	-7.5	25.4	39.7
5. NSW Tablelands	Jan	47.0	9.8	74.2	-37.2	64.4	88.3
5. NSW Tablelands	Feb	14.2	6.3	34.2	-7.8	27.8	43.2
5. NSW Tablelands	Apr	4.3	2.1	9.0	-2.2	6.9	11.1
5. NSW Tablelands	Sep	18.9	16.8	38.7	-2.1	21.9	50.7
5. NSW Tablelands	Oct	27.7	12.4	38.3	-15.4	26.0	50.7
5. NSW Tablelands	Dec	22.4	8.6	71.3	-13.8	62.7	84.3
6. QLD Eastern Darling Downs	Mar	13.6	7.5	21.9	-6.2	14.5	20.9
6. QLD Eastern Darling Downs	May	12.2	6.2	11.2	-6.0	4.9	14.1
6. QLD Eastern Darling Downs	Jun	14.3	5.5	28.0	-8.8	22.6	24.0
6. QLD Eastern Darling Downs	Aug	26.4	13.2	76.7	-13.1	63.4	83.1
6. QLD Eastern Darling Downs	Sep	39.3	15.0	135.9	-24.3	120.9	132.0
6. QLD Eastern Darling Downs	Oct	41.9	46.7	79.6	4.8	32.9	95.0
6. QLD Eastern Darling Downs	Nov	48.5	22.9	82.9	-25.5	59.9	91.0
6. QLD Eastern Darling Downs	Dec	39.4	17.4	75.8	-22.0	58.4	65.4
7. QLD Southern Coastal	Feb	11.0	3.3	21.1	-7.7	17.8	27.0
7. QLD Southern Coastal	Mar	5.7	5.2	10.7	-0.5	5.5	13.9
7. QLD Southern Coastal	Jun	7.9	2.1	14.7	-5.8	12.6	16.6
7. QLD Southern Coastal	Jul	13.0	5.4	30.0	-7.6	24.7	29.3
7. QLD Southern Coastal	Aug	6.4	8.9	30.9	2.5	22.0	34.1
7. QLD Southern Coastal	Sep	7.5	11.6	41.6	4.1	30.0	42.9
7. QLD Southern Coastal	Nov	9.3	6.5	27.9	-2.9	21.4	24.6
7. QLD Southern Coastal	Dec	12.6	5.1	23.3	-7.5	18.2	24.8
8. QLD Western Downs	Mar	11.2	7.0	16.9	-4.2	9.9	20.1
8. QLD Western Downs	May	5.8	5.1	12.9	-0.7	7.8	16.9
8. QLD Western Downs	Jun	12.5	5.0	25.7	-7.5	20.8	24.5
8. QLD Western Downs	Jul	16.2	13.3	39.1	-2.9	25.7	40.1
8. QLD Western Downs	Aug	20.5	15.5	44.3	-5.0	28.9	45.3
8. QLD Western Downs	Sep	22.3	16.0	75.4	-6.2	59.4	83.8
8. QLD Western Downs	Nov	39.7	17.1	56.6	-22.6	39.6	56.5
8. QLD Western Downs	Dec	43.3	18.1	58.1	-25.2	40.1	64.1
9. SA Eyre Peninsula	Feb	31.3	57.1	120.3	25.9	63.1	108.7
9. SA Eyre Peninsula	Apr	14.2	23.7	73.3	9.5	49.6	92.1
9. SA Eyre Peninsula	Jul	11.6	11.8	21.1	0.2	9.2	23.0
9. SA Eyre Peninsula	Sep	18.1	38.8	54.3	20.6	15.5	71.2
9. SA Eyre Peninsula	Oct	34.5	29.7	108.6	-4.7	78.8	105.6
9. SA Eyre Peninsula	Nov	29.2	37.7	125.1	8.5	87.4	129.1
9. SA Eyre Peninsula	Dec	28.4	37.7	145.4	9.3	107.7	187.6
10. SA Murray-Lands Yorke Pen.	Feb	38.7	38.2	59.4	-0.5	21.2	67.5
10. SA Murray-Lands Yorke Pen.	Apr	22.2	17.5	47.4	-4.7	30.0	54.6
10. SA Murray-Lands Yorke Pen.	Nov	52.1	34.1	54.1	-18.1	20.0	69.4
11. SA Northern Pastoral	Feb	14.1	18.9	52.9	4.9	34.0	57.2
11. SA Northern Pastoral	Apr	8.6	10.5	27.1	1.8	16.6	28.9
11. SA Northern Pastoral	Jun	11.2	15.2	31.2	4.0	16.0	39.7
11. SA Northern Pastoral	Aug	32.1	24.8	53.0	-7.3	28.2	65.4
11. SA Northern Pastoral	Oct	18.6	29.1	56.5	10.5	27.4	55.9

11. SA Northern Pastoral	Nov	15.2	22.4	47.2	7.1	24.8	46.5
12. SA South East	Feb	16.7	30.1	39.1	13.4	9.0	50.6
12. SA South East	Mar	21.8	18.1	59.8	-3.7	41.7	76.2
12. SA South East	Apr	8.2	11.3	33.8	3.1	22.5	38.1
12. SA South East	Oct	13.7	16.0	32.5	2.3	16.5	43.0
13. TAS Tasmania	Jan	3.7	26.8	49.1	23.1	22.3	54.9
13. TAS Tasmania	Feb	4.4	21.8	29.3	17.4	7.5	36.9
13. TAS Tasmania	Mar	1.9	6.8	33.1	4.9	26.3	37.3
13. TAS Tasmania	Apr	3.3	11.0	12.4	7.7	1.4	15.0
13. TAS Tasmania	May	1.2	5.8	10.9	4.6	5.1	13.9
13. TAS Tasmania	Jul	1.3	4.4	6.5	3.1	2.1	5.9
13. TAS Tasmania	Aug	1.8	2.6	9.7	0.8	7.1	11.8
14. VIC Central North	Feb	83.5	28.8	112.1	-54.7	83.3	125.5
14. VIC Central North	Mar	41.7	22.1	104.1	-19.6	82.0	119.6
14. VIC Central North	Apr	27.0	9.3	49.5	-17.7	40.2	51.1
14. VIC Central North	Nov	82.6	58.9	111.8	-23.7	52.9	139.0
14. VIC Central North	Dec	111.3	31.0	271.5	-80.3	240.5	315.1
15. VIC Mallee	Feb	45.6	39.2	117.2	-6.4	78.0	107.9
15. VIC Mallee	Mar	46.9	21.6	82.6	-25.2	61.0	104.4
15. VIC Mallee	Apr	31.2	15.7	49.9	-15.5	34.2	53.3
15. VIC Mallee	Sep	33.1	28.4	53.8	-4.7	25.3	70.1
15. VIC Mallee	Oct	55.7	35.5	83.4	-20.2	48.0	108.9
15. VIC Mallee	Nov	65.2	42.4	90.3	-22.8	47.8	87.8
15. VIC Mallee	Dec	86.4	32.3	221.1	-54.1	188.8	289.1
16. VIC Southern and Eastern	Jan	23.6	19.4	122.9	-4.2	103.5	125.2
16. VIC Southern and Eastern	Feb	18.6	11.6	30.1	-6.9	18.4	33.9
16. VIC Southern and Eastern	Mar	11.6	3.2	46.4	-8.5	43.3	49.4
16. VIC Southern and Eastern	Apr	8.2	1.8	21.2	-6.4	19.4	23.5
16. VIC Southern and Eastern	Jul	2.2	2.9	11.7	0.7	8.8	14.8
16. VIC Southern and Eastern	Sep	11.7	7.3	30.0	-4.3	22.7	29.0
16. VIC Southern and Eastern	Oct	13.3	3.3	59.7	-10.0	56.4	76.3
16. VIC Southern and Eastern	Nov	20.6	9.5	65.7	-11.0	56.1	74.7
16. VIC Southern and Eastern	Dec	28.9	5.3	145.4	-23.7	140.2	172.3
17. VIC Wimmera	Feb	46.0	33.2	93.3	-12.9	60.1	113.4
17. VIC Wimmera	Mar	53.8	18.5	92.1	-35.3	73.7	117.7
17. VIC Wimmera	Apr	19.4	13.4	57.5	-5.9	44.1	63.1
17. VIC Wimmera	Sep	29.3	23.0	46.7	-6.3	23.7	48.4
17. VIC Wimmera	Oct	43.0	26.7	110.4	-16.3	83.7	141.5
17. VIC Wimmera	Nov	67.9	58.0	158.9	-9.9	100.9	204.9
18. WA Central-Southern WB	Aug	5.8	3.6	23.0	-2.2	19.4	19.9
18. WA Central-Southern WB	Oct	10.7	19.5	54.3	8.8	34.8	60.0
18. WA Central-Southern WB	Nov	14.3	38.6	69.8	24.3	31.2	71.0
19. WA Northern-Eastern WB	Aug	12.9	12.6	38.8	-0.3	26.2	36.2
19. WA Northern-Eastern WB	Oct	26.7	34.5	74.9	7.8	40.4	74.0
19. WA Northern-Eastern WB	Nov	29.8	45.0	87.1	15.3	42.1	93.6
20. WA South West Coastal	Apr	3.1	7.8	73.9	4.7	66.1	85.2
20. WA South West Coastal	Jun	3.0	4.2	6.2	1.2	2.0	6.6
20. WA South West Coastal	Jul	3.8	1.2	6.9	-2.7	5.7	9.0
20. WA South West Coastal	Aug	6.9	2.8	18.2	-4.1	15.4	21.1
20. WA South West Coastal	Oct	1.8	11.6	48.0	9.9	36.4	60.1
20. WA South West Coastal	Nov	14.0	37.2	100.8	23.2	63.6	105.9

Table V. Yield anomalies and regional CDHE Frequency and Severity >75th Percentile

ABARES Region	Year	CDHE Regional Severity	CDHE Regional Freq	Yield Anomaly
8. QLD Western Downs	1990	387.78	8.85	sorghum
1. NSW Central West	1995	965.87	42.18	wheat
3. NSW North West Slopes		250.72	13.25	wheat
6. QLD Eastern Darling Downs		266.93	21.28	wheat
8. QLD Western Downs		308.70	23.01	wheat
9. SA Eyre Peninsula		585.86	20.81	wheat
11. SA Northern Pastoral		842.70	17.90	wheat
15. VIC Mallee		278.47	13.59	wheat
1. NSW Central West		1017.56	46.21	oats
9. SA Eyre Peninsula		597.25	21.28	oats
1. NSW Central West		1016.55	45.68	barley
3. NSW North West Slopes		259.66	14.04	barley
6. QLD Eastern Darling Downs		270.21	22.09	barley
8. QLD Western Downs		312.13	22.19	barley
9. SA Eyre Peninsula		585.86	20.81	barley
11. SA Northern Pastoral		848.28	18.34	barley
15. VIC Mallee		284.12	13.91	barley
6. QLD Eastern Darling Downs	2001	503.75	32.53	wheat
6. QLD Eastern Darling Downs		490.56	28.27	barley
8. QLD Western Downs		274.56	20.33	barley
1. NSW Central West	2003	294.97	43.52	wheat
7. QLD Southern Coastal		337.36	37.00	wheat
1. NSW Central West		342.08	48.39	oats
1. NSW Central West		341.23	47.66	barley
8. QLD Western Downs		752.37	37.25	sorghum
6. QLD Eastern Darling Downs	2005	418.97	23.00	wheat
9. SA Eyre Peninsula		1715.76	54.58	wheat
10. SA Murray Lands-Yorke Pen.		244.86	21.39	wheat
15. VIC Mallee		270.33	21.76	wheat
9. SA Eyre Peninsula		1513.80	45.87	barley
15. VIC Mallee		296.32	17.40	barley
6. QLD Eastern Darling Downs	2006	297.63	31.51	wheat
6. QLD Eastern Darling Downs		276.34	23.71	barley
1. NSW Central West	2007	721.57	59.23	wheat
4. NSW Riverina		299.03	21.27	wheat
9. SA Eyre Peninsula		462.77	26.28	wheat
14. VIC Central North		336.00	32.53	wheat
15. VIC Mallee		341.77	20.95	wheat
16. VIC Southern and Eastern		323.35	34.03	wheat
17. VIC Wimmera		362.16	37.19	wheat
1. NSW Central West		983.13	87.36	oats
4. NSW Riverina		369.52	28.79	oats
9. SA Eyre Peninsula		487.16	28.17	oats
14. VIC Central North		448.83	37.39	oats
16. VIC Southern and Eastern		442.73	39.62	oats
17. VIC Wimmera		501.55	41.95	oats
1. NSW Central West		918.95	67.82	barley
4. NSW Riverina		348.85	23.78	barley
6. QLD Eastern Darling Downs		249.96	26.85	barley
9. SA Eyre Peninsula		423.34	23.71	barley
14. VIC Central North		433.15	34.66	barley
15. VIC Mallee		418.28	21.64	barley
16. VIC Southern and Eastern		425.80	37.18	barley
17. VIC Wimmera		477.74	35.77	barley
6. QLD Eastern Darling Downs		317.50	33.24	sorghum
1. NSW Central West	2008	672.01	38.32	oats
9. SA Eyre Peninsula		597.09	25.81	oats
12. SA South East		305.95	10.19	oats
15. VIC Mallee		631.59	20.02	oats

1. NSW Central West		330.47	23.17	barley
14. VIC Central North		366.86	23.81	barley
9. SA Eyre Peninsula	2009	258.05	26.62	wheat
14. VIC Central North		224.41	25.43	wheat
17. VIC Wimmera		270.17	31.31	wheat
14. VIC Central North		266.57	25.74	barley
18. WA Central-Southern WB.	2010	360.20	17.45	oats
18. WA Central-Southern WB.	2011	309.80	29.70	wheat
19. WA Northern-Eastern WB.		263.68	29.22	wheat
20. WA South West Coastal		284.50	45.27	wheat
18. WA Central-Southern WB.		454.68	36.26	oats
19. WA Northern-Eastern WB.		383.82	35.02	oats
20. WA South West Coastal		761.47	64.98	oats
18. WA Central-Southern WB.		411.62	30.04	barley
19. WA Northern-Eastern WB.		360.26	29.59	barley
20. WA South West Coastal		713.84	46.77	barley
18. WA Central-Southern WB.	2013	299.15	27.94	wheat
19. WA Northern-Eastern WB.		440.93	31.29	wheat
18. WA Central-Southern WB.		299.22	27.99	oats
19. WA Northern-Eastern WB.		441.60	31.47	oats
19. WA Northern-Eastern WB.		268.64	22.17	barley
8. QLD Western Downs	2014	626.00	38.41	wheat
8. QLD Western Downs		617.89	33.81	barley
3. NSW North West Slopes		449.29	19.97	sorghum
6. QLD Eastern Darling Downs		771.23	41.75	sorghum
17. VIC Wimmera	2015	256.96	20.98	wheat
17. VIC Wimmera		264.21	22.60	barley
12. SA South East	2016	448.31	24.26	wheat
13. TAS Tasmania		377.81	32.90	wheat
16. VIC Southern and Eastern		923.20	42.47	wheat
17. VIC Wimmera		1410.97	49.15	wheat
2. NSW Far West		401.14	26.44	oats
14. VIC Central North		2256.44	70.83	oats
17. VIC Wimmera		1787.56	61.00	oats
12. SA South East		426.25	23.28	barley
13. TAS Tasmania		324.25	30.66	barley
14. VIC Central North		1386.28	50.77	barley
15. VIC Mallee		1026.69	29.93	barley
16. VIC Southern and Eastern		893.47	39.30	barley
17. VIC Wimmera		1392.71	46.41	barley
5. NSW Tablelands	2018	216.22	21.01	wheat
8. QLD Western Downs		503.41	26.97	wheat
9. SA Eyre Peninsula		741.13	15.67	wheat
16. VIC Southern and Eastern		490.39	22.44	wheat
1. NSW Central West		1559.93	99.77	oats
13. TAS Tasmania		1029.59	26.51	oats
6. QLD Eastern Darling Downs		754.33	28.78	barley
16. VIC Southern and Eastern		894.52	27.31	barley
14. VIC Central North	2019	240.21	18.65	wheat
1. NSW Central West		563.24	12.80	oats
10. SA Murray Lands-Yorke Pen.		374.93	17.06	oats
14. VIC Central North		671.60	30.40	oats
16. VIC Southern and Eastern		391.16	20.52	oats
17. VIC Wimmera		315.26	17.43	oats
1. NSW Central West		563.24	12.80	barley
4. NSW Riverina		322.98	9.46	barley
6. QLD Eastern Darling Downs		237.32	16.31	barley
14. VIC Central North		391.03	16.11	barley
3. NSW North West Slopes		733.74	21.18	sorghum
6. QLD Eastern Darling Downs		445.68	42.46	sorghum
18. WA Central-Southern WB.	2020	680.69	21.64	wheat
19. WA Northern-Eastern WB.		1049.37	23.61	wheat

19. WA Northern-Eastern WB.		1605.81	31.92	oats
20. WA South West Coastal		853.46	37.79	oats
18. WA Central-Southern WB.		797.27	22.37	barley
19. WA Northern-Eastern WB.		1435.47	25.80	barley
20. WA South West Coastal	2021	463.45	38.35	wheat